Second Series *March, 1925* *Vol. 25, No. 3*

THE

PHYSICAL REVIEW

THE ISOTOPE EFFECT IN BAND SPECTRA, II: THE SPECTRUM OF BORON MONOXIDE

By Robert S. Mulliken[1]

Abstract

Band spectrum of boron monoxide.—Previous measurements of Jevons on the BO bands (ascribed by him to BN) have been extended, with the help of *new spectrograms*. Over 100 β and about 200 α heads were measured or identified and are tabulated with their intensities. (1) Complete *verification of the predicted vibrational isotope effect* is found for both α and β systems. Each is composed of two closely similar superposed systems, of which the weaker and larger scale one is due to the less abundant isotope $B^{10}O$, the other to $B^{11}O$. There was no indication of any other B isotopes than B^{10} and B^{11}. The measured positions of all the heads can be represented by the equations:

$$B^{10}O:\ \nu_\alpha = \begin{Bmatrix} 23{,}652.2\ ;\ 23{,}638.9 \\ 23{,}526.0\ ;\ 23{,}512.7 \end{Bmatrix} + 1285.6n' - 11.7n'^2 - 1926.8n'' + 12.21n''^2$$

$$B^{11}O:\ \nu_\alpha = \begin{Bmatrix} 23{,}661.6\ ;\ 23{,}648.3 \\ 23{,}535.4\ ;\ 23{,}522.1 \end{Bmatrix} + 1247.9n' - 10.6n'^2 - 1873.2n'' + 11.68n''^2$$

$$B^{10}O:\ \nu_\beta = 42{,}874.6 - 0.19n'n'' + 1304.6n' - 10.43n'^2 - 1927.9n'' + 12.66n''^2$$

$$B^{11}O:\ \nu_\beta = 42{,}880.9 - 0.17n'n'' + 1268.8n' - 9.98n'^2 - 1872.9n'' + 11.84n''^2$$

For the linear terms in n' and n'' (the initial and final vibrational quantum numbers), the weighted mean ratio for corresponding coefficients of the two isotopes is 1.0291 ± 0.0003; for the quadratic terms, 1.062 ± 0.008. The theoretical values are 1.0292 and 1.059 for BO, 1.0276 and 1.056 for BN. The complete agreement with theory for BO, but not for BN, in the absence of contradiction from more direct experimental evidence, makes practically certain the BO origin of the bands, and at the same time quantitatively confirms the predicted vibrational isotope effect and gives powerful new support to the quantum theory of band spectra. Further evidence supporting the assignment of the bands to BO is presented. A comparative *energy-level diagram* for both isotopes is given, showing also the existing transitions with their intensities. The α and β systems correspond to the same final state of the BO molecule, which is in all probability its normal state. (2) The inequality of the constant terms for the two isotopes in the above equations indicates an electronic isotope effect of wholly unprecedented magnitude. This vanishes, however, if one makes the assumption that the minimum values of n' and n'' are not zero, but $\frac{1}{2}$. This result makes probable the existence of *half-integral vibrational quantum numbers* in BO, and of a *null-point vibrational energy* of $\frac{1}{2}$ quantum for BO (and doubtless for other molecules). (3) Measurements on the structure lines of three β bands gave an approximate confirmation of the *rotational*

[1] National Research Fellow.

isotope effect. (4) They also permitted a partial *analysis of the band structure*, so that approximate equations for the origins of the α and β bands were obtained, as well as values for the internuclear distance for BO. (5) Measurements are given on a *new system of BO bands* of low intensity lying in the visible, and corresponding to a transition from the β initial state to two (probably the first and third) of the four α initial states. The agreement with calculation is very close for both isotopes (on the assumption that the new bands consist of Q branches). This result confirms the preceding analyses of the α and β systems. The grouping of the new bands is of an unusual type, due to the values of the constants involved. (6) *Comparison of the arc and active nitrogen spectra of BO.* The β bands, when generated in active nitrogen, appear to consist usually of an isolated positive branch. A negative branch appears to be weakly present in a few cases. In the arc, doublets appear in place of the single positive branch lines, a new component being added. The intensity distribution of the BO bands in active nitrogen among various n' and Δn values is discussed. The n' distribution, unlike the m' distribution, corresponds to a high effective temperature.

Possible analogy of BO and CN to the Na atom.—If the α and β systems of BO, and the red and violet CN bands, are respectively analogous to the first two members of the principal series of Na, the *electronic resonance potentials* of BO at 2.9 and 5.3 volts (calculated from the constant terms of the above equations), and of CN at 1.8 and 3.2 v, may be compared with the values 2.10 and 3.74 for Na. The weakness of the transition $\beta \rightarrow \alpha$ in BO is then analogous to that of the "forbidden" transition $2p-3p$ in Na. BO and CN, like Na, have nine outer electrons (outside the nucleus and K electrons) of which the first eight possibly form an octet somewhat as in Na, leaving the ninth in a loosely bound orbit. If the preceding analogy is correct, BO and CN should have *ionizing potentials* at about 7.0 and 4.4 volts, respectively (Na ionizes at 5.1 v). If this is true the alternation from higher to lower ionization potentials observed in the case of atoms, according as the number of electrons is even or odd, also holds for the series of molecules BO, CN, N_2^+; CO, N_2; NO; O_2, with 9, 10, 11, and 12 outer electrons, respectively.

QUALITATIVE CONFIRMATION OF THE VIBRATIONAL ISOTOPE EFFECT IN THE BAND SPECTRUM OF BORON MONOXIDE

IN a previous paper[2] the subject of the isotope effect in electronic band spectra has been discussed from a general and theoretical standpoint on the basis of the quantum theory. In the following pages this paper will be referred to as (I). Reference should be made to (I)[1] for the notation and terminology here used. The present paper deals with the confirmation[3] of some of the predictions of the theory, in the case of a band spectrum which was originally ascribed to boron nitride[4] but which the present writer now attributes to a compound boron monoxide.

[2] R. S. Mulliken, Phys. Rev., **25**, 119 (February, 1925).

[3] Preliminary accounts by the writer have appeared in Science, Aug. 31, 1923 (BN accepted as emitter); Nature, March 22, 1924 (BO; SiN is also discussed here); Nature, September 6, 1924 (evidence as to BO vs BN; half vibrational quantum numbers).

[4] W. Jevons, Proc. Roy. Soc. **91A**, 120-134 (1914).

Either BN or BO would have an unusually favorable value of $(\rho-1)$, the isotope coefficient [cf. (I), Eqs. (11), (16)]. It may be recalled that $\rho=\sqrt{(1/M_2+1/M')/(1/M_1+1/M')}$, where M_2 and M_1 are the atomic weights of the less abundant and the more abundant isotope, respectively, and M' is that of the other element. According to Aston,[5] boron contains two isotopes of atomic weights 10.0 and 11.0. According to the chemical atomic weight, 10.82, as recently determined by Baxter and Scott[6] and by Hönigschmidt and Birkenbach,[7] isotope 11 must be 4.6 times as abundant as isotope 10. Accordingly the band spectrum of BO should consist of two superposed spectra, the stronger due to $B^{11}O$, the weaker to $B^{10}O$.

The band spectrum here ascribed to BO was first obtained by Lord Rayleigh in 1913, by the reaction of BCl_3 vapor with active nitrogen. The heads from λ2100 to λ6400 were then measured by Jevons,[4] using photographs taken with Hilger glass and quartz spectrographs of moderately high dispersion. Jevons gives a good set of reproductions of the spectrum. This consists of two band systems. The α system of Jevons is a doubly double-headed system extending probably from about λ12000, certainly from λ8500, to below λ3100.[8] The relative spacing and intensities of the α heads are well shown in a diagram by Jevons. The single-headed β system extends from near λ3700 to below λ2100.[8] In both systems the heads are shaded toward the red, and are sharply defined. Jevons was able to express the positions of the heads of each system in terms of a Deslandres equation. In addition to the main systems of bands, Jevons found some fainter bands, most of which he grouped in two "subsidiary systems," β_1 and β_2, related to the main β system.

Granting that a difference exists between isotopes, the main α and β systems of Jevons should obviously be ascribed to the more abundant isotope $B^{11}O$. According to the theory, every $B^{11}O$ band should be accompanied by a $B^{10}O$ band about one fifth as intense, forming an α′ and a β′ system. The α and α′ systems should have a *common origin*;[3] on either side of this origin each $B^{10}O$ band should be at a distance about 2.9 per cent greater than the corresponding $B^{11}O$ band, since $(\rho-1)=0.0292$. The same statement holds for the β and β′ systems.

[5] F. W. Aston, "Isotopes", London, Edw. Arnold Co., 2nd ed., 1924.

[6] Baxter and Scott, Proc. Am. Acad. Arts Sci. **59**, 21 (1923).

[7] Hönigschmidt and Birkenbach, Anales Soc. Españ. Fís. Quim. **20**, 167 (1922); also, Stock and Küss (Ber. Deutsch. Chem. Ges. **56B**, 314, 1923) get a preliminary value 10.81.

[8] Jevons' identified data cover the range λ 6370-3370 for the α system, and λ 3256-2140 for the β system.

Assignment of vibrational quantum numbers. Before attempting to verify these predictions with Jevons' data, it is necessary to assign vibrational quantum numbers to the α and β bands. This can readily be done with the aid of two criteria of Heurlinger and Kratzer, (I) p. 136. (It could also be done, (I), p. 136, with the aid of the isotope effect, if it were assumed in advance that the latter would be in accordance with theory.) Jevons arranged the bands in a rectangular diagram (m vs p)—compare the rather similar arrangement of the circles containing estimated intensities of bands, in Fig. 1—in such a way that it is necessary only to change his empirical designations $n=62,61 \ldots 57$ for the β system to $n'=0,1, \ldots 5$; and $p=79,78 \ldots 69$ to $n''=0,1, \ldots 10$, where n' and n'' are the vibrational quantum numbers for the initial and final states, respectively. For the α system, the change is from $m=61, 60, \ldots 56$ to $n'=0,1, \ldots 5$, and from $p=79, 78, \ldots 74$, to $n''=0,1, \ldots 5$. A corresponding transformation can be made in Jevons' formulas for the band-heads.

Confirmation of isotope effect with Jevons' data. The α and β system origins for $B^{11}O$ can now be located. Jevons' β_2 bands on the high frequency side and his β_1 bands on the low frequency side of the β origin fulfill the requirements for $B^{10}O$ in respect to both position and intensity. Jevons' reproduction shows this well. His β_1 and β_2 bands evidently become more and more separated from the corresponding (adjacent) β bands with increasing distance from the origin ($m=62$, $p=79$). The results afford an excellent qualitative confirmation of the vibrational isotope effect, as will be seen by comparison with a theoretical diagram [(I) Fig. 1 (a)]. However, not all the expected $B^{10}O$ β bands, and none of the $B^{10}O$ α bands, are to be found in Jevons' data. The only evidence for $B^{10}O$ α heads consisted in some faint indications at the red end of the spectrum in Jevons' reproduction (not in his data), and a few unidentified measured heads in the ultraviolet.[9]

Confirmation with new data. The BO bands have now all been remeasured, extending Jevons' data into the near infra-red, and slightly in the ultraviolet. Many weak heads not recorded by Jevons have been measured, especially those due to $B^{10}O$. Careful examination and

[9] It is not surprising that the heads referred to at the red end were passed by in the absence of a guiding theory, since they are heavily masked by structure lines of the neighboring strong $B^{11}O$ heads (cf. Plate I(d) and Fig. 2). The masking is even more complete throughout the central part of the system; this is due particularly to the quadruplet character of the system. The bands of the two isotopes are well separated in the infra-red and also in the ultra-violet, but Jevons did not reach the former region, and in the latter the CN bands apparently interfered.

measurement of the photographs taken in this connection show in every case, so far as can be determined, with two or three doubtful exceptions, a $B^{10}O$ head, of about the correct intensity, for each $B^{11}O$ head, in both α and β systems. This may be seen by reference to the wave-length tables below (Tables I and II). Confirmation of the vibrational isotope effect for each of a very large number of bands is thus obtained in the present work, as compared with its former confirmation in the case of only a *single* infra-red HCl band.[10]

In the identification on the $B^{10}O$ heads, the procedure was first to calculate their positions, using for each $B^{10}O$ system a formula obtained by theory from the corresponding formula for $B^{11}O$. The calculation was made originally on the assumption that BN was the emitter of the bands. The much better agreement with BO became apparent only after careful measurements [cf. Eqs. (1) and (2)], since $(\rho-1)=1.0276$ for BN, as compared with 1.0292 for BO.

Plate I shows enlargements of various portions of the BO spectrum. Plate I (b) shows the $(2\rightarrow 2)$ β bands near the origin, and (a) shows other β bands farther away. It will be seen that the pattern of the band lines from each $B^{11}O$ head is repeated in lower intensity for the corresponding $B^{10}O$ head. Plate I (e) shows this on a larger scale for the $(0\rightarrow 1)$ band. In (c) the $(3\rightarrow 0)$ and $(2\rightarrow 0)$ α bands show well the isotope effect on the ultraviolet side of the α system. The pattern of the two stronger ($B^{11}O$) head-pairs is repeated, with a shift toward the violet, by the two weaker pairs of $B^{10}O$ heads, the two sets of pairs interlocking. Plate I (d) shows how in the red, at the other end of the α system, the $B^{10}O$ heads are well separated from the $B^{11}O$ heads, being displaced toward lower frequencies. Plate II shows some of the α heads nearer the origin, in the green; here the A heads $B^{10}O$ cannot be seen, but the presence of the B heads is evident, although their exact positions are masked by $B^{11}O$ structure lines.

The largeness of the separations between corresponding bands of the two isotopes (Table I and II) is notable. Thus for the $(4\rightarrow 0)$ band near the extreme ultraviolet end of the β system, the wave number difference $[\nu(B^{10}O)-\nu B^{11}O]$ is $(\nu_2-\nu_1)=+129$, while $\Delta\lambda=-5.6$, from $\lambda 2091$. At the other end of the β system, the separation for the $(3\rightarrow 10)$ band is $(\nu_2-\nu_1)=-370$, while $\Delta\lambda=+44.4$, from $\lambda 3442$. In the α system, the largest measured separation on the ultraviolet side was $(\nu_2-\nu_1)=+174$, with $\Delta\lambda=-18.4$ at $\lambda 3263$, for the $(6\rightarrow 0)$ band. On the infra-red side, the largest certainly measured separation was $(\nu_2-\nu_1)=-281$, with $\Delta\lambda=$

[10] F. W. Loomis, Astrophys. J. **52**, 248 (1920); A. Kratzer, Zeit. f. Phys. **3**, 460 (1920)

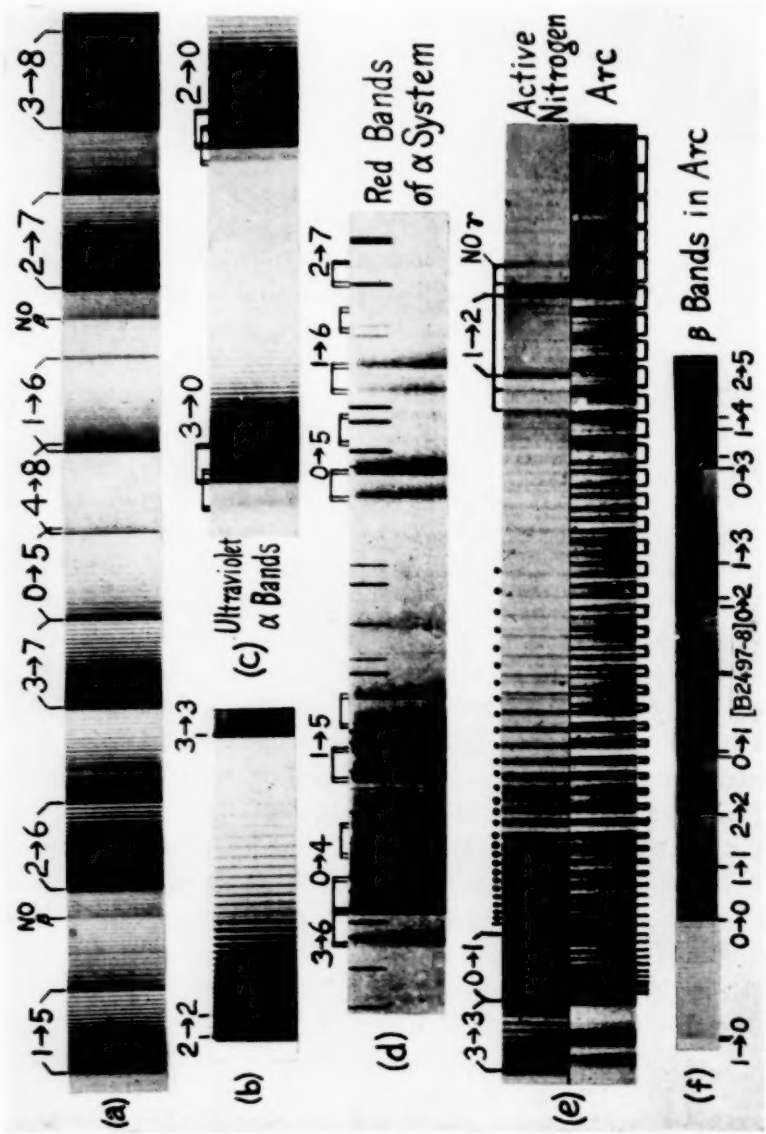

Plate I. *Enlargements of boron monoxide bands.*

Description of Plate I

In all cases the $B^{10}O$ heads and structure lines are *weaker* than the corresponding $B^{11}O$ heads and lines. *All* the BO α and β heads are shaded toward the red.

(*a*) Region λ2850-3120, showing heads and structure lines for bands of both isotopes, and isolated positive branch character. The two heads marked NO β are two of the "β bands of active nitrogen" (probably due to NO); they are shaded toward the red.

(*b*) (2→2) β bands, showing weak $B^{10}O$ structure lines among strong $B^{11}O$ lines.

(*c*) Region λ3650-3900, showing α bands on high-frequency side of origin; each band has four heads (A_1, A_2, B_1, and B_2 in order) for each isotope.

(*d*) Region λ5950-7550, showing α bands far on low-frequency side of origin, with $B^{10}O$ heads well separated from those of $B^{11}O$ (too weak to show in 3→6 and 2→7). Comparison, neon plus argon. Some unmarked heads are present due to N_2 (α bands of active nitrogen).

(*e*) Comparison of (0→1) β band in arc and active nitrogen (showing also 3→3 and 1→2); greatly enlarged. The $B^{11}O$ arc doublets are marked below; the high-frequency component of each doublet is alone present in the active nitrogen photograph above (in the reproduction, the juxtaposition of corresponding lines in the two sources is somewhat imperfect, especially at a distance from the head). The $B^{10}O$ lines of the 0→1 band in active nitrogen are marked by dots above; many of them can also be identified in the arc, together with their doublet companions in some cases. The four heads marked NO γ, whose structure lines, extending toward the 0→1 head, cause some confusion, belong to one of the "γ bands of active nitrogen" (probably due to NO). In the arc photographs there are several extra lines due to impurities.

(*f*) Region λ2260-2800 in arc, only slightly enlarged, showing overlapping of succeeding bands. The weaker $B^{11}O$ heads, and the $B^{10}O$ heads, are difficult or impossible to identify (contrast (*a*)).

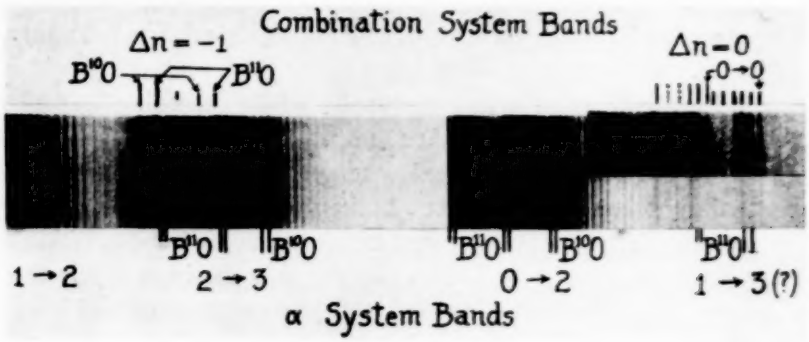

Plate II. Combination system bands, sequences $\Delta n = 0$ and $\Delta n = -1$.—The reproduction is enlarged from a single photograph, except for the insert in the upper right hand corner made from a longer exposure photograph, and showing better the $\Delta n = 0$ sequence. Note the faintness of the combination system bands as compared with the α system bands.—In both systems *A* heads are indicated with shorter, *B* heads with longer, lines adjacent to the reproduction.—Sequence $\Delta n = 0$. $B^{10}O$ and $B^{11}O$ heads superposed. Right to left—*A* heads 0→0, 1→1, 2→2, 3→3, 4→4, 5→5; then *B* heads 0→0, 1→1, 2→2, ... 5→5(?).—Sequence $\Delta n = -1$. Right to left,—superposed *A* heads, first of $B^{11}O$, then of $B^{10}O$; possible *P* branch head of *B* sequence of $B^{11}O$; superposed *B* heads, first of $B^{11}O$, then of $B^{10}O$.

+161A, for the (2→7) band. For the last $B^{11}O$ head measured, in the (2→8) band, the calculated separation is $\Delta\nu = -342$, $\Delta\lambda = +250$A.

In agreement with Aston's results, no indication was found of any other isotope of boron than those of atomic weights 10 and 11.

New Measurements

The experimental methods were much the same as those of Jevons. BCl_3 vapor was led into active nitrogen just as the latter left the exciting discharge tube and entered the afterglow tube, and the resulting spectrum of BO was observed through a quartz window. The BCl_3 used was pure material kindly supplied by Prof. G. P. Baxter, which was some remaining from the recent work by Prof. Baxter and Dr. A. Scott on the atomic weight of boron.[6] This was evidently free from CCl_4, since (in contrast to Jevons' experience) the strongest CN bands were hardly visible on the photographs.[11] In activating the nitrogen, a high-potential discharge from a $\frac{1}{2}$kw, type E, Clapp-Eastham transformer was used, with two large Leyden jars in the circuit. The nitrogen was used at the rate of about 50 liters (at atmospheric pressure) per hour. A pure grade of commercial nitrogen was found satisfactory, in one case without further treatment. Further details are to be found in the later section on direct experimental evidence as to the (BO or BN) origin of the bands. (See also Jevons' paper[4]).

The use of active nitrogen in producing the BO bands has pronounced advantages. Of particular importance is the fact that the heads are sharp and not badly overrun by structure lines from preceding heads; this is due to the low temperature. At the same time, the band systems are very well developed, in spite of the low temperature. Also, the spectrum is particularly free from continuous background and impurities (except for some trouble with the strongest active nitrogen bands). The intensity, however, is only moderate. In the arc, the intensity is much greater, but the advantages that go with low temperature are lost, so that it is difficult to pick out any but the strongest of the $B^{11}O$ heads, while very few of the $B^{10}O$ heads can be identified at all (cf. Plate I (f) with (a)).

For the ultraviolet, photographs were taken with a Hilger type C quartz spectrograph; the dispersion varied from about 4 A/mm at λ2100 to 35 A/mm at λ4000. A smaller quartz spectrograph was used to examine the region below λ2100. For the visible and near infra-red a

[11] This was in spite of the fact that the BCl_3 vapor was allowed to pass through a greased stopcock (the grease was slowly attacked).

Hilger glass spectrograph was used, with a dispersion varying from about 12 A/mm at λ4000 to 100 A/mm at λ6500. For the extreme red and infra-red, dicyanin-stained plates were used, and by exposures of a number of hours the bands were followed to λ8500. For some of the very strong a bands in the visible, brief exposures were sufficient, but for many weaker bands, especially those in the ultraviolet β system, exposures up to several hours were used. In order to render the measurements precise, the best possible focus and a very narrow slit were used, as well as fine-grained plates. The comparison spectra used were the iron arc for most of the ultraviolet, the copper arc at the extreme ultraviolet end, and helium, neon, and argon lines for the infra-red and visible. The correctness of the placing of the comparison lines was checked by measurements on two or more plates. Every effort was made to get as precise data as possible with the instruments used. For this reason and because of internal consistency, it is believed that the results are on the whole more precise than those of Jevons, at least in the ultraviolet. The dispersion used was somewhat less favorable, especially in the visible. Particular care was taken in the identification of the heads, which in some cases are easy to confuse with structure lines. In several cases apparent errors in Jevons' data were corrected; in cases of disagreement special care was taken to check the result. In connection with a study of intensity distribution among the bands, it was attempted to determine definitely the presence or absence of all possible bands.

The results of the measurements are recorded in Tables I and II. From the figures in the J-M column it will be noted that, apart from occasional differences, there is a systematic displacement of 1 to 5 (mostly 2 to 3) wave-number units toward the red in the present data as compared with Jevons'. In the a system, the magnitude of this difference is about inversely proportional to the dispersion. The measurement of band-heads is notoriously uncertain, and the systematic displacement is in all probability due to a difference in method of setting on the heads.[12] In the present measurements, the setting was made on the most intense part of the head, thus treating the latter as if it were a single line. If Jevons' settings were made on the *edge* of each head, which is toward higher frequencies, the difference would be explained. Of course neither procedure is theoretically correct, and the true position of the head should lie between the two, since the true wave-number of the head should be that

[12] That it is not due to displaced comparisons in either Jevons' or the writer's measurements is fairly well shown by its consistency throughout the spectrum, for measurements on several plates. It is certainly not due to displaced comparisons in the present measurements.

of the center of the line of highest frequency (since all the bands are shaded toward the red) in the band, as revealed under high dispersion. Under low dispersion, this blends with neighboring lines, so that the *intensity maximum* would be too far toward the red, by an amount which should vary somewhat with the intensity and dispersion, while the *high-frequency edge* of the blend must obviously be too far in the other direction, by an amount obviously depending on the intensity and the dispersion.

The present very complete measurements on the BO heads are suited for a quantitative test of the vibrational isotope effect. The small more or less constant error presumably present due to the necessary inaccuracy of the settings on the heads should not appreciably affect the determination of the coefficients. Measurements on origins would of course have been preferable, but in view of the difficulty in locating these, involving the use of much higher dispersion and correspondingly reduced intensity, this was impracticable. A detailed analysis of some of the strongest bands, with the use of higher dispersion, is contemplated in the near future.

TABLE I

Bands of the β System

Vibr. quantum nos.		$B^{11}O$ heads					$B^{10}O$ heads				
n'	n''	Int.	λ(I. A)	Wave-no.	C-O	J-M	Int.	λ(I. A)	Wave-no.	C-O	J-M
5	0	00?	.....	[48975.3]	..		000?	.....	[49137.0]	..	
6	1	00?	.....	[48272.2]	..		000?	.....	[48410.5]	..	
4	0	1^+	.....	[47796.5]	..		0	.....	[47926.3]	..	
5	1	1	2121.80	47114.8	−1		0	2117.04	47220.8	0	
3	0	3	2145.37	46597.2	0	2	1	2140.93	46693.8	1	3
4	1	2	2176.32	45934.7	0	1	1^-	2172.80	46009.1	1	2
2	0	4	2202.97	45379.0	0	2	2	2199.92	45441.9	0	2
3	1	4	2234.65	44735.8	0	3	2	2232.55	44777.7	1	3
1	0	6	2264.76	44141.1	−1	3	4	2263.33	44169.0	0	2
2	1	3	2297.21	43517.7	0	(4)	1^+	2296.74	43526.6	0	(−5)
5	3	—	On $B^{10}O$	[43460.9]	−4		2	2299.98	43465.3	−1	2
3	2	6	2330.44	42897.0	1	5	1	2330.96	42887.6	1	
0	0	7	2331.33	42880.8	0	4	*2^+	2331.83	42871.5	3	
4	3	1?	2364.10	42286.6	−4	(−2)				1	
1	1	8	2364.54	42279.7	−1	(5)	*3^+	2365.97	42253.1	0	
2	2	10	2398.53	41679.6	0	4	*6	2401.00	41636.6	−1	
3	3	6	2433.34	41083.2	1	3	—	On (0,1)	[41023.1]	(3)	
0	1	+10	2437.10	41019.9	0	3	*5	2440.71	40959.2	0	
1	2	5	2472.00	40440.8	0		*2^+	2476.67	40364.6	−1	
5	5	2	2505.33	39903.0	0	1	—	Masked	[39809.3]	—	
2	3	6	2507.67	39865.5	0	3	*4	2513.61	39771.4	0	4
6	6	2^-	2542.40	39321.2	−4	(0)	—	Masked	[39208.5]	—	
3	4	7^+	2544.25	39292.5	1	3	—	On (0,2)	[39183.3]	(1)	
0	2	+9	2551.40	39182.4	0	4	6	2568.75	39069.8	0	0
4	5	4	2581.63	38723.6	1	0	*2?	2590.13	38596.7	3	
1	3	8	2588.01	38628.3	−1	2	4	2596.62	38500.1	−2	7
5	6	*2	2619.78	38159.9	0	−8	—	Masked	[38019.7]	—	
2	4	6	2625.64	38074.7	0	3	2^+	2635.43	37933.3	−2	−3

TABLE I—continued

Vibr. quant. nos.		$B^{11}O$ heads					$B^{10}O$ Heads				
n'	n''	Int.	λ(I. A)	Wave-no.	C-O	J-M	Int.	λ(I. A)	Wave-no.	C-O	J-M
3	5	4	2664.09	37525.2	1	2	—	On (0,3)	[37368.8]	(0)	
0	3	+8	2675.27	37368.4	0	1	4	2687.02	37204.9	0	2
4	6	4	2703.37	36979.9	2	1	*2	2715.71	36811.9	−2	
1	4	10	2713.81	36837.7	−1	3	5	2726.91	36660.7	−2	0
5	7	2	2743.42	36440.1	0	−1	*1	Masked	[36255.5]	—	
2	5	9	2753.38	36308.3	0	3	7	2767.86	36118.3	−1	2
6	8	*2?	2784.35	35904.5	−3				[34614.7]		
3	6	7	2793.87	35782.1	1	2	—	On (0,4)	[35579.6]	(2)	
0	4	+8	2809.90	35578.0	1	3	2	2826.86	35364.5	1	1
1	5	8	2850.56	35070.5	0	3	3	2878.97	34845.5	−1	2
5	8	*2+	2877.38	34743.7	0	0	—	Masked	[34516.4]	—	
2	6	10	2892.23	34565.3	0	4	7	2912.17	34328.6	0	2
6	9	*3?	2920.01	34236.5	−8				[34000.5]		
3	7	9	2934.90	34062.7	1	2	—	On (0,5)	[33815.8]	—	
0	5	+6	2956.56	33813.3	−1	3	1	2979.56	33552.2	−1	
4	8	6	2978.47	33564.5	1	2	2	3001.56	33306.4	1	
1	6	7	2999.67	33327.3	0	2	3	3024.22	33056.8	−1	1
2	7	9	3043.64	32845.9	0	2	5−	3069.93	32564.6	0	1
3	8	9	3088.63	32367.5	1	1	3	3116.70	32076.0	2	(−3)
0	6	*1?	3117.35	32069.3	0	4	*2?	3147.46	31762.5	1	−6
4	9	6+	3134.59	31892.8	1	4	3+	3164.33	31593.2	1	
1	7	4+	3162.79	31608.6	0	3	2	3194.62	31293.6	−1	(−16)
5	10	4	3181.34	31424.2	−2	1	—	Masked	[31114.8]	—	
2	8	7	3209.32	31150.3	0	3	4	3243.22	30824.7	2	(15)
6	11	*2?	3228.91	30961.3	−7		1?	3263.25	30635.5	−4	
3	9	9	3256.94	30694.8	1	5	4	3292.75	30361.1	3	(21)
4	10	8	3305.43	30244.6	1	(22)	4−	3343.06	29904.1	2	
5	11	5?	3354.62	29801.1	−4	(12)			[29451.8]		
2	9	*5	3391.22	29479.5	−1		1−	3434.09	29111.5	2	
3	10	6	3441.61	29047.9	0	(−8)	4	3485.97	28678.3	−2	
4	11	4+	3493.06	28620.0	0		—	Masked	[28242.9]	—	
3	11	1	3645.65	27422.1	1				[27013.8]		
4	12	—	Masked?	[27018.5]	—						

Notes for Table 1. The vibrational quantum numbers given should probably all be increased by ½ (see text), but this ½ is conveniently omitted in the table.—Bands not previously measured are indicated by blanks in the J-M column. This column gives in whole wave-number units differences between wave-numbers as measured by Jevons and by the writer. Parentheses around values in this column indicate doubt as to whether the head measured by Jevons was the same as that measured by the writer, or indicate bands probably measured but not identified by Jevons.—The calculated values used for the column C-O (calculated minus observed) were obtained from Eq. (2).—Wave-numbers in brackets are calculated values inserted where measurements were not obtained.—A+? following an intensity value indicates doubt as to the *identity* of the measured head; this usually applies to weak heads among heavy structure lines. A++ preceding an intensity value indicates that the intensity given really applies to two superposed heads. Heads marked "masked" were heavily concealed by structure lines from a preceding head, so that they could not be measured, although in some cases they were identified. Heads marked "On (−,−)" were so close to a head (−,−) that the two were not distinguishable.—Heads not recorded in the table are definitely absent or exceedingly weak.—Additional unidentified heads (or lines), all of intensity 2, were found at ν=33,051.1, 33,003.5, 29891.1, and 28,944.9.

* The head in question is superposed on a structure line so that its estimated intensity is too high and its measured position may be slightly more in error than usual.

TABLE II

Bands of the α System

Vibr. quant. nos. v' v''	Head	$B^{11}O$ heads					$B^{10}O$ heads				
		Int.	λ(I. A)	Wave-no.	C-O	J-M	Int.	λ(I. A)	Wave-no.	C-O	J-M
8 0	A_1		(Possibly	[32966]	—						
	A_2		present)	[32953]	—						
	B_1			[32840]	—						
	B_2			[32827]	—						
7 0	A_1	1	3136.1	31878	0			Faintly			
	A_2	2	3137.0	31869	−4			visible			
	B_1	•2	3148.6	31751	0						
	B_2	•2	3149.7	31740	−2						
8 1	A_1	—	Masked	[31105]	—						
	A_2	—	by NO	[31092]	—			Masked			
	B_1	1?	3226.6	30983	−4			by NO_β			
	B_2	•2?	3227.8	30972	−7						
6 0	A_1	2+	3249.4	30766.	1		—	Masked	[30944]	—	
	A_2	2	3250.6	30755	−1		—	by (8,1)	[30931]	—	
	B_1	2+	3262.8	30640	1		•2?	3244.4	30813	5	
	B_2	2−	3264.2	30627	1		•2	3245.6	30802	3	
7 1	A_1	1	3330.2	30019	−3			Very			
	A_2	2	3331.8	30006	−3			faint			
	B_1	2+	3344.5	29891	−2			or in-			
	B_2	3	3346.2	29876	0			visible			
5 0	A_1	2	3373.2	29637	−1	4	—	Masked	[29788]	—	
	A_2	5	3374.7	29624	−1	4	—	by (5,11)$_\beta$	[29774]	—	
	B_1	7	3387.6	29510	−1	(13)	3?	3370.5	29660	1	(12)
	B_2	5	3389.1	29498	−1	(13)	•2?	3372.1	29647	1	
6 1	A_1	1	3458.9	28903	3		—	Masked	[29030]	—	
	A_2	2	3460.5	28889	3	(−3)	—	by (5,0)	[29017]	—	
	B_1	2	3473.8	28779	1		—	and (3,10)$_\beta$	[28904]	—	
	B_2	3	3475.3	28766	0	(−6)	—	etc.	[28891]	—	
4 0	A_1	5	3510.0	28482	2	3	1−	3494.7	28607	0	
	A_2	6	3511.3	28472	−1	−1	2	3495.9	28596	−2	(0)
	B_1	7	3525.5	28356	1	(12)	—	Masked	[28481]	—	
	B_2	7	3526.8	28346	−2	(8)	—	by $B^{11}O$, A	[28468]	—	
5 1	A_1	1−	3599.6	27773	1			Weak,			
	A_2	1	3601.3	27760	1			masked			
	B_1	1	3615.8	27648	0			by NO_β			
	B_2	1+	3617.2	27638	−3			and (4,0)			
3 0	A_1	5	3660.8	27309	1	5	1	3648.2	27403	0	
	A_2	6	3662.3	27297	−1	2	2	3649.7	27392	−1	
	B_1	8	3677.8	27182	1	4	5	3664.9	27278	−1	
	B_2	10	3679.1	27173	−2		5	3666.6	27265	−1	
6 2		Weak, masked by (3,0), or absent									
4 1		Very weak, masked by (3,0), absent									
2 0	A_1	6?	3828.3	26114	1		1+	3819.4	26175	2	
	A_2	8	3830.2	26101	0		3	3821.2	26163	1	
	B_1	9	3847.0	25987	2	1	3	3837.5	26051	−1	
	B_2	10	3848.7	25976	0	1	—	Masked	[26037]	—	

TABLE II—continued

Vibr. quant. nos. n'	n''	Head	$B^{11}O$ heads Int.	λ(I. A)	Wave-no.	C-O	J-M	$B^{10}O$ heads Int.	λ(I. A)	Wave-no.	C-O	J-M
5	2		Weak, masked by (2,0), or absent									
3	1	A_1	1?	3928.4	25448	0						
		A_2	2?	3930.3	25436	−1			Masked			
		B_1	3	3948.3	25320	2			by (2,0)			
		B_2	4	3950.5	25306	3						
6	3	A_1	*2?	3959.1	25251	2						
		A_2	*2?	3960.8	25240	−1			Masked			
		B_1	2	3979.5	25122	5						
		B_2	*3	3981.9	25106	7						
1	0	A_1	5	4015.1	24899	0	3	1	4010.5	24927	−1	
		A_2	6	4017.1	24887	−1	2	1	4012.8	24913	−1	
		B_1	7	4035.5	24773	−1	3	*3+	4031.4	24798	2	
		B_2	8	4037.4	24761	−2	3	3−	4033.3	24787	0	
4	2	A_1	1?	4033.9	24783	1						
		A_2	—	Masked	[24770]	—			Masked			
		B_1	*3?	4054.7	24656	2			by (1,0)			
		B_2	*2?	4057.0	24642	2						
2	1	A_1	2	4121.9	24254	0	2	1	4120.6	24262	0	
		A_2	4	4124.1	24241	−1	3	2	4122.9	24248	1	
		B_1	6	4143.4	24128	−1	2	*1?	4141.9	24137	−1	
		B_2	7	4145.5	24116	−2	2	2?	4144.2	24123	−1	
5	3		Very weak, masked by (2,1), or absent									
0	0	A_1	2	4225.0	23662	0	2	1−	4226.3	23655	−3	
		A_2	4	4227.5	23648	0	2	*3?	4229.3	23638	1	
		B_1	4?	4247.9	23534	1	(9)	*5?	4249.4	23526	0	(3)
		B_2	5?	4250.4	23521	1	(8)	4?	4251.9	23512	1	
3	2	A_1	*3	4234.4	23609	1						
		A_2	2	4236.5	23598	−1			Masked			
		B_1	*4?	4257.4	23482	2			by (0,0)			
		B_2	*4?	4259.5	23470	0			and by $B^{11}O$,(3,2)			
1	1	A_1	8	4339.6	23037	0	4					
		A_2	8	4342.0	23024	0	4		Masked			
		B_1	10	4363.4	22911	0	9		by $B^{11}O$			
		B_2	8	4365.9	22898	0						
4	3		Very weak, masked by (1,1), or absent									
2	2		Apparently absent									
5	4	A_1	1−	4476.7	22331	−1		—	Obviously			
		A_2	1−	4479.2	22319	−2		—	present,			
		B_1	2+	4502.3	22205	−1		—	but			
		B_2	2+	4504.7	22193	−2		—	masked by $B^{11}O$			
0	1	A_1	7	4586.0	21799	1	3	*2	4600.0	21733	5	
		A_2	8	4588.8	21786	1	3	*5	4602.0	21724	1	
		B_1	10+	4612.7	21673	0	4	*7	4626.0	21611	0	
		B_2	10+	4615.4	21661	0	2	*5	4627.9	21602	−4	

TABLE II—continued

Vibr. quant. nos. n'	n''	Head	$B^{11}O$ heads Int.	λ(I. A)	Wave-no.	C-O	J-M	$B^{10}O$ heads Int.	λ(I. A)	Wave-no.	C-O	J-M
3	3		Very weak, masked by (0,1), or absent									
1	2	A_1	5	4715.6	21200	−1	2	–	Masked	[21121]	–	
		A_2	5	4718.7	21186	−1	3	5?	4736.8	21105	3	
		B_1	8	4744.0	21074	−1	4	5?	4761.7	20995	0	
		B_2	8	4746.9	21060	−1	4	5?	4765.0	20980	−1	
2	3	A_1	1^-	4852.8	20601	0		–	Masked	[20506]	–	
		A_2	1^+	4855.7	20589	−2	2	–	"	[20493]	–	
		B_1	2	4882.9	20474	0		•2	4904.8	20382	−3	
		B_2	3	4885.7	20462	−1	2	1^+	4909.1	20364	2	
0	2	A_1	2	5008.0	19962	0	3	–		[19848]		
		A_2	4^-	5011.6	19948	0	3	–	Masked	[19834]		
		B_1	•9	5040.1	19835	0	4	–	by $B^{11}O$	[19722]		
		B_2	6	5043.5	19822	0	4	–		[19708]		
1	3	A_1	0?	5158.8	19379	5						
		A_2	0?	5161.1	19370	1						
		B_1	2^-?	5189.3	19265	−7						
		B_2	1?	5195.5	19242	3						
4	5		Possibly very weakly present									
2	4	A_1	0	5315.1	18809	0	5	–	Masked	[18665]	–	
		A_2	1	5319.0	18795	0	6	–	by $B^{11}O$	[18651]	–	
		B_1	2^+	5351.1	18683	0	5	1	5393.2	18537	2	
		B_2	3	5354.6	18670	−1	6	1	5397.1	18523	2	
3	5	A_1	1^-	5481.1	18240	−2						
		A_2	1	5485.6	18224	−4			Masked			
		B_1		Masked	[18110]	–			by (0,3)			
		B_2		by (0,3)	[18096]	–						
0	3	A_1	3	5508.8	18148	−1	4	–	Masked	[17982]	–	
		A_2	5	5513.0	18134	0	4	–	by $B^{11}O$	[17968]	–	
		B_1	7	5547.5	18021	0	5	3	5599.0	17856	0	
		B_2	8	5551.5	18008	−1	5	5	5603.7	17840	2	
1	4	A_1	2^-	5681.9	17595	−2	3	–	Masked	[17414]	–	
		A_2	2^-	5687.1	17579	1	5	–	by $B^{11}O$	[17401]	–	
		B_1	3^-	5723.1	17468	−2	5	2	5781.6	17291	−3	
		B_2	3^-	5727.4	17455	−2	6	2	5787.6	17274	1	
2	5	A_1	00?	5866.5	17041	0			Masked			
		A_2	0	5872.2	17025	3			by N_2			
		B_1	0	5910.9	16916	−1						
		B_2	0	5916.0	16898	4						
3	6	A_1	00	6062.1	16491	0						
		A_2	0	6067.5	16477	1			Masked			
		B_1	0	6107.6	16368	−4			by (0,4)			
		B_2	– On (0,4)A_1		[16352]	–						

TABLE II—continued

Vibr. quant. nos. n'	n''	Head	$B^{11}O$ heads Int.	λ(I. A)	Wave-no.	C-O	J-M	$B^{10}O$ heads Int.	λ(I. A)	Wave-no.	C-O	J-M
0	4	A_1	3	6113.1	16354	2	7	—	Masked	[16140]	—	
		A_2	3	6118.2	16340	2	6	—	by $B^{11}O$	[16127]	—	
		B_1	5	6159.7	16230	−1	5	2	6242.2	16016	−2	
		B_2	5	6165.4	16215	1	5	2	6248.2	16000	1	
1	5	A_1	2	6317.1	15826	−1	3	1	6409.4	15598	−1	
		A_2	3	6323.5	15810	2	5	1	6414.1	15586	−2	
		B_1	5	6368.5	15698	1	8	2	6460.3	15475	−4	
		B_2	5	6374.8	15682	3	8	2	6467.2	15458	−1	
2	6	A_1	00	6538.0	15291	5			Very			
		A_2	00	6543.0	15279	4			weak,			
		B_1	0	6590.0	15170	0			masked			
		B_2	0	6596.3	15156	1			by N_2, etc.			
0	5	A_1	0	6854.2	14586	2		0	6977.6	14328	−4	
		A_2	1	6861.8	14569	5		0	6986.2	14310	0	
		B_1	2	6913.5	14460	−1		1	7041.4	14198	−1	
		B_2	3	6921.5	14444	4		1	7049.2	14182	2	
1	6	A_1	0	7098.9	14083	−3		00	7240.7	13807	−2	
		A_2	1	7108.0	14065	2		00	7251.0	13788	−4	
		B_1	1	7163.6	13956	−2		0	7307.8	13680	−2	
		B_2	2	7173.2	13937	4		1	7316.8	13663	2	
2	7	A_1	00	7362.3	13579	−4						
		A_2	0	7373.8	13558	4		00	7528	13281	0	
		B_1	0	7434.8	13446	2						
		B_2	1?	7441.8	13434	1		00?	7600	13154	−1	
0	6	A	00	7790	12833	3		000?	7977	12532	−8	
		B	0	7870	12703	6		—		[12398]		
1	7	A	00	8093	12353	−1		000?	8319	12017	12	
		B	0	8174	12230	−5		—		[11904]		
2	8	A	000	8419	11875	−3		—		[11532]	—	
		B	000	8519	11735	11		—		[11406]	—	

Notes:—The notes of Table I in general apply here. The calculated values for the C-O column are from Eq. (1).—The masking of heads by structure lines from a preceding strong head is much more frequent in the α than in the β system; there is also some interference near the long wave-length end by N_2 1st positive bands (α bands of active nitrogen).—The recorded intensities here lack much in value because of the varying sensitivity of the plates used to cover the range. The estimated intensities of the bands in the infra-red are probably relatively too low; and a considerable extension of the α system into the infra-red, very likely to the (2,10) bands near λ 12000, might be expected if the plate sensitivity could be maintained.

QUANTITATIVE CONFIRMATION OF VIBRATIONAL ISOTOPE EFFECT

The following equations represent within experimental error the measured positions of all the heads in Tables I and II, assuming, as is customary, that the minimum values of n' and n'' are zero.

$$\begin{aligned}
&B^{10}O{:}\nu_a = \begin{Bmatrix} 23{,}652.2; 23{,}638.9; \\ 23{,}526.0; 23{,}512.7 \end{Bmatrix} +1285.6n' -11.7n'^2 \quad -1926.8n'' +12.21n''^2 \\
&B^{11}O{:}\nu_a = \begin{Bmatrix} 23{,}661.6; 23{,}648.3; \\ 23{,}535.4; 23{,}522.1 \end{Bmatrix} +1247.9n' -10.6n'^2 \quad -1873.2n'' +11.68n''^2 \\
&\text{Ratio: (difference} = -9.4) \quad 1.0302 \qquad 1.104 \qquad 1.0286 \qquad 1.045
\end{aligned} \tag{1}$$

$$\begin{aligned}
&B^{10}O{:}\nu_\beta = 42{,}874.6 - 0.19n'n'' \quad +1304.6n' -10.43n'^2 \quad -1927.9n'' +12.66n''^2 \\
&B^{11}O{:}\nu_\beta = 42{,}880.9 - 0.17n'n'' \quad +1268.8n' -9.98n'^2 \quad 1872.9n'' \quad +11.84n''^2 \\
&\text{Ratio: (difference} = -6.3) \quad 1.0282 \qquad 1.045 \qquad 1.0294 \qquad 1.069
\end{aligned} \tag{2}$$

These were obtained independently for the α and β systems of each isotope.[13,14] In determining the coefficients of n' and n'' for the α system of each isotope, the average measured wave-number for the four α heads was used. This was justifiable, since the mutual separations of the four heads appear to be constant within experimental error. This latter conclusion was also reached by Jevons, although the measured separations here obtained differ slightly from his results. The intervals between the four heads are the same within experimental error for both isotopes. This is to be expected since the four heads are presumably due to a multiple electronic level [(I) p. 123], and since no appreciable electronic isotope effect, and certainly no differential effect between the different sub-levels, is to be expected [(I) p. 124].

The $n'n''$ terms of Eq. (2) arise from the fact that the measurements are on heads instead of on band-origins, and are due to the variation with n' and n'' of the distance from origin to head. All the other coefficients, as well as the constant term, also necessarily contain relatively small contributions from this source [cf. (1), Eqs. (20), (20′) of ref. 29, and (21)]. Except for these small contributions, the ratios for the two isotopes of corresponding coefficients of n' and of n'' should give experimental values of ρ, and the ratios for the coefficients of n'^2 and n''^2 should give experimental values of ρ^2 [see (I), Eq. following (13)]. The experimental ratios are given above in connection with Eqs. (1) and (2). It is possible to state, from an approximate determination of the magnitudes of the small head contributions (see later section), that these produce an error of not

[13] Applying the combination principle, the energy term was determined for each vibrational level. This unexpectedly revealed the $n'n''$ terms of Eq. (2). It would also reveal any irregularities (perturbations) in the spacing of the energy levels, but none was found within experimental error.

[14] Eq. (2) was formulated without attaching much weight to the data for $n'=6$, for which the identity of the heads was uncertain. A positive cubic term would, however, make possible a considerable improvement in the difference "calc.−obs." for the $n'=6$ bands, and a decided improvement for the $n'=5$ bands, and should probably be included.

more than 1 unit in the last figure in these ratios as given above. Hence the latter may be accepted as correct within experimental error. The question of the constant terms will be discussed later.

Attention may conveniently be drawn at this point to the very close agreement of the coefficients of n'' and n''^2 in the α and β systems; the less good agreement for $B^{10}O$ than for $B^{11}O$ may be ascribed to the relative lack of reliable data, especially in the α system, due to masking of $B^{10}O$ heads by strong $B^{11}O$ structure lines. The agreement for $B^{11}O$ is such as to show practically without question that the α and β systems have their final state in common. This is confirmed (see below) by the existence of a combination system.

From Eqs. (1) and (2) the weighted mean values of the ratios are 1.0291 ± 0.0003 for ρ and 1.062 ± 0.008 for ρ^2.[15] Comparing these with the theoretical values $\rho = 1.0292$ and $\rho^2 = 1.0593$ for BO, $\rho = 1.0276$ and $\rho^2 = 1.0560$ for BN, it will be seen that the experimental result for ρ is in extremely good agreement for BO, and in disagreement for BN by an amount far beyond the probable error in the experimental value. The comparison is also favorable to BO in the case of the mean quadratic term ratio, although this result is not at all decisive.

In the preceding it has been tacitly assumed that the choice lay only between BO and BN. The arguments used above in favor of BO against BN also apply against any other diatomic boron compound; in addition the direct evidence (see below) definitely excludes any compound other than an oxide or nitride. The diatomic character of the emitter is attested, according to the quantum theory of band spectra, by the simple structure of the α and β systems and bands. The familiar diffuse and ordinarily apparently headless boric oxide bands in the visible are, however, probably due to a complex emitter, which may be assumed, as apparently in the past, to be B_2O_3.

Although the above theoretical evidence in favor of BO is extremely definite and convincing, it is of course necessary to establish the absence of contradictory evidence of a more directly experimental nature.

Chemical Evidence as to the Identity of the Emitter of the Bands

The BO bands were originally ascribed by Jevons to a nitride of boron, presumably the well-known stable white compound BN. This was a natural supposition, since the bands are developed in active nitrogen, and since, according to Jevons, the (white) product deposited on the walls of the

[15] The ratios for the coefficients of n' (α), n' (β), n'' (α), and n'' (β), were given the respective weights 2, 3, 4, and 6, in accordance with the writer's judgment of their relative reliabilities. The *unweighted* means are $\rho = 1.0291 \pm 0.0004$; $\rho^2 = 1.065 \pm 0.010$.

afterglow tube contains combined nitrogen. Again, when $(CH_3)_3BO_3$ was substituted for BCl_3 the bands were developed as before, indicating that *chlorine* was not required for their production. Also they were ***not*** obtained in the uncondensed discharge through pure BCl_3, indicating the necessity of *some* other element than boron. Jevons concluded that boron and nitrogen alone were necessary. The writer at first accepted this conclusion.[3]

Before considering the experimental evidence for BO, it will be desirable to consider the occurrence of the BO and B_2O_3 bands in various sources. Jevons[4] found the BO bands in the B_2O_3 arc in air; also in the boron arc in air, oxygen, and nitrogen, but weaker in oxygen. This last result appeared to support the nitride origin of the bands, but was admittedly inconclusive, since neither the oxygen nor the nitrogen was entirely pure. Kayser and Konen point out (Handbuch der Spektroscopie, vol. VII, section on boron) that Exner and Haschek had previously obtained the stronger of the β bands in the arc, and Hagenbach and Konen a number of the α bands in the arc, and indications of them in the spark. Apparently these, as well as certain bands obtained by Plücker, Ciamician, and others (see Kayser and Konen, vols. V and VII on boron) by the discharge through BF_3, and some others measured by Kühne, were formerly referred to collectively without distinction as the "boron bands," in contradistinction to the boric oxide bands. The *latter* are particularly prominent in the flame, and also occur in the arc in air, and in the spark under proper conditions. The BO bands are absent in the flame, according to Jevons and others. Probably thermal dissociation of B_2O_3 to yield BO occurs in the arc, but not in the flame. Jevons failed to find the BO bands in the spark in an atmosphere either of oxygen or of nitrogen.

The intensity of the BO bands in relation to the oxygen content of the nitrogen used in generating them by its reaction with BCl_3, gave the first piece of direct experimental evidence in favor of BO as their emitter. In the present work, a cylinder of commercial nitrogen, stated to be 99.6 per cent pure, was first used. This was purified by contact with wet phosphorus, according to the method used by Jevons,[4] and then passed through calcium chloride, soda lime, and phosphorus pentoxide. Under these conditions, the BO bands showed a very pronounced maximum of intensity for a purification period of about 45 minutes. Spectroscopic and visual observations on the afterglow showed that the α and β bands *of active nitrogen* were present in more or less equal intensity at this stage. When the purification period was greatly reduced, the nitrogen α bands became much weaker, the β bands much stronger; when it was increased

to several hours (or days) the α bands became considerably stronger, the β bands much weaker.

Now E. P. Lewis,[16] and also Rayleigh,[17] have shown that the β (and γ) bands of active nitrogen require the presence of oxygen. Rayleigh collected much evidence on the occurrence of these bands in various sources; this evidence points very strongly to NO as their emitter. Lewis had also previously obtained strong evidence of the NO origin of the γ bands, and thought that the β bands might also be due to NO. Recent work indicates[18] that the β and γ bands probably have a common final state, so that there is little doubt that both are due to NO, especially since the structural simplicity of both systems indicates a diatomic emitter in each case. The α bands, however, are due to N_2.

Jevons has suggested,[19] in criticizing the writer's conclusions as to the origin of the BO bands, that the favorable influence of oxygen on their intensity might be due to its known effect (cf. papers by E. P. Lewis, and by Rayleigh and Fowler) in promoting the formation of active nitrogen. The above account evidently disproves this, since, beginning at a stage of purification where the BO bands are at their strongest, the *removal* of oxygen actually increases the yield of active *nitrogen*, as measured by the intensity of its α bands, while greatly decreasing the intensity of the NO and the BO bands. If a stage was reached where there was a lack of oxygen for the catalysis of the formation of active nitrogen, it is probable that the phosphorus vapor which was present fulfilled the same function.

In later experiments with a cylinder of nitrogen stated to be 99.7 per cent pure, but evidently much purer than the first, the oxygen content was already too small for the best results with BO, even when the phosphorus treatment was omitted. In fact, the intensity of the BO bands was markedly increased when a small amount of air was admitted. The behavior of $SiCl_4$ with this nitrogen was in striking contrast to that of BCl_3. Although too pure for maximum BO intensity, it was by far too impure to permit more than a faint indication of the purple glow of the SiN bands. The SiN bands[3] did not reach full intensity until the nitrogen had been purified as far as possible (at least 2 hours). Apparently oxygen destroys or inhibits the formation of SiN.

[16] E. P. Lewis, Astrophys. J. **20,** 49 and 58 (1904); Phil. Mag. **25,** 826 (1913)

[17] Rayleigh, Proc. Roy. Soc. A **93,** 254 (1917). Rayleigh found one objection which seemed to him to make it impossible to ascribe the bands to NO or any oxide of nitrogen. This objection, however, hardly seems vital in the light of present knowledge.

[18] R. T. Birge, Nature, Nov. 1, 1924. The writer had also tentatively reached the same conclusions.

[19] W. Jevons, Nature, May 24 and May 31, 1924; Proc. Roy Soc. A **106,** 174 (1924)

The simultaneous presence, when the BO bands are at their strongest, of active nitrogen and of active[20] or excited NO may be accounted for by a pair of reactions such as the following (the prime denotes an electronically excited molecule):

(A) $BCl_3+N_2' \rightarrow BN$ (or BN')$+NCl_3$; (B) $BN+NO' \rightarrow BO'+N_2$. (3)

Or possibly,

(a) $BCl_3+NO' \rightarrow BO+NCl_3$; (b) $BO+N_2' \rightarrow BO'+N_2$. (3′)

Both pairs of reactions assume that NO′ has not enough energy to form BO′ from BCl_3 in one step. However, the high intensity of the BO bands favors a one-stage reaction, and it may be that the presence of N_2' is not essential. Reaction (A), whether or not involved in the formation of BO′, would account for the presence of nitride nitrogen observed by Jevons in the reaction-product; BN, although thus probably present, apparently does not emit a spectrum. The conclusion recently expressed by Birge[21] that active nitrogen consists of metastable excited nitrogen molecules in the state necessary for the emission of the α bands,[22] affords the simplest explanation of the behavior of active nitrogen in producing chemical reactions and exciting spectra. Its action would thus be analogous to that of excited mercury atoms in the work of Franck and Cario.[23]

The exact mechanism of formation of BO′, although of much interest in itself, is not essential to the present argument, but the above analysis shows that the oxide origin of the bands is reasonable and probable. If the bands were due to BN, the unlikely assumption would be needed that N'_2, although alone capable of producing the SiN bands, is much less effective than NO′ in producing the BN bands.

Noting that the BO′ molecules are formed in a medium consisting largely of inert unexcited nitrogen molecules, with a small proportion of NO and NO′ and doubtless O_2 and other molecules, it is not surprising that the BO spectrum is strong and that of B_2O_3 negligibly weak

[20] Evidence for the existence of active, that is metastable, excited NO is to be found in observations of Lord Rayleigh[17] and of the writer that the bluish glow of the β bands shows an even greater persistence than the yellow glow of the α bands. The fact that in impure active nitrogen the β bands may appear without the α bands also indicates an independent metastable existence.

[21] R. T. Birge, Phys. Rev. **23,** 295 (1924); Nature, Nov. 1, 1924; cf. also M. N. Saha and N. K. Sur, Phil. Mag. **48,** 421 (1924).

[22] The emitting state of active nitrogen can, however, hardly be identical with the metastable state. Presumably the transfer from the latter to the former is accomplished in collisions with other molecules.

[23] Franck and Cario, Zeit. für Physik **9,** 259; **10,** 185; **11,** 161 (1922); **17,** 202 (1923). This suggestion has been made independently by Birge (unpublished), by the writer (Nature, Sept. 6, 1924; also indicated in connection with the Cu halides in Phys. Rev. **23,** 767, 1924), and by Saha and Sur.[21]

or absent. A BO molecule would have to make a very large total number of encounters with other molecules before a molecule of B_2O_3 could result. In order to give the B_2O_3 spectrum, this molecule might also have to make a favorable encounter with an excited N_2 or NO molecule.

Jevons recently brought forward evidence which he considered irreconcilable with the oxide origin of the BO bands. In experiments with the uncondensed discharge through mixtures of oxygen with various chlorides ($TiCl_4$, $SiCl_4$, CCl_4) he uniformly obtained oxide bands. With BCl_3 he obtained the B_2O_3 bands—each of which now showed a series of heads—but not the BO bands. The writer has confirmed this result for the visible region, observing incidentally that the B_2O_3 bands are best brought out with a great excess (80:1 was used) of O_2 over BCl_3 molecules. Although these results do not help the cause of BO, they are after all not wholly surprising. If B_2O_3 and BO molecules are equally easily excited by the discharge, it is necessary only that the number of BO molecules present at any moment shall be negligible compared with the number of B_2O_3 molecules. This may well be the case, in an atmosphere consisting of oxygen atoms and molecules, in view of the chemically highly unsaturated character which BO must have.

Photographs of a carbon arc whose anode contained in various experiments BN, B_6C, or B_2O_3, gave very strong evidence against BN and in favor of BO. The arc was run in a Pyrex bulb which could be evacuated and filled with gas as desired. In the case of all three compounds, the BO β bands always appeared, in moderate intensity, when an atmosphere of air, or oxygen (about 99.7 per cent pure, the rest N_2) was used; but under like conditions, as gauged by the intensity of the boron doublets at $\lambda 2497$ and $\lambda 2089$, in pure nitrogen (phosphorus-treated) and in nearly pure nitrogen (containing a little oxygen), they were completely absent. The α bands, and with them the B_2O_3 bands, were similarly present with air or oxygen, but disappeared when nitrogen was used.

HALF-INTEGRAL VIBRATIONAL QUANTUM NUMBERS

In Eq. (1) there is a difference of unexpected magnitude between the constant terms for the α systems of $B^{10}O$ and $B^{11}O$, and similarly in Eq. (2) for the β systems. According to the theory, these constant terms are "electronic" (ν' terms) except for a small "rotational" contribution due to the use of data on heads. When approximate allowance is made, on the basis of a study of band structure (see below) for the latter, the differences of Eqs. (1) and (2) are slightly *increased* in magnitude, to (-10.1) and (-7.2), respectively. According to the quantum theory of band

spectra as hitherto accepted, these corrected differences should represent *purely electronic* isotope effects. According to the Bohr theory, applicable to an atom with one electron [(I) Eq. (9)], differences of -0.12 and -0.21, respectively, might be expected.[24] The much larger results here observed are absolutely out of harmony with considerations previously presented [(I) pp. 124-5]. Hence any alternative explanation that does not do violence to the theory is greatly to be preferred.

If, in formulating Eqs. (1) and (2), we had assumed the minimum values of n' and n'' to be $1/2$, instead of 0, the linear term coefficients and the constant terms would obviously be somewhat different. The transformation can be effected by replacing n' by $(n'-1/2)$ wherever n' appears in Eqs. (1) and (2), similarly replacing n'' by $(n''-1/2)$, and recasting in the original form of (1) and (2). It can easily be verified that such a transformation alters the corrected differences of corresponding constant terms for $B^{10}O$ and $B^{11}O$, from -10.1 to -2.3 for the α system, and from -7.2 to $+2.4$ for the β system. The electronic isotope effect thus becomes zero in both cases within an amount which can reasonably be attributed to the combined effect of errors in the determination of the constants and coefficients of Eqs. (1) and (2). This result cannot be accomplished by any other assignment of minimum values of n' and n'', if we restrict ourselves to the possibilities 0, $+1/2$, $+1$. Since half-integral values of n' and n'' with a minimum value $+1/2$ are by far more probable than a large electronic isotope effect or other serious failure in the theory, they may be quite definitely accepted—unless one wishes to entertain the possibility of fractional values other than $1/2$. It is hoped that later more accurate measurements will make the evidence more nearly quantitative.

It may be noted (cf. Eqs. (8) and (9) below) that the transformation to half quantum numbers alters the mean experimental value of ρ from 1.0291 to 1.0293. The new value is, however, in just as good agreement as before with the theoretical value 1.0292 for BO; and is slightly worse than before for BN. With very accurate data, the dependence of the experimental ρ on the absolute numbering would furnish an independent check on the latter, additional to that of the previous paragraph.

The existence of half vibrational quantum numbers is in line with recent work in line and band spectra.[25] Several investigators have re-

[24] No isotope effect has as yet been reported in the boron line spectrum. The doublets at λ 2497 and λ 2089 are obviously, from the relative intensity of their components, not of isotopic origin.

[25] The work of Sommerfeld and Landé on the structure and Zeeman effect of multiplets may be cited. A. M. Mosharaffa (Proc. Roy. Soc. A **105**, 641, 1924) has also found half quantum numbers useful in the Stark effect.

cently shown that half-integral rotational quantum numbers are the rule rather than the exception in band spectra.[26] There is also evidence from specific heat data.[27] The situation in the BO molecule—and doubtless in many or perhaps most molecules—may parallel that assumed by Heisenberg in explaining the structure and Zeeman effect in doublets and triplets in line spectra. Thus, for example, in the normal state of the Na atom, the valence electron was assumed to have 1/2 quantum each of radial and of azimuthal motion.[28] Analogously in BO, the vibrational and rotational quantum numbers may both be half-integral, the sum of the two being integral. This would involve a null-point energy of 1/2 quantum each of vibration and rotation.[29]

Structure of BO Bands and Rotational Isotope Effect

Absence of negative branch. A preliminary account of salient features of the structure of the BO bands will be given here, but a more detailed analysis will be reserved until measurements can be made with higher dispersion photographs. All the BO bands are shaded toward the red, so that the head is always on what is presumably a positive branch, capable of representation by an equation of the form $\nu^{m} = A + Bm + Cm^2$, C here being negative; m is the rotational quantum number. There is no evidence of a null-line: this is probably very close to the head (see below). In only two of the β bands is more than one set of strong lines associated with each head; in the $(2\frac{1}{2} \rightarrow \frac{1}{2})$ and $(4\frac{1}{2} \rightarrow 1\frac{1}{2})$ bands additional lines of a presumably negative branch about 2/3 and 1/3 as intense, respectively, as those of the positive branch, are present. Weak negative branch lines also appear in the $(2\frac{1}{2} \rightarrow 2\frac{1}{2})$, $(1\frac{1}{2} \rightarrow 3\frac{1}{2})$, and $(3\frac{1}{2} \rightarrow 5\frac{1}{2})$ bands.[30] Similar peculiarities probably exist in the α system. Other cases of inequality of intensity of posi-

[26] A. Kratzer, Münch. Ber. p. 107 (1922); Ann. der Phys. **71**, 72 (1923); R. Frerichs, Zeit. f. Phys. **20**, 170 (1923); E. Hulthén, Ann. der Phys. **71**, 41 (1923); E. F. Barker, Astrophys. J. **58**, 201 (1923); W. F. Colby, Astrophys. J. **58**, 303 (1923); etc.

[27] R. C. Tolman (Phys. Rev. **22**, 470, 1923) has shown that the assumption of a null-point energy of 1/2 quantum fits the experimental data for the rotational specific heat of hydrogen just as well as the earlier assumption of a minimum of 1 quantum. The assumption of zero null-point energy definitely does *not* fit the facts. See F. Reiche, Ann. der Phys. **58**, 657 (1919); E. C. Kemble and J. H. Van Vleck, Phys. Rev. **21**, 653 (1923).

[28] W. Heisenberg, Zeit. f. Phys. **8**, 273 (1922)

[29] This may have a bearing on the question of the relative vapor pressures of isotopes; in this connection cf. Lindemann and Aston, Phil. Mag. (6) **37**, 523 (1919), and Lindemann, Phil. Mag. (6) **38**, 173 (1919).

[30] Probable faint traces are present in the $(3\frac{1}{2} \rightarrow \frac{1}{2})$, $(3\frac{1}{2} \rightarrow 5\frac{1}{2})$, $(3\frac{1}{2} \rightarrow 6\frac{1}{2})$, $(2\frac{1}{2} \rightarrow 6\frac{1}{2})$, and doubtful faint traces in the $(4\frac{1}{2} \rightarrow 6\frac{1}{2})$, $(1\frac{1}{2} \rightarrow 5\frac{1}{2})$, $(3\frac{1}{2} \rightarrow 7\frac{1}{2})$, $(2\frac{1}{2} \rightarrow 7\frac{1}{2})$, and $(3\frac{1}{2} \rightarrow 8\frac{1}{2})$ bands. Doubtless in a few additional cases negative branch lines are present which accidentally coincide, at the dispersion used, with the positive branch lines.

tive and negative branches are on record. The usual absence of more than one series of structure lines from each head is well shown in Plate I, especially in (*a*).

Confirmation of rotational isotope effect. Careful measurements were made for both isotopes of all possible lines in the ($\frac{1}{2}\rightarrow 3\frac{1}{2}$), ($2\frac{1}{2}\rightarrow 3\frac{1}{2}$), and ($2\frac{1}{2}\rightarrow 5\frac{1}{2}$) β bands. The lines begin to be resolved at about the fifth from the head, and can be followed to about the 40th from the head. By plotting the first differences between successive lines against successive integers, values of the coefficient C, presumably moderately accurate, were obtained from the average second differences. The results for all three bands (using the half-quantum vibrational numbering) may be expressed by the following pair of equations, the values of $B^{10}O$ being considerably less reliable than for $B^{11}O$.

$$B^{10}O: \quad C_\beta = C_0 - \alpha' n' + \alpha'' n'' = -0.2849 - 0.0204 n' + 0.0175 n''$$

$$B^{11}O: \quad C_\beta = C_0 - \alpha' n' + \alpha'' n'' = -0.2715 - 0.0206 n' + 0.0172 n'' \qquad (4)$$

Ratio of coefficents:				
	(theory)	1.059	1.090	1.090
	(experiment)	1.049	0.99	1.02

The ratios of corresponding coefficients for the two isotopes give an approximate confirmation of the theory [cf. (I), Eqs. (7A), (18), and ref. 28] for the constant part of C; for the coefficients α' and α'' the result is unsatisfactory; the disagreement, however, is probably in all three cases within the limits of experimental error.[31] Another approximate confirmation of the rotational isotope effect has been shown to exist in the case of CuH.[32]

Determination of coefficients of band structure. Assuming only that the lines measured belong to a series (presumably a positive branch) of substantially the usual form $\nu = B' + 2B'm + Cm^2$, where $B' = B_0' - \alpha' n'$, and $C = B' - B'' = C_0 - \alpha' n' + \alpha'' n''$, it is possible from the data of Eq. (4), together with the coefficient of $n'n''$ in Eq. (2), to determine B' and B''.[33] According to (I) ref. 29, Eq. (20′), the coefficient p of $n'n''$ should be equal to $p = [(2B_0'^2/C_0 - 2B_0' + (3B_0'^2/C_0^2 - 4B_0'/C_0)\alpha' n' - (3B_0'^2/C_0^2 - 2B_0'/C_0)\ \alpha'' n'' + \ldots\ldots)]\alpha'\alpha''/C_0^2$. The experimental p may be assumed to correspond to the average values $n' = 2\frac{1}{2}$, $n'' = 3\frac{1}{2}$. Inserting these values in the p equation together with the values of α', α'',

[31] The effect of higher power terms in m should cause an error of 0.001 or 0.002 in C; the relative error from this cause for the two isotopes should be completely negligible.

[32] R. S. Mulliken, Nature, April 5, 1924.

[33] It is *possible* (cf. A. Kratzer, Ann. der Phys. **71**, 72, 1923; Zeit. f. Phys. **23**, 298 1924) that the bands are of a type for which ν is of a somewhat different form.

and C_0 from Eq. (4), and putting $p=-0.17$ according to Eq. (2), one obtains for $B^{11}O$, by successive approximations, $B_0'=2.03$. Then[33] for $B^{11}O$,[34] with a probable error of perhaps 5 per cent,

$$B^{11}O:\ B_\beta'=2.03-0.021n' \text{ and } B_\beta''=B_\beta'-C_\beta=2.30-0.017n''. \quad (5)$$

It may be noted that α' and α'' have the usual sign, and that α', α'', C_0 and the B's, have entirely reasonable numerical values; thus, e.g., in the violet CN bands, $B'=1.96-0.022n'$; $B''=1.89-0.017n''$.

The values of Eq. (5), and corresponding values[34] for $B^{10}O$, can now be used to obtain approximate corrections so as to reduce Eq. (2) to the corresponding equation for a system of band origins, with the help of (I) ref. 29, Eq. (20′). It was in this way that the *corrected* differences, for the constant (ν^e) terms of Eqs. (1) and (2), used in the preceding section, were obtained. This procedure also shows that the heads of the various bands must be very near the origins, the calculated values of m_{head} being between 5 and 12 for most of the bands; it is then not surprising that it is at just about this number of lines from the head that the bands begin to be resolved.

Although no $n'n''$ terms were detected in the measurement of the α heads, use can be made of the fact that the α and β bands have a common final state. Then one may assume $B_\alpha''=2.30-0.017n''$ for $B^{11}O$. Measurements on some of the bands give, assuming the coefficient of n'' from the β system measurements,[35]

$$B^{11}O;\ C_\alpha=-0.38-0.014n'+0.017n'' \quad (6)$$

B_α' can now be calculated, and,

$$B^{11}O:\ B_\alpha'=1.92-0.01n';\ B_\alpha''=2.30-0.017n'' \quad (7)$$

From the data now available, it can be calculated that the coefficient of $n'n''$ for the α system should be -0.04: this small value is in agreement with the failure to detect the coefficient experimentally.

Equations for band origins. From the data now available, it is possible to obtain in place of (1) and (2) the following probably moderately accurate equations for the *origins* of the BO bands, using the half-quantum numbering;

[34] A separate calculation for $B^{10}O$ from the experimental values of p, α_1' α'', and C_0 would not be very reliable; the theoretical values are $B'=2.15-0.023n'$ and $B''=2.44-0.019n''$.

[35] It is possible that the values of B' and C differ appreciably for the four different α heads. Eq. (6) was determined from measurements on A_2 and B_2 structure lines; there was some indication of a systematic difference between the two, but an average was used for Eq. (6).

$$B^{10}O:\ \nu_\alpha = \left\{\begin{matrix}23{,}960.6;23{,}947.3\\23{,}834.4;23{,}821.1\end{matrix}\right\} + (1298.0n' - 11.7\ n'^2) - (1939.4n'' - 12.19n''^2) \tag{8}$$

$$B^{11}O:\ \nu_\alpha = \left\{\begin{matrix}23{,}962.9;23{,}949.6\\23{,}836.7;23{,}823.4\end{matrix}\right\} + (1259.1n' - 10.6\ n'^2) - (1885.2n'' - 11.66n''^2)$$

Ratio: (Diff. $= -2.3$) 1.0309 1.038 1.0288 1.045

$$B^{10}O:\ \nu_\beta' = 43{,}168.6 + (1316.7n' - 10.53n'^2) - (1941.5n'' - 12.58n''^2)$$
$$B^{11}O:\ \nu_\beta' = 43{,}166.2 + (1280.3n' - 10.07n'^2) - (1885.7n'' - 11.77n''^2) \tag{9}$$

Ratio: (Diff. $= +2.4$) 1.0284 1.046 1.0296 1.069

Each equation is in the form $\nu = \nu^e + \nu^n = (E'^e - E''^e)/h + (E'^n - E''^n)/h$, and so yields values of ν^e, E'^n, and E''^n.

Combination System Bands

In all the photographs of the α system of BO, the $(1\frac{1}{2} \rightarrow 3\frac{1}{2})$ band is obscured by a peculiar structure (see Plate II) which looks like a group of lines or band-heads, some of which appear distinctly shaded toward the violet. Similar peculiarities appear very markedly in the $(2\frac{1}{2} \rightarrow 3\frac{1}{2})$ band, (Plate II), and less prominently near the $(\frac{1}{2} \rightarrow 1\frac{1}{2})$ and $(\frac{1}{2} \rightarrow 3\frac{1}{2})$ bands and on the $(2\frac{1}{2} \rightarrow 5\frac{1}{2})$ band.

These extra lines or heads do not agree in position with any of the B_2O_3, the N_2, or the NO band-heads, nor have they been found in the spectrum of BCl_3.[36] It seemed possible that they might be due to transitions from β system initial states to α system initial states. The positions of the *origins* of such a combination system of bands should obviously be calculable from Eqs. (8) and (9). The result is:

$$B^{10}O:\ \nu = \nu^e + 1316.7n' - 10.53n'^2 - 1298.0n'' + 11.7n''^2 \tag{10}$$
$$B^{11}O:\ \nu = \nu^e + 1280.3n' - 10.07n'^2 - 1259.1n'' + 10.6n''^2$$

Here $\nu^e = 19,205.6$, 19218.9, 19331.8, and 19345.1, corresponding to the A_1, A_2, B_1, and B_2 α levels.[37] These equations might be expected to give results in error by a few wave-number units, on account of the uncertainties involved in the determination of the coefficients in Eqs. (1) and (2) for the α and β bands, and especially in the corrections subsequently applied in obtaining Eqs. (8) and (9).

From the previously estimated values of B_β' and B_α', one should have for the new bands, for $B^{11}O$, $B' = B_\beta' = 2.03 - 0.021n'$: $C = +0.11 -$

[36] Photographs of the B_2O_3 bands, and data on the bands produced by the discharge through BCl_3, are given by Jevons[19].

[37] The ν^e values directly calculated from Eqs. (8) and (9) are 2.3 less than here for $B^{11}O$ and 2.4 units more for $B^{10}O$. The use of the same mean value here for both isotopes is justified by the likelihood that the apparent discrepancy between the ν^e values of the two isotopes is due to errors in the determination of ν^e in the α and β systems. It may be noted that the directly calculated values give as good (or slightly better) agreement with the data of Table III as the mean values here used.

$0.021n'+0.014n''$. The positive value of C shows that the new bands, unlike the α and β bands, should be shaded toward the violet; the head should be on the negative (P) branch, and on account of the relatively small numerical value of C, at a considerable distance from the origin, -35 wave-number units, for example, in the case of the $\frac{1}{2}\rightarrow\frac{1}{2}$ band. No conspicuous heads were, however, found in the calculated positions. But it was found that practically all the unidentified lines or heads mentioned above could be explained by assuming each to correspond to the beginning of a Q branch. Such a Q branch would have its head at the band-origin, and, with a low value of C, a low-temperature source, and under moderate dispersion, as here, this head might not differ much in appearance from that of a P or R branch. The weakness of the first few lines should, however, cause an apparent small shift toward the violet, giving the appearance of a diffuse line or head shaded toward the violet, as observed. On this basis, assuming a shift of $+3$ units from the origins as calculated from Eq. (10), the agreement between observed and calculated wave-numbers is complete for the transitions $\beta\rightarrow\alpha(A_1)$ and $\beta\rightarrow\alpha(B_1)$, for both isotopes. There is, however, no definite evidence of transitions to the A_2 and B_2 α levels; such transitions, if present, must give less than one tenth the intensity of those to the A_1 and B_1 levels. The transition to B_1 shows greater intensity than that to A_1, except in the $\Delta n=0$ sequence, where the reverse is true. It is possible that R branches are present in the new bands, but escape observation because of the lack of a head. In no case were individual structure lines visible in the new bands, presumably because of insufficient intensity as compared with the background of relatively intense α system bands. All the bands of the new system are very weak as compared with like-numbered α and β bands. In one or two cases there is a suggestion of a P branch; e.g., on the low-frequency side of the B_1 head at 20,609 there is a shaded region beginning at about 20,572 and extending toward the violet (cf. Plate II). The usual absence of P branches in the combination bands may be correlated with their absence in the β (and α?) bands.

In spite of various peculiarities and irregularities noted above, the agreement recorded in Table III is so remarkable as to leave no reasonable doubt that the data really correspond to a system of bands involving a transition from β to α states of BO.[38] For instance, the arrangement of the new bands in sequences is of a very unusual character, entirely in accord with prediction, due to the near-equality of the coefficients of n'

[38] There is of course a possibility that the heads here observed correspond to transitions to some third pair of α levels A_3 and B_3; and the interpretation as Q branches *may* not be correct.

TABLE III

Bands of the Combination System

Vibr. Quant. Nos. n' n''		$B^{11}O$ Heads				$B^{10}O$ Heads			
		Int.	λ(I. A)	Wave-no.	C-O	Int.	λ(I. A)	Wave-no.	C-O
2 0	A_1		(Masked by 0,1a)	[21719]			Masked	[21789]	
	B_1	1^-(v)	4576.5	21845	1	*0^+	4561.5	21916	−1
3 1	A_1		Masked	[21702]			Masked	[21768]	
	B_1	1(v)	4580.8	21824	4	*1^-	4566.1	21894	0
4 2	A_1		Masked	[21684]			Masked	[21748]	
	B_1	—	.....	[21811]	—	*0^-	4570.7	21872	3
5 3	A_1		Masked	[21669]			Masked	[21732]	
	B_1	0	4586.9	21795	0	*0^-	4574.1	21856	2
1 0	A_1				−2				−2
	B_1				−3				−3
2 1	A_1								
	B_1	*4	4881.2	20481 (A_1)	1	*1^+	4872.8	20516	−2
3 2	A_1	5(v)	4850.9	20609 (B_1)	−1	2(v)	4842.9	20643	−3
	B_1				3				0
					1				0
0 0	A_1	1	5201.2	19221	−2				−3
	B_1	0(v)	5167.3	19347	−1				−2
1 1	A_1	*1^-	5195.5	19242	1		Heads		−2
	B_1	*00	5161.1	19370	−1		superposed		−4
2 2	A_1	1	5189.3	19265	0		on $B^{11}O$		−3
	B_1	1(v)	5155.5	19391	0		heads		−2
3 3	A_1	0?	5184.7	19282	7				8
	B_1	—		[19416]	—				—
4 4	A_1	0?	5176.1	19314	0				3
	B_1	—		[19441]	—				—
5 5	A_1	00?	5170.3	19336	5	On 0,0	$B_1B^{11}O$	[19347]	—
	B_1	0?	5135.5	19467	1	1?(v)	5133.6	19474	0
0 1	A_1	—	Masked	[17981]	—	—	Masked	[17944]	
	B_1	—	by 0,3a	[18108]	—	—	by 0,3a	[18070]	
1 2	A_1	—		[18025]	—	—	Masked	[17988]	
	B_1	On 0,3 A_1 head		[18154]			by 0,3a	[18115]	
2 3	A_1	—	Masked	[18070]		—		[18036]	
	B_1	1^-	5493.7	18197	0	0(v)	5503.5	18165	−3
3 4	A_1	—	Masked	[18114]	—	—	Masked	[18085]	
	B_1	*0	5481.1	18240	2	0	5489.4	18212	−1
0 2	A_1			[16765]				[16692]	
	B_1	*1^+	5916.2	16898	−7	00?	5943.5	16821	−2
1 3	A_1	00?	5939.7	16831	−1	—		[16761]	—
	B_1	1^-(v)	5895.3	16958	−1	—		[16887]	—
2 4	A_1	—	On 0,2 B_1	[16895]	(−3)	—		[16831]	—
	B_1	0^+	5872.2	17025	−3	—	On 1,3 B_1	[16957]	—
3 5	A_1	—	On 1,3 B_1	[16961]	—	—	$B^{11}O$	[16903]	—
	B_1	—		[17088]	—	—		[17030]	—

Notes. The use of brackets, ? and *, and the dropping of half quantum numbers, are as explained under Table I, except that in the case of the (1,1), the (3,4)B, and the (0,2)B heads, the use of the * indicates superposition or merging with weak a system *heads* (cf. Table II) instead of structure lines. A (v) after an intensity value is here used to indicate distinct shading toward the violet. The calculated wave-numbers for the C-O column were obtained by adding 3 units to the values calculated from Eq. (10). Unidentified lines or heads occur at 16,785 (int. 00); 16,809 (00); 16864(00).—*P* head of 0,2 B_1?; 16928(0+),—*P* head of 1,3 B_1?; 19303(00); 19325(00); 19359(00); 19428(00+).

and n''. In the sequence for which $\Delta n = 0$ (and presumably in those in which it is positive), the heads proceed toward the violet; in the sequence for which $\Delta n = -1$, the members of the sequence are all superposed to give what appears to be a single strong head: in the sequence $\Delta n = -2$, the heads proceed toward the red. In the $\Delta n = 0$ sequence the $B^{10}O$ and $B^{11}O$ bands coincide; in the -1 sequence, the superposed members for $B^{10}O$ form an apparent single head which is correctly related, in respect both to position and intensity, to the corresponding $B^{11}O$ head; and so on. The above statements hold, furthermore, for both A_1 and B_1 heads, between which the $\Delta\nu$ separation is the same as that observed in the α system. The existence of these combination bands therefore affords striking confirmation of the general correctness of the preceding analysis of the α and β systems, and of their possession of a common final state.[39]

THE EXCITED STATES OF THE BO MOLECULE

Energy levels in BO. The electronic energy levels, with their associated vibrational levels, which are revealed by the foregoing analysis of the BO spectrum, and which may be deduced from Eqs. (8) and (9), are indicated in Fig. 1 by horizontal lines arranged on a vertical energy scale.[40] A set of more closely spaced rotational levels ($E^m = Bm^2 + \ldots$.) should be imagined as superimposed above each vibrational level (and extending up across two or three higher vibrational levels).

The levels for both isotopes are shown on the same scale, thus illustrating the actual magnitude of the difference between them. The frequency corresponding to any band-origin is proportional to the distance from one of the upper (α or β) levels to one of the lower (N) levels. The vertical beaded lines indicate observed transitions for $B^{11}O$, the figure in each circle being the estimated photographic intensity of the head of the corresponding band. The difference in frequency for the two isotopes (isotopic displacement) for a given band, in relation to the position of the band with respect to the system-origin, depends on differences in energy of corresponding levels of the two isotopes in a way that can readily be seen from the diagram.

Constants of the BO molecule. The spacing of successive vibrational levels gives a measure of the corresponding molecular vibration frequency

[39] No new evidence is afforded as to the existence of half-vibrational quantum numbers. The calculated frequencies would not be appreciably changed if Eqs. (8) (9), and (10), like (1) and (2), had been formulated in terms of integral quantum numbers; this is because of the near-equality of the coefficients of n' and n''.

[40] Such diagrams were first used by R. T. Birge (Abstract, Phys. Rev. **23**, 294, 1924).

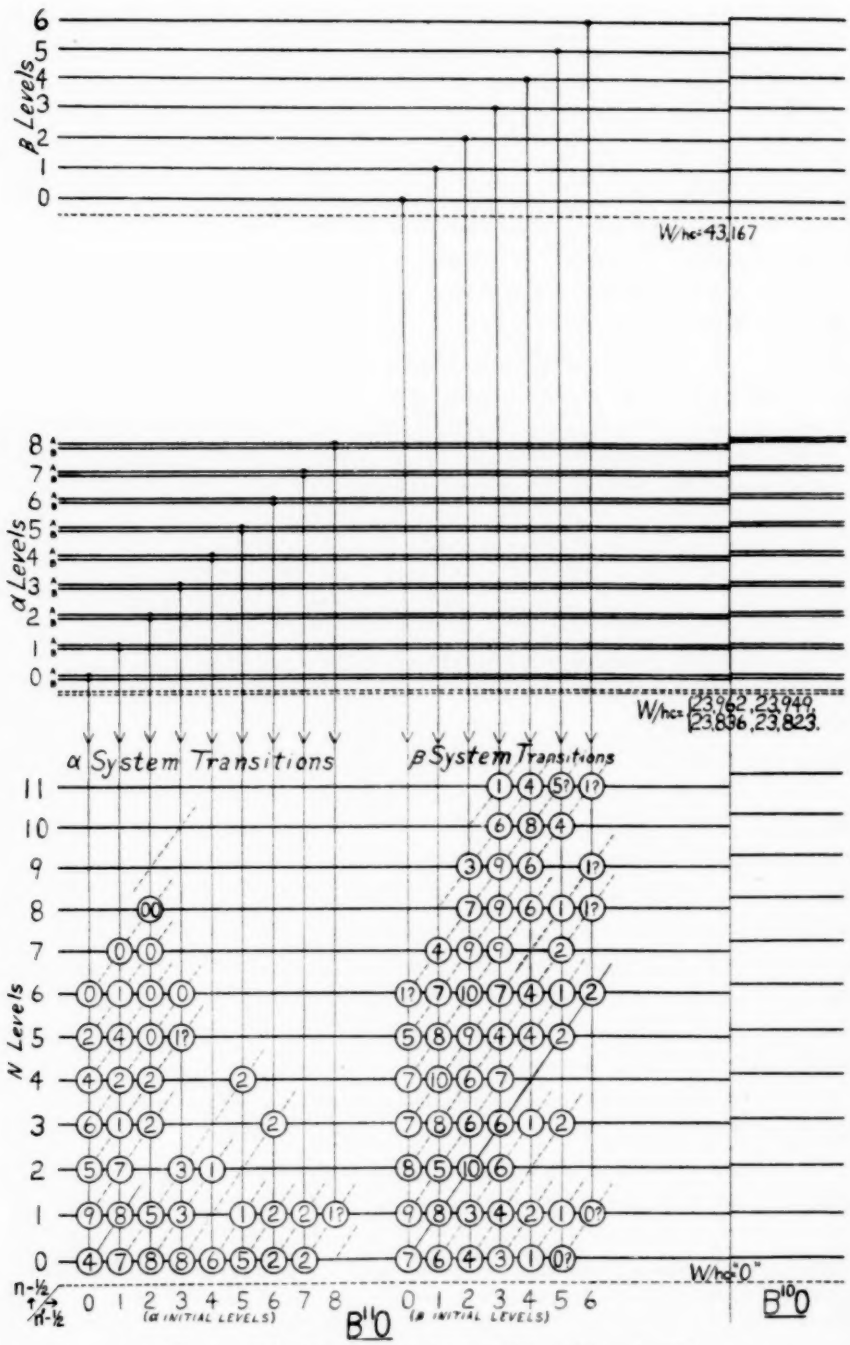

Fig. 1. *Vibrational energy levels and transitions in BO.*

DESCRIPTION OF FIG. 1

The α and β bands of BO involve two electronically excited sets of initial levels designated β and α, and a common final level designated N to indicate that it probably corresponds to the normal state of the molecule. The three electronic levels are shown for the vibrationless molecule ($n=0$), which probably does not exist, by dotted lines in Fig. 1; the lowest (N) is arbitrarily marked $E=0$. (In the figure, W was inadvertently used in place of E, also n in place of n''.) The vibrational levels, beginning with $n=\frac{1}{2}$, $1\frac{1}{2}$, . . . , which are associated with each electronic level, are drawn to scale in Fig. 1, the energy values being calculated from Eqs. (8) and (9). The $B^{10}O$ levels are shown on the extreme right, those of $B^{11}O$ occupying most of the figure. The α levels, shown *double* in Fig. 1, are really quadruple, each level of Fig. 1 being actually a close double.

A vertical line is drawn from each of the α levels toward the N levels; each intersection which is marked by a circle represents an observed $B^{11}O$ band, whose (estimated photographic) intensity is given by a number. For convenience in examining the intensity pattern, the initial vibrational quantum number (minus $\frac{1}{2}$) for each vertical row of circles is repeated at the bottom of the diagram. The diagonal lines between the circles serve to indicate *band-sequences*, i.e., sets of bands characterized by a particular value of $(n''-n')$.—Similar statements hold for the β system of bands. Note the very different character of the intensity distribution in the α and β systems. —The $B^{10}O$ transitions, which are not separately shown, are similar to those of $B^{11}O$.—In addition to the two systems of transitions shown, there is a third, of low intensity, corresponding to transitions from the β to the two α levels of Fig. 1.

ω. Quantitatively, according to the Bohr theory, $\omega = (1/h)\ (dE^n/dn)$. Then from Eqs. (8) and (9), for $B^{11}O$:

$$\omega_\beta = (1280.3 - 20.1n)\ c;\ \omega_\alpha = (1259.1 - 21.2n)\ c;$$
$$\omega_N = (1885.5 - 23.5n)\ c. \qquad (11$$

The subscripts of ω refer to the initial states of the β and α systems, respectively, and to their common final state; c is the velocity of light.

From the value of B_0 in Eqs. (5) and (7), since $B_0 = h/8\pi^2\mu r_0^2$, the equilibrium internuclear distances r_0 for the three states can be calculated. These should of course be the same for both isotopes. The results are, in 10^{-8} cm, with a probable error of ± 0.03 in each case,[41]

$$r_\beta = 1.16;\ r_\alpha = 1.20;\ r_N = 1.09. \qquad (12)$$

Note that the value of r_0 is very near that for CN, where $r_n = 1.17$.

Possible analogy of BO and CN molecules to Na atom. There is considerable evidence for the existence of an analogy between CN and BO, both chemically unsaturated "odd molecules," and the Na atom. In all three cases, there are nine electrons outside the nuclei and K electrons. The CN molecule, like BO, emits two band systems having a common final state, which is in all probability the normal state of the molecule, as probably also in BO.[42] The α and β systems of BO then correspond to electronic resonance potentials 2.9 and 5.3 volts, and the red and violet bands of CN to 1.8 and 3.2 v. These may be compared with 2.10 and 3.74 v for the Na resonance potentials corresponding to the first two lines ($1s-2p$ and $1s-3p$) of the principal series of Na. Note that the ratio of the second to the first is 1.8 in all three cases. The "forbidden" transition $2p-3p$ in Na is furthermore paralleled by the absence in either BO or CN of a conspicuous band system corresponding to an

[41] It is *possible* that these results are incorrect: cf. ref. 33 and related discussion preceding Eq. (5).

[42] The maximum energy of the emitters of the BO β bands is about 6 v greater than that of a BO molecule in the N state (without vibration). If the N state were not the normal state, transitions to lower states would be expected. Barring the possibility of a metastable N state, such transitions should be accompanied by band emission. No bands of unknown origin are, however, observed between λ2000 and λ8500. It is very improbable that there is a system of bands lying wholly beyond λ8500. If there were bands beginning below λ2000, this would require for the BO molecule in its β state an energy of probably 14 volts. It is improbable that the BO molecule, with its odd number of electrons (N_2 ionizes at 16.3 v, NO at 9.4 v, etc.), could possess so high an electronic energy below ionization. Such a high energy is also improbable when one considers the energy of active N_2 (probably 10 or 11 v [22]) and of excited NO (probably about 6 v) in relation to the formation of excited BO molecules.—In regard to CN, see R. S. Mulliken, Nature, Dec. 13, 1924.

analogous transition from the upper to the lower of the two excited electron levels of the molecule. The occurrence in Na in low intensity of forbidden lines of this type is, however, matched in BO by the appearance of the weak $\beta \rightarrow \alpha$ system of bands.

The above analogies suggest the possibility that the first eight outer electrons in BO and CN may be arranged around the two nuclei in 2_1 and 2_2 orbits somewhat as in the octet of Na, the ninth electron being bound relatively loosely, perhaps in a 3_1 orbit, as in Na. Such binuclear octets would be in line with the probable structure of molecules of the HCl type, and with Langmuir's suggestion as to the structure of N_2, CO, CN^- ion, and the like. Proceeding from N_2 through O_2, one would then expect a gradual transition toward the typical shared octet of F_2.

If the α and β bands of BO, and the red and violet bands of CN, are really analogous, in respect to the electron transition involved, to the first two members of the principal series of Na, one may calculate approximate values of s and p spectral terms for these molecules. On this basis, the ionization potentials (equal to the $1s$ terms) should be about 4.4 volts for CN and about 7.0 v for BO. Higher members of the principal series of BO, if present, should lie in the unexplored ultraviolet below λ2000. In the case of CN, the origins of higher members should lie between about λ2800 and λ3300. Although the presence of additional CN band systems in this region has not been demonstrated, the *absence* of bands *below* the calculated series limit at λ2800 may well be significant. The ionization potentials just calculated for BO and CN suggest the existence of a parallelism among molecules to the alternation of higher and lower ionization potentials which is observed, in the case of atoms, as the number of valence electrons changes from even to odd. Thus: CN, BO (9 outer electrons), 4.4, 7.0 v; CO,N_2 (10 outer electrons), 14-15 v; 16. 3v; NO (11 outer electrons), 9.4 v; O_2 (12 outer electrons), 16.1 v.[43]

Intensity Relations and Structural Differences in Arc and Active Nitrogen Spectra of BO

Rotational energy distribution. As in the case of the CN bands,[44] and as would be expected for thermal equilibrium, the BO bands when generated in active nitrogen show a much smaller range of m' values (m = rotational quantum number) and a much lower maximum value of m',

[43] In regard to alteration of atomic ionization potentials cf. F. A. Saunders, Science, Jan. 18, 1924. Ionization potentials of CO, N_2, NO and O_2 are from compilation by K. T. Compton and F. L. Mohler, Bulletin of National Research Council on Critical Potentials, (1924).

[44] R. T. Birge, Astrophys. J. **55**, 273 (1922). Cf. also E. C. Kemble, Phys. Rev. **8**, 689 (1916); T. Heurlinger, Dissertation (Lund), pp. 65-6.

than when produced in the arc. This is illustrated in the case of the $(\frac{1}{2}\rightarrow 1\frac{1}{2})$ band in Plate I(*e*). Plate I(*f*) shows the general appearance of the β bands in the arc. Jevons' reproductions show their appearance in active nitrogen, and also show part of the α bands in both sources. The heads (for which m' is small), especially of $B^{10}O$, are notably less conspicuous in the arc, due to their reduced intensity and their concealment by structure lines of high m' from preceding heads.

Vibrational energy distributon. A study of the intensity data of Tables I and II, displayed in Fig. 1, gives interesting information. Thus by adding the intensity figures for all bands having a given n', one can get a rough idea of the initial n' distribution for the emitting molecules. In the β system, the number of molecules for a given value of n' appears to rise slightly from $n'=\frac{1}{2}$ to $n'=$ about $2\frac{1}{2}$ or $3\frac{1}{2}$, falling off sharply after that, with a maximum n' of $5\frac{1}{2}$ or $6\frac{1}{2}$. In the α system, $n'=\frac{1}{2}$ and $1\frac{1}{2}$ are about equally prominent, after which there is a gradual falling off of intensity to n' values as high as $8\frac{1}{2}$. These n' distributions are evidently non-thermal, since for thermal equilibrium there should be a steady falling off of intensity with increasing n', with $n'=\frac{1}{2}$ by far the most prominent. The *arc spectra* of BO appear to approximate thermal equilibrium in respect to n' distribution. With respect to initial vibrational energy, the effective temperature appears to be actually higher in active nitrogen, which is really only a little above room temperature, than for the arc, while the reverse is the case with respect to rotational energy. The difference is well exemplified in Plate I(*e*), where the $(3\frac{1}{2}\rightarrow 3\frac{1}{2})$ β band appears strongly in active nitrogen, but is weak or apparently absent in the arc.

High n' values, unaccompanied by high m' values, also occur in other band spectra excited by active nitrogen, in cases where a chemical reaction is involved (e.g., CN, SiN). The high n' values developed by active nitrogen may presumably be attributed to the fact that the excitation of the second molecule is accomplished during a molecular collision, which one might naturally expect to produce a considerable amount of atomic vibration. The apparent absence of any appreciable increase of m' by such collisions is perhaps also to be expected.

Lenz, following a procedure first outlined by Heurlinger, has recently applied the Bohr correspondence principle with marked success to the problem of the relative intensity of groups of bands corresponding to different values of $(n''-n')$.[45] Using a simplified model, he has shown that the intensity distributions observed in various types of electronic band spectra may be accounted for, at least qualitatively. The important

[45] T. Heurlinger, Zeits. f. Phys. **1**, 87 (1920); W. Lenz, Zeit. f. Phys. **25**, 299 (1924)

factors are the nuclear vibration frequency, the frequency of motion of the emitting electron, and the amplitude of the perturbation of the electronic frequency by the vibrational motion. In the α system of BO, the intensity distribution of Δn values is fairly symmetrical about $\Delta n = 0$: the sequences $\Delta n = \pm 1$ are somewhat more intense than $\Delta n = 0$; for higher Δn's the intensity gradually diminishes; the maximum observed values are $\Delta n = -7$ and $+6$ ($\Delta n = +7$ lies too far into the infra-red for observation). In the β system, the observed Δn values range from -5 to $+8$, with a preponderance of intensity in favor of the positive Δn's. The latter are all about equally intense from 0 to $+6$, after which a rapid fall in intensity occurs. The comparative weakness of the negative Δn sequences may be due in part to the scarcity of molecules having $n' > 3\frac{1}{2}$; also it is *in part* only apparent, due to decreasing plate sensitivity. Lenz's theory predicts an approach to equality for numerically equal Δn values of opposite sign.

There appear to be a number of peculiar restrictions in the BO bands for particular changes $n' \rightarrow n''$. Thus in the α system, the sequence $\Delta n = 0$ is represented only by $(\frac{1}{2}, \frac{1}{2})$ and $(1\frac{1}{2}, 1\frac{1}{2})$, while in the β system, all values of n' except $4\frac{1}{2}$ are represented. Also, in the α system, the $(1\frac{1}{2}, 3\frac{1}{2})$, $(3\frac{1}{2}, 4\frac{1}{2})$, $(4\frac{1}{2}, 1\frac{1}{2})$, and $(4\frac{1}{2}, 3\frac{1}{2})$ bands are unexpectedly absent or nearly so, while the $(5\frac{1}{2}, 4\frac{1}{2})$ band is unexpectedly present. In the β system, many of the bands for which $n' = 4\frac{1}{2}, 5\frac{1}{2}$, and $6\frac{1}{2}$ are missing; e.g., $(4\frac{1}{2}, 2\frac{1}{2})$, $(4\frac{1}{2}, 3\frac{1}{2})$, $(4\frac{1}{2}, 4\frac{1}{2})$, $(4\frac{1}{2}, 7\frac{1}{2})$. A characteristic tendency shown by both systems is for the preferred values of Δn (either positive or negative) to increase with increasing n'.

A phenomenon probably closely related to the occurrence of large Δn values in the emission of band spectra seems to be indicated by the non-thermal occurrence of large n' values in gas spectra excited electrically in vacuum tubes at low temperatures. Apparently the excitation of a molecular electron by impact of an external electron is normally accompanied by a considerable increase in n. Direct evidence that electronic impacts readily produce nuclear vibration is to be found in the work of Brandt[46] on the 7 volt resonance potential in nitrogen.

Arc doublets. A very striking difference between the BO bands in the arc and in active nitrogen gives further information on the subject of collisions with excited molecules. In the case of the easily examined strong β bands $(1\frac{1}{2} \rightarrow \frac{1}{2})$, $(\frac{1}{2} \rightarrow \frac{1}{2})$, $(\frac{1}{2} \rightarrow 1\frac{1}{2})$, $(\frac{1}{2} \rightarrow 2\frac{1}{2})$, and $(\frac{1}{2} \rightarrow 3\frac{1}{2})$, each

[46] E. Brandt (Zeit. f. Phys. **8**, 32, 1921) finds that this is composed of a series of small breaks, of which each is doubtless an electronic resonance potential plus one of a variety of vibrational changes (cf. Fig. 1) analogous to a series of absorption bands $(0 \rightarrow 0)$ $(0 \rightarrow 1)$, ... , —or $(\frac{1}{2} \rightarrow \frac{1}{2})$, etc.

single positive branch line of the active nitrogen photographs is joined on the arc photographs by a companion, of equal intensity, in the direction of lower frequencies, so as to form a *doublet*.[47] The doublets are not resolved near the head; the separation first becomes noticeable at the 34th, 34th, 22nd, 18th, and 16th line, respectively, from the head for the above bands;[48] from this the doublet separation would seem to be considerably dependent on the final vibrational quantum number. At large distances from the head, neighboring doublets overlap. In Plate I(*e*) enlargements of the $(\frac{1}{2}\rightarrow 1\frac{1}{2})$ band in the arc and active nitrogen have been juxtaposed, and show well the arc doublets for $B^{11}O$; some of the $B^{10}O$ doublets can also be identified. In examining the reproduction, one must of course remember that the weak lines of the $(\frac{1}{2}\rightarrow 1\frac{1}{2})$ band of $B^{10}O$ are interspersed among (and sometimes superposed on) the stronger $B^{11}O$ lines; they are comparatively inconspicuous in the arc, but give in places a false doublet appearance in the active nitrogen photograph. The appearance of the doublets is entirely similar in the other bands mentioned.

Kratzer has shown that doublet bands may be explained by the assumption that the emitting molecules may possess resultant electronic angular momentum, either positive or negative, in the direction of molecular rotation.[49] If this explanation is correct, it would appear that in the instant of formation or excitation in active nitrogen, *one* only of the two possible relative directions of rotation is imparted to the BO molecule; while *both* directions appear under the conditions, presumably approaching thermal equilibrium, in the arc. Further elucidation of these interesting doublets and of the problem of the isolated positive branch must, however, be left until further more accurate measurements have been made.

In conclusion, it is a pleasure to acknowledge indebtedness to Prof. F. A. Saunders for his initial encouragement and later valuable advice and help. Much is also due to the kindness of the director of the laboratory, Prof. T. Lyman, and to the suggestions and criticism of Prof. E. C. Kemble. The writer is also indebted to Prof. G. P. Baxter of the Department of Chemistry for the pure boron chloride used.

JEFFERSON PHYSICAL LABORATORY,
HARVARD UNIVERSITY,
Sept. 12, 1924 (revised Dec. 11, 1924)

[47] The new lines appearing in the arc are almost certainly *not* the missing negative branch lines.

[48] It should be recalled that the dispersion is *decreasing* in the direction from $(1\frac{1}{2}\rightarrow\frac{1}{2})$ toward $(\frac{1}{2}\rightarrow 3\frac{1}{2})$.

[49] A. Kratzer, Ann. der Phys. **71**, 72 (1923); see also Zeit. f. Phys. **23**, 298 (1924).

THE SERIES SPECTRA OF THE STRIPPED ATOMS OF PHOSPHORUS (P_V), SULPHUR (S_{VI}), AND CHLORINE (Cl_{VII})

By I. S. Bowen and R. A. Millikan

Abstract

Spectra of stripped atoms, sodium to chlorine.—Grating spectrograms of order three to eight have been obtained of the hot-spark spectra of these elements, which have yielded more accurate values for the ($3p_2-3p_1$), ($3s-3p_2$) and ($3p_1-3d$) terms of Al_{III}, Si_{IV}, P_V and S_{VI}, and have enabled the identification and determination within about 5 frequency units (1) of 18 series lines of P_V, and thence of the 14 most important term values ($3s$ to $6f''$), (2) of 11 series lines of S_{VI}, and 10 corresponding term values ($3s$ to $5f'$), and (3) of the first doublet of the principal series of Cl_{VII} at 800.70 and 813.00 A. The position of this doublet was first predicted by use of the method developed in a previous paper,[1] based on observed regularities in these spectra. Further evidence is presented for the fact that both the regular and the irregular doublet laws of x-ray spectra, hold also throughout the field of optics. A plot of $\sqrt{\nu/R}$ for the stripped atom levels as a function of atomic number gives approximately straight lines (Moseley law), those for the $3s$, $3p$ and $3d$ terms and for the $4s$, $4p$, $4d$ and $4f$ terms being approximately parallel (irregular doublet law). The doublet separations d_1d_2, however, do not fit well into the relativity doublet law, the ratio of observed to theoretical values decreasing from about .8 for S_{VI} to less than .2 for Si_{IV}, while Al_{III} and Mg_{II} are anomalous, d_1 having a greater frequency than d_2. The general similarity of the spectra of all these elements is strikingly shown in spectrograms on which appear the "D" doublet of Na and the corresponding "D" doublets of the stripped atoms of Mg, Al, Si, P, S, and Cl in the second, third, fourth, fifth, sixth and seventh orders, respectively, all near 5600 A, that for Na being farthest from the mean position. The frequencies of all the known terms found for the stripped atoms of Na to S, are collected in a table. Ionization potentials of P_V and Si_{VI}, computed from the $3s$ levels of P_V and S_{VI}, come out 64.7 and 87.6 volts.

I. Method of Proving the Existence in our Hot Sparks of the Stripped Atoms of the Whole Second Row of Elements of the Periodic Table, from Sodium through Chlorine.

IN a preceding article[1] we have shown (1) that both the regular and the irregular doublet laws developed for the interpretation of x-ray spectra hold also throughout the whole field of optics, and (2) that this discovery puts into our hands a new method for predicting with certainty (a) the precise frequencies or wave-lengths which must be emitted by an atom of a given stage of ionization, and (b) the precise doublet-separations to be expected in these frequencies.

[1] Bowen and Millikan, Phys. Rev. **24**, 209 (1924)

By the application of this method we have now proved that our hot-sparks have the power of completely stripping all the valence electrons from the whole group of atoms from sodium through chlorine, thus reducing all of the atoms of this series to one single electronic structure in which, however, the effective nuclear charge increases from one in sodium to seven in chlorine.

Tables I and II represent the revision and extension of Tables V and VI of the preceding article. Table I exhibits the application of the relativity, or regular doublet law, to this series of similar atomic structures, and Table II exhibits in a similar way the applicability of the irregular doublet law to this same series.

TABLE I

$(3p_2-3p_1)$ separations of stripped atoms Na_I to Cl_{VII}

	$\Delta\nu$	$Z-s$	s
Na_I	17.18	3.550	7.450
Mg_{II}	91.55	5.394	6.606
Al_{III}	234.00	6.820	6.180
Si_{IV}	461.84	8.084	5.916
P_V	794.82	9.259	5.741
S_{VI}	1267.10	10.404	5.596
Cl_{VII}	1889.5	11.496	5.504

The way in which the position of these stripped-atom-lines was predicted from the irregular doublet law of Table II and their doublet separations from the regular doublet law of Table I, has been heretofore detailed for the atoms from sodium through sulphur. The exact values given in these tables differ slightly from those previously published for

TABLE II

	$3s-3p_2$	Diff.	2nd diff.	$3p_1-3d$	Diff.
Na_I	16956.17			12199.48	
		18713.25			23529.96
Mg_{II}	35669.42		701.14	35729.44	
		18012.11			26308.34
Al_{III}	53681.53		408.15	62037.78	
		17603.96			26585.63
Si_{IV}	71285.49		240.03	88623.41	
		17363.93			26131.82
P_V	88649.42		147.31	114755.23	
		17216.62			25557.64
S_{VI}	105866.04		81.43	140312.87	
		17135.19			
Cl_{VII}	123001.23				

the reason that new and very much better plates have been taken in the case of all these atoms save Na and Mg, and in consequence the present tables contain data of a considerably higher order of precision than that of preceding tables. The separations, from aluminum through sulphur, in the present table have all been taken upon spectra of order from three to eight and may be relied upon to one frequency unit. On account of

this increase in precision the present tables are to be regarded as not merely extending but rather completely replacing the old ones.

To show the power of the method it is to be observed from Table II that the column of 2nd differences progresses systematically by a factor a little more than $\frac{1}{2}$ (quite accurately .58), so that it was possible to predict where the first term of the principal series of the stripped atom of chlorine would lie to within considerably less than 15 frequency units which here corresponds to *one tenth of an angstrom.* We used aluminum electrodes with NaCl in their cores and obtained at once in both the first and second order a definite line of intensity 2 or 3 *at exactly the right place, namely, at wave-length 813.00 A.*

Next, from the progression of the values of the screening constant s in Table I it was seen that this constant for the stripped chlorine must have a value very close to 5.5. Substitution of this value in the equation $\Delta\nu = .108(Z-s)^4$ gave a value of $\Delta\nu$ which could not be in error by more than one-tenth angstrom. *At precisely the predicted distance from the* $(3s-3p_2)$ *line, the position of which had been predicted from Table II, our plate showed a new and sharp chlorine line, at* $\lambda 800.70A$, of the same intensity as its companion.

This then completes the stripping of all the valence electrons from the whole row of the seven different atoms which in the periodic table intervene between neon and argon. This stripping reduces all of these atoms to the same electronic structure which is possessed by neon.

II. Photographic Exhibition of Similarity of Stripped Atom Spectra

Although there is identity of the electronic structure of the stripped atoms of Na, Mg, Al, Si, P, S and Cl the central charge pulling upon the radiating electron increases in going from sodium through chlorine in the ratios 1, 2, 3, 4, 5, 6, 7, provided the screening of the 10 electrons in the K and L shells is perfect.

These atoms should then all possess the same spectrum as that of sodium, save that the "D" doublet in going from Na to Cl should increase in frequency in view of the irregular doublet law (Table II), in the ratios 1, 2, 3, 4, 5, 6, 7. Hence, if this "D" or sodium doublet were observed in its first order for sodium, second order for magnesium, etc., down to the seventh order for chlorine, it should be found in the same spectral position for the whole seven stripped atoms. Because, however, the screening is not perfect, and therefore the irregular doublet law is not exact (see Table II), the actual spectral positions of these "D" doublets

will lack somewhat of coincidence, sodium being the farthest out as Table II shows.

Plate I shows this whole series of "D" doublets, for the stripped atoms Na to Cl, all taken in the same narrow region on the plate—between $\lambda = 5600$ and $\lambda = 5900$—and with an unchanged position of the grating. This plate shows how beautifully the first order of the sodium, the second of the magnesium, the third of the aluminum, the fourth of the silicon, the fifth of the phosphorus and the sixth of the sulphur fall into the same narrow region of the spectrum. It was impossible to get the chlorine in the seventh order and consequently its position, as obtained from first and second order photographs, is merely indicated .

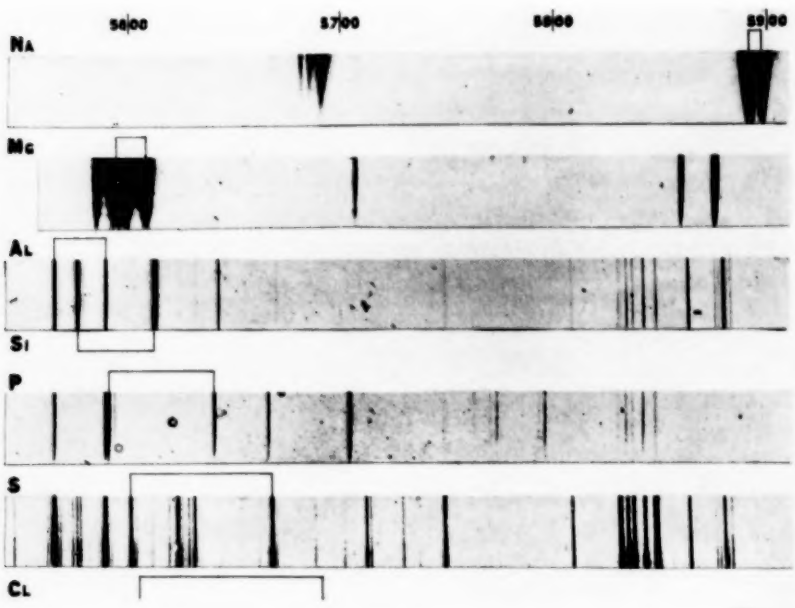

Plate I. Photographic exhibition of similiarity of stripped-atom spectra.

Although the frequency separation of the components of this "D" doublet increases rapidly in going from Na to Cl (regular doublet law), the large increase in wave-length separation shown in the photographs is due primarily to increasing spectral orders, for since $d\lambda = d\nu/\nu^2$, $d\lambda$ does not increase with anything like the rapidity of $d\nu$. It will be understood that the "D" doublet is in every case the pair of lines indicated by the brackets.

III. The Series of the Stripped Atoms of Phosphorus P_V and Sulphur S_{VI}

The positions of the principal lines due to jumps between the hydrogen-like terms (circular or nearly circular orbits) in the spectrum of the stripped atom of phosphorus can be predicted by means of the procedure which we have previously exposed in the case of the stripped atom of boron.[2] Thus, the $5f'$ orbit is a circle, the energy value of which should

TABLE III

Spectrum of stripped phosphorus PV

Intensity	λ(I.A. vac.)	ν	Δν		Term values	
2	542.52	184325.0	815.2	$3p_2-4s$	$3s$	524491.19
					$4s$	251540.66
2	544.93	183509.8		$3p_1-4s$	$5s$	147858.7
3	673.92	148385.6		$3d-4f$	$3p_1$	435046.95
					$3p_2$	435841.77
4	865.475	115543.49	788.26	$3p_2-3d$	$4p_1$	220055.11
5	871.420	114755.23		$3p_1-3d$	$4p_2$	220339.02
					$3d$	320295.0
2	997.637	100236.86	277.84	$3d-4p_1$	$4d$	179101.1
2	1000.410	99959.02		$3d-4p_2$	$4f$	171909.4
					$5f$	110036.5
15	1118.015	89444.24	794.82	$3s-3p_1$	$5f'$	109818.4
12	1128.039	88649.42		$3s-3p_2$	$6f'$	76278.5
0	1385.11	72196.4		$4p_1-5s$	$6f''$	76255.2
1	1447.92	69064.6		$4d-5f$		
2	1610.54	62091.0		$4f-5f'$		
2	2425.08	41235.75	279.50	$4p_2-4d$		
2	2441.63	40956.25		$4p_1-4d$		
2	2962.26	33758.0		$5f-6f'$		
3	2979.45	33563.2		$5f'-6f''$		
5	3176.06	31485.55	283.91	$4s-4p_1$		
3	3204.96	31201.64		$4s-4p_2$		

be almost exactly 5^2 times that of the $5f'$ orbit of sodium, or $(5/3)^2$ times the $5f'$ orbit of aluminum. Since this latter term value is known from Paschen's work,[3] we could compute the former at once to about one part in five thousand by this method. It could be obtained still more accurately by extrapolating to phosphorus from the progression shown in

[2] Bowen and Millikan, Proc. Nat. Acad. **10**, 199 (1924)

[3] Paschen, Ann. der Phys. **71**, 142 (1923)

the $5f'$ terms in Table VII. In this way $5f'$ for stripped phosphorus was found to be $25\times4392.74=109818.4$ correct within about ±5.

The jump $4f-5f'$ can be predicted quite accurately from a similar extrapolation on the $4f$ term. This locates the $4f-5f'$ line to a fraction of an angstrom and enabled us to identify unambiguously the line of measured wave-length 1610.54 A as the $4f-5f'$ line. Adding this observed frequency to the $5f'$ term fixed the $4f$ term at 171,909.4.

TABLE IV

Spectrum of stripped sulfur SVI

Intensity	λ (I.A. vac.)	ν	Δν		Term values	
0	388.91	257128.9	1256.6	$3p_2-4s$	$3s$	710264.2
0	390.82	255872.3		$3p_1-4s$	$4s$	347264.0
					$3p_1$	603131.1
1	464.63	215225.0		$3d-4f$	$3p_2$	604398.2
					$4p_1$	308625.9*
1	706.503	141542.2	1229.3	$3p_2-3d_2$	$4p_2$	309083.5*
2	712.693	140312.9		$3p_1-3d_1$	$3d_1$	462818.2*
0	712.868*	140278.4	34.5	$3p_1-3d_2$	$3d_2$	462854.4*
					$4f$	247612.1
5	933.418	107133.1	1267.1	$3s-3p_1$	$5f'$	158159.5
4	944.590	105866.0		$3s-3p_2$		
0	1117.91	89452.6		$4f-5f'$		
1	2588.12*	38638.1	457.6	$4s-4p_1$		
0	2619.14*	38180.5		$4s-4p_2$		

* Added to proof, January 27, 1925.

Exactly similar analysis identified the $3d-4f$ line as the line of measured wave-length 673.92 A and then fixed the $3d$ level as in the table.

The $(3p_1-3d)$ is the first term of the diffuse series and its wave-length could be predicted accurately from the progression (irregular doublet law) shown in Table II. These considerations show that the measured line at $\lambda=871.420$ A is the line sought. The regular doublet-separation law of Table I then fixes the 865.475 line as $3p_2-3d$.

Thus by a combination of the regular and irregular doublet laws for the non-hydrogen-like terms and the simple Bohr theory for the hydrogen-like ones the whole group of results contained in Table III has been worked out. All these results have been checked by the use of the older methods represented in the Rydberg formula.[4]

[4] In Table III the wave-lengths from 2400 up are taken from Geuter's data given in Kayser, vol. 6, p. 246. These are reduced to I. A. (vacuum).

A precisely similar analysis applied to the stripped atom of sulphur has been responsible for the assignment of lines and the computation of term-values shown in Table IV for the spectrum of the stripped atom of sulphur. The fixing of the $3s$ levels of P_V at 524491.19 (Table III) and of S_{VI} at 710264.2 (Table IV) fixes the *ionizing potential* of P_V at 64.7 volts and that of S_{VI} at 87.6 volts.

Table V contains the observed wave-lengths and the frequencies, determined as already indicated, of the two components of the "D" doublet of the stripped atom of chlorine.

TABLE V

Lines of stripped chlorine ClVII

Intensity	λ (I.A. vac.)	ν	$\Delta\nu$	
3	800.70	124890.7	1889.5	$3s-3p_1$
2	813.00	123001.2		$3s-3p_2$

IV. THE FREQUENCY SEPARATION OF THE d_1d_2 DOUBLETS FROM MAGNESIUM THROUGH SULPHUR

The data which we published in Table V of our preceding article[1] upon the $3d$ and $4d$ orbits in Mg_{II} and Al_{III} and the $4f$ orbits in Al_{III} and Si_{VI} showed that the relativity formula predicted accurately the observed separations, or in other words that the value of the screening constant s came out 10 within the limits of observational error.

But when upon our new plates, taken with high resolution, we studied the $3d$ and $4d$ terms in Si_{IV}, P_V, and S_{VI} this agreement broke down. Thus the relativity formula predicts a separation of the $3d_13d_2$ levels in phosphorus of 22.5 frequency units (see column 4 Table VI). When,

TABLE VI

d_1d_2 doublets for stripped atoms Na_I to S_{VI}

	By direct measurement	$3d_2-3d_1$ Principal minus diffuse	From theory $.036(Z-10)^4$	By direct measurement	$4d_2-4d_1$ Principal minus diffuse	From theory $.0152(Z-10)^4$
Na_I			.036			.0152
Mg_{II}	−.99	−.91	.576			.243
Al_{III}	−2.28	−1.70	2.92	−1.28		1.23
Si_{IV}		1.57	9.2		.08	3.9
P_V		6.32	22.5		4.41	9.5
S_{VI}	34.5	37.75	46.6			19.7

however, the $(3d-4f)$ line 673.92 was observed in the fifth order it could not be seen to be a doublet at all despite the fact that our high resolution should have revealed it. This could only mean that the doublet was

actually much too narrow to fit the relativity equation. This doublet should also have appeared in the $(3p_1-3d)$ line at 871.420 A with a separation of .17 A (for this is the equivalent at this point of 22.5 frequency units), and also in the $(3d-4p_1)$ line at 997.637 A with a separation of .22 A. Though these lines were obtained in the seventh and third orders respectively they showed no resolvable doubling.

The actual separation could be obtained as follows: It is well known that in the diffuse series the separation of the two strongest components is equal to the difference of the p_1p_2 separation and the d_1d_2 separation. Hence a fairly good estimate of the d_1d_2 separation, which we could not directly observe, could be obtained from the difference between the observed diffuse separation and the true p_1p_2 separations as obtained from the principal series. As will be seen from Table III the difference between these two separations, namely $(3s-3p)=794.82$, and $(3p-3d)=788.26$ is 6.56, while the difference between $(4s-4p)=283.91$ and $(3d-4p)=277.84$ is 6.07. These two numbers agree fairly well and their mean, namely 6.32, is taken as the true $3d$ separation and is so recorded in Table VI. *It will be seen that this d_1d_2 separation, thus fairly reliably obtained, is less than one third of the separation predicted by the relativity equation, namely, 22.5.* The reason that this method succeeds when a direct observation of doubling fails is found in the fact that it is possible to set on the center of gravity of a line with an error not greater than a thirtieth of the width of the line.

In a similar way all the numbers in the 3rd and 6th columns of Table VI were obtained from measurements of this sort upon our own plates, except in the case of $3d_1-3d_2$ for Mg, which was taken from Fowler's book (p. 120), and $4d_1-4d_2$ for Si, which was taken from one of Fowler's papers.[5] The numbers in the second and fifth columns are those used in Table V of our preceding article, and represent Fowler's and Paschen's direct measurements, respectively.

The negative signs used with the Mg and Al separations signify that d_1 has, quite anomalously, a larger term value than d_2. This had been previously pointed out by Paschen.[6] It means that in Mg and Al the separation of the two principal components of the diffuse series is, altogether anomalously, greater than the true p_1p_2 separation.

It will be seen that the departures of the separations predicted by the relativity-doublet formula and shown in columns 4 and 7, from the observed separations in columns 2, 3, 5, and 6, are quite unambiguous,

[5] Fowler, Proc. Roy. Soc. **103**, 423 (1923)

[6] Paschen, Ann. der Phys. **71**, 151 (1923), footnote.

although by the time sulphur is reached the observed separation seems to be rapidly nearing the theoretical value, as it might be expected to do since the observed and theoretical values are known to agree moderately well in the x-ray field.

The foregoing behavior of the *d* doublets, then, while it is clearly not predicted by the relativity equation yet seems to be tending to conformity with that equation.

TABLE VII

Comparison of frequencies of series terms for stripped atoms Na_I to S_{VI}.

	N =	3	4	5	6
	R/N^2 =	12192.78	6858.44	4389.40	3048.19
s	Na/1	41449.0	15709.5	8248.3	5077.3
	Mg/4	30316.9	12865.6	7120.3	4517.3
	Al/9	25494.89	11476.82	6535.29	
	Si/16	22756.83	10633.65	6168.72	
	P/25	20979.65	10061.63	5914.35	
	S/36	19729.56	9646.22		
p_1	Na/1	24475.7	11176.1	6406.3	4151.3
	Mg/4	21376.6	10154.0	5949.6	3909.2
	Al/9	19504.01	9526.85	5664.93	
	Si/16	18272.62	9105.53	5471.16	
	P/25	17401.88	8802.20		
	S/36	16753.64			
d	Na/1	12276.2	6900.4	4412.5	3061.9
	Mg/4	12444.3	6988.8	4461.6	3091.6
	Al/9	12611.00	7074.30	4508.72	3119.96
	Si/16	12733.65	7131.84	4539.22	
	P/25	12811.80	7164.04		
	S/36	12856.59			
	Na/1		6860.4	4390.4	3043.
	Mg/4		6866.8	4394.3	3051.2
	Al/9		6871.28	4397.61	3053.83
	Si/16		6874.19	4399.97	3055.97
	P/25		6876.38	4401.46	
	S/36		6878.11		
f''	Na/1			4388.8	
	Mg/4				3048.7
	Al/9			4391.80	3050.30
	Si/16			4392.31	3050.84
	P/25			4392.74	3051.14
	S/36			4393.32	
f'''	Na/1				3046.3
	Mg/4				
	Al/9				3049.64
	Si/16				3049.81
	P/25				3050.21

V. COMPARISON OF SERIES TERMS OF Na_I, Mg_{II}, Al_{III}, Si_{IV}, P_V, and S_{VI}

For convenience of reference and comparison we have arranged in Table VII all of our series terms in the form previously used by both

Fowler and Paschen. This form is dictated by the consideration that for remote orbits all of these stripped atoms should have term values which are proportional to the square of the effective nuclear charge, so that if these term values are divided by the squares of the numbers 1, 2, 3, 4, 5, 6, respectively, the same number should result.

In the present table the Na, Mg, and Al terms are taken directly from Paschen.[3] The silicon follows Fowler's identification, but the term values have been recalculated with the use of new experimental data of our own and also with the use of the Rydberg constant which is appropriate to silicon, Fowler having used the hydrogen value of this constant. The remaining data are calculated from Tables III and IV of this paper.

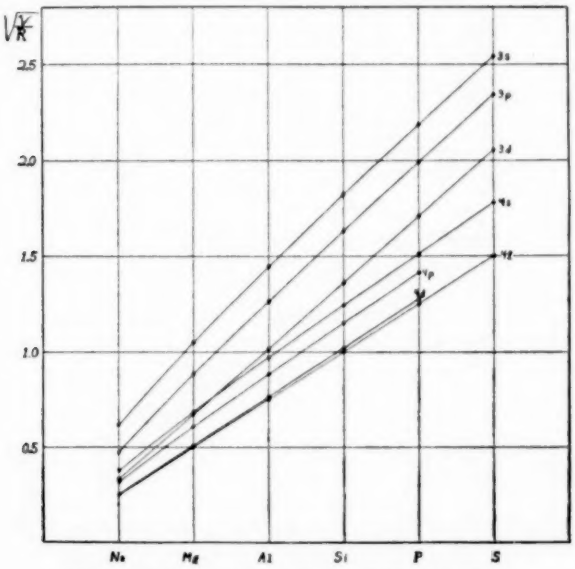

Fig. 1. Moseley's law in the field of optics.

This whole comparison may be very beautifully made graphic in precisely the way in which Moseley first exhibited the relations between atomic number and x-ray spectra. Indeed, no more striking demonstration of the fact that x-ray laws hold throughout the *optical* region as well can be made than is found in Fig. 1. In this figure we have plotted all our stripped atom levels, corresponding to the second row of the periodic table, in a Moseley diagram. That these optical levels follow the *Moseley law* is exhibited by the linear relation everywhere found between $\sqrt{\nu/R}$ and atomic number. That they follow the irregular doublet law is shown by the parallelism of the $3s$, $3p$, and $3d$ lines, all of which have constant screening differences, corresponding as they do to 3_1, 3_2, and 3_3 orbits,

respectively. Quite similarly, the irregular doublet law appears in the near parallelism of the $4s$, $4p$, $4d$, and $4f$ lines, which correspond to 4_1, 4_2, 4_3, and 4_4 orbits, respectively. The lack of perfect parallelism in all these cases we interpret, as in our preceding papers, as due to decreasing perfectness in the screening, and a fortiori therefore, to the difference in the screening between differently shaped orbits, as the radiating electron's distance from the nucleus decreases relatively to the screening electrons' mean distance. The diagram thus furnishes a very satisfactory graphical illustration of the extension of two of the three x-ray laws, namely, the Moseley law and the irregular doublet law into the field of optics. That it fails to illustrate the extension of the third, or regular doublet law, is merely due to the fact that the regular doublet separations are so small as not to be visible at all upon a drawing of this scale.

NORMAN BRIDGE LABORATORY OF PHYSICS,
CALIFORNIA INSTITUTE OF TECHNOLOGY,
PASADENA, CALIFORNIA.
November 20, 1924.

MEASUREMENTS OF β-RAYS ASSOCIATED WITH SCATTERED X-RAYS

By Arthur H. Compton and Alfred W. Simon

Abstract

Stereoscopic photographs of beta-ray tracks excited by strongly filtered x-rays in moist air have been taken by the Wilson cloud expansion method. In accord with earlier observations by Wilson and Bothe, two distinct types of tracks are found, a longer and a shorter type, which we call P and R tracks, respectively. Using x-rays varying in effective wave-length from about 0.7 to 0.13 A, the ratio of the observed number of R to that of P tracks varies with decreasing wave-length from 0.10 to 72, while the ratio of the x-ray energy dissipated by scattering to that absorbed (photo-electrically) varies from 0.27 to 32. This correspondence indicates that about 1 R track is produced for every quantum of scattered x-radiation, assuming one P track is produced by each quantum of absorbed x-radiation. The *ranges* of the observed R tracks increase roughly as the 4th power of the frequency, the maximum length for 0.13 A being 2.4 cm at atmospheric pressure. About half of the tracks, however, had less than 0.2 of the maximum range. As to *angular distribution*, of 40 R tracks produced by very hard x-rays (111 kv), 13 were ejected at between 0 and 30° with the incident beam, 16 at between 30° and 60°, 11 at between 60° and 90° and none at a greater angle than 90°. The R electrons ejected at small angles were on the average of much greater range than those ejected at larger angles. These results agree closely in every detail with the theoretical predictions made by Compton and Hubbard, and the fact that in comparing observed and calculated values, no arbitrary constant is assumed, makes this evidence particularly strong that the assumptions of the theory are correct, and that whenever a quantum of x-radiation is scattered, an R electron is ejected which possesses a momentum which is the vector difference between that of the incident and that of the scattered x-ray quantum.

IN recently published papers, C. T. R. Wilson[1] and W. Bothe[2] have shown the existence of a new type of β-ray excited by hard x-rays. The range of these new rays is much shorter than that of those which have been identified with photo-electrons. Moreover, they are found to move in the direction of the primary x-ray beam, whereas the photo-electrons move nearly at right angles to this beam.[3] Wilson, and later Bothe,[4] have both ascribed these new β-rays to electrons which recoil from scattered x-ray quanta in accordance with the predictions of the quantum theory

[1] C. T. R. Wilson, Proc. Roy. Soc. A **104**, 1 (1923)
[2] W. Bothe, Zeits. f. Phys. **16**, 319 (1923)
[3] See, e.g., F. W. Bubb, Phys. Rev. **23**, 137 (1924)
[4] W. Bothe, Zeits. f. Phys. **20**, 237 (1923)

of x-ray scattering.[5] In support of this view, they have shown that the direction of these rays is right, and that their range is of the proper order of magnitude. The present paper describes stereoscopic photographs of these new rays which we have recently made by Wilson's cloud expansion method. In taking the pictures, sufficiently hard x-rays were used to make possible a more quantitative study of the properties of these rays.

The cloud expansion apparatus used in our work was patterned closely after Wilson's well-known instrument except that all parts other than the glass cloud chamber itself were made of brass. The timing was done by a single pendulum, which carried a slit past the primary beam and actuated the various levers through electric contacts. The Coolidge x-ray tube, enclosed in a heavy lead box, was excited by a transformer and kenotron rectifiers capable of supplying 280 peak kilovolts. For illumination we used a mercury spark, similar to that of Wilson, through which discharged a 0.1 microfarad condenser charged by a separate transformer and kenotron to about 40 kv. The photographs were made by an "Ontoscope" stereoscopic camera, equipped with Zeiss Tessar $f/4.5$ lenses of 5.5 cm. focal length. Eastman "Speedway" plates (45×107 mm) were found satisfactory.

A typical series of the photographs[6] obtained are reproduced in Plate I, (a) to (f), which show the progressive change in appearance of the tracks as the potential across the x-ray tube is increased from about 21 to about 111 kv.

Especially in view of the fact that the original photographs are stereoscopic, the negatives of course show much more detail than do the reproductions. These suffice to show, however, the two types of tracks, the growth of the short tracks with potential, and the fact that while the long tracks are most numerous for the soft x-rays, the short tracks are most in evidence when hard rays are used. These results are in complete accord with Wilson's observations.

Number of tracks. It has been shown[7] that if the above interpretation of the origin of the two classes of β rays is correct, the ratio of the number of short tracks (type R) to that of long tracks (type P) should be

$$N_R/N_P=\sigma/\tau \qquad (1)$$

where σ is the scattering coefficient, and τ the true absorption coefficient of the x-rays in air; for σ is proportional to the number of scattered

[5] A. H. Compton, Bulletin Nat. Res. Council, No. 20, p. 19 (1922); and P. Debye, Phys. Zeits. (Apr. 15, 1923)

[6] These photographs were shown at the Toronto meeting of the British Association in August 1924.

[7] A. H. Compton and J. C. Hubbard, Phys. Rev. **23**, 448 (1924)

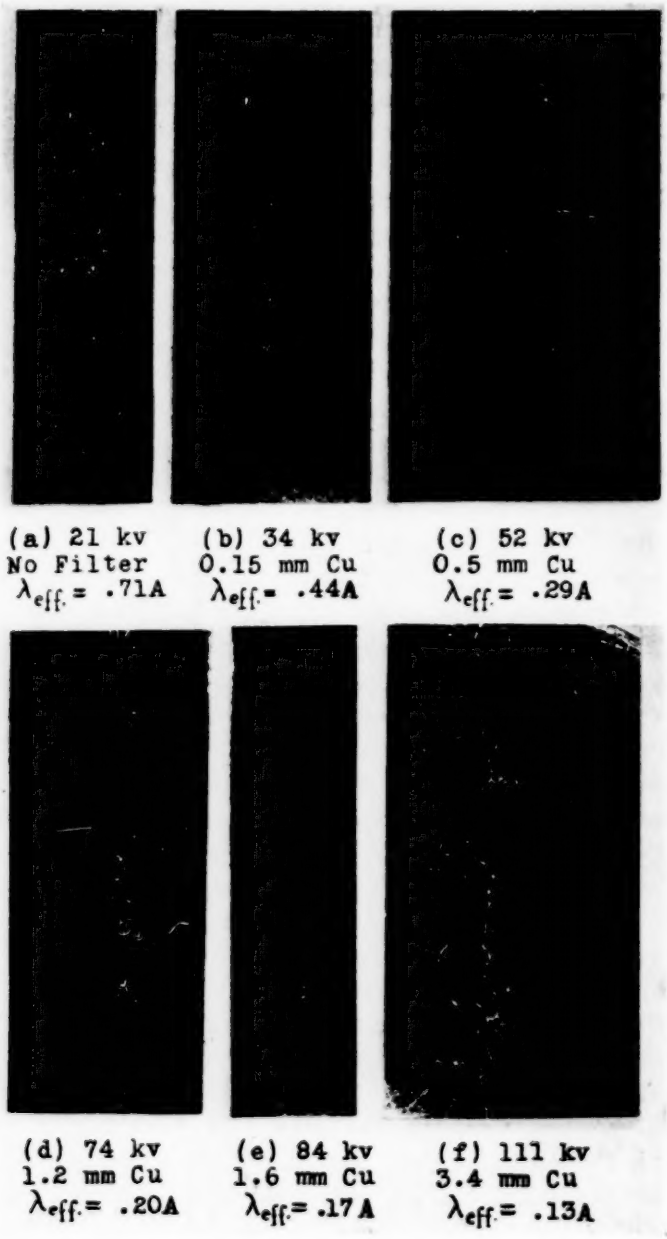

Plate I. The x-rays pass from top to bottom. In addition to the copper filter, they traverse glass walls 4 mm thick. For the short waves the shorter (R) tracks increase rapidly in length and number. Thus while in (a) nearly all are P tracks, in (f) nearly all are R tracks.

quanta, and τ to the number of quanta spent in exciting photo-electrons, per centimeter path of the x-rays through the air.

In Table I we have recorded the results of the examination of the best 14 of a series of 30 plates taken at different potentials. The potentials given in column 1 of this table are based on measurements with a sphere gap. The potential measurements required corrections due to a slight warping of the frame holding the spheres, and to the lowering of the line voltage when the condenser was charged for the illuminating spark. The latter error was eliminated in the later photographs, at 34, 21, and 74 kv, and the former error was corrected by a subsequent measurement of the sphere gap distances, checked by a measurement of the lengths of the P tracks obtained at the lowest potential. The probable errors of potential measurements are thus unfortunately large, amounting to perhaps 10 percent in every case except that of 74 kv, which is probably accurate to within 5 per cent.

TABLE I

Number of tracks of types R and P.

Potential	Effective wave-length	Total tracks N	R tracks N_R	P tracks N_P	N_R/N_P	σ/τ
21kv	.71A	58	5	49	0.10	0.27
34	.44	24	10	11	0.9	1.2
52	.29	46	33	12	2.7	3.8
74	.20	84	74	8	9	10
84	.17	73	68	4	17	17
111	.13	79	72	1	72	32

The effective wave-lengths as given in column 2 are the centers of gravity of the spectral energy distribution curves after taking into account the effect of the filters employed. Because of the strong filtering, the band of wave-lengths present in each case is narrow, and the effective wave-length is known nearly as closely as the applied potential.

All the tracks originating in the path of the primary beam are recorded in column 3. Of these, the nature of some was uncertain. At the lower voltages it was difficult to distinguish the R tracks from the "sphere" tracks which Wilson has shown are often produced near the origin of a β-ray track by the fluorescent K rays from the oxygen or nitrogen atoms from which the ray is ejected. At the highest voltage the length of some of the R tracks is so great as to make it difficult to distinguish them from the P tracks. The numbers of R and P tracks shown in columns 4 and 5 are those of the tracks whose nature could be recognized with considerable certainty, the uncertain ones not being counted. This procedure probably

makes the values of N_R/N_P in column 6 somewhat too small for the lower potentials and somewhat too great for the higher potentials.

The values of σ and τ given in column 7 are calculated from Hewlett's measurements[8] of the absorption of x-rays in oxygen and nitrogen. We have taken from his data the value of τ for 1 A to be 1.93 for air, and to vary as λ^3. The difference between the observed value of $\mu=\tau+\sigma$ and this value of τ gives the value of σ which we used.

The surprisingly close agreement between the observed values of N_P/N_R and the values of σ/τ we believe establishes the fact that the *R tracks are associated with the scattering of x-rays.* In view of the evidence that each truly absorbed quantum liberates a photo-electron or P track,[9] the equality of these ratios indicates that *for each quantum of scattered x-rays about one R track is produced.*

The fact that for the greater wave-lengths the ratio N_R/N_P seems to be smaller than σ/τ may mean that not all of the scattered quanta have R tracks associated with them. This would be in accord with the interpretation which has been given of the spectrum of scattered x-rays. The modified line has been explained by assuming the existence of a recoil electron, and the unmodified line as occurring when the scattering of a quantum results in no recoil electron. On this view the fact that the unmodified line is relatively stronger for the greater wave-lengths goes hand in hand with the observation that N_R/N_P is less than σ/τ for the greater wave-lengths. In view, however, of the meager data as yet available on this point, we do not wish to emphasize this correspondence too strongly.

Ranges of the R tracks. The range of the recoil electrons has been calculated on the basis of two alternative assumptions.[10] First, assuming that the electron recoils from a quantum scattered at a definite angle, its energy is found to be

$$E=h\nu\frac{2\alpha\cos^2\theta}{(1+\alpha)^2-\alpha^2\cos^2\theta}, \tag{2}$$

where $\alpha=h\nu/mc^2$, and θ is the angle between the primary x-ray beam and the direction of the electron's motion. This energy is a maximum when $\theta=0$, and is then,

$$E_m=h\nu\frac{2\alpha}{1+2\alpha}. \tag{3}$$

[8] C. W. Hewlett, Phys. Rev. **17**, 284 (1921)

[9] See, e. g., A. H. Compton, Bull. Nat. Res. Council No. 20, p. 29, 1922

[10] See Compton and Hubbard, loc. cit.[7]

The second assumption is that the R electron moves forward with the momentum of the incident x-ray quantum. In this case the energy acquired is

$$E' = h\nu \cdot \tfrac{1}{2}\frac{a}{1+2a}(1-\tfrac{1}{4}a^2+\cdots) . \quad (4)$$

Eq. (3) was found to agree considerably better than Eq. (4) with Wilson's experimental results.

The lengths of the tracks shown on our photographs could be estimated probably within 10 or 20 per cent. These measured values, reduced to a final pressure of 1 atmosphere, are summarized in Table II. In column 2 are recorded the lengths of the longest tracks observed at each potential. S_m is the range calculated from Eq. 3, using C. T. R. Wilson's result[1] that the range of a β-particle in air is $V^2/44$ mm, where V is the potential in kilovolts required to give the particle its initial velocity, and the frequency ν employed is the maximum frequency excited by the voltage applied to the x-ray tube. S' is similarly calculated from Eq. (4).

TABLE II

Maximum lengths of R tracks.

Potential	Observed	Calc. (S_m)	Calc. (S')
21kv	0mm	0.06mm	0.004mm
34	0	0.3	0.02
52	2.5	1.8	0.1
74	6	6	0.4
88	9	12	0.7
111	24	25	1.5

It is evident that the observed lengths of the R tracks are not in accord with the quantity S' calculated from Eq. (4). They are, however, in very satisfactory agreement with the values of S_m given by Eq. (3). This result agrees with the conclusion drawn from Wilson's data,[11] but is now based upon more precise measurements. It follows that *the momentum acquired by an R particle* is not merely that of the incident quantum, but *is the vector difference between the momentum of the incident and that of the scattered quanta.*[12]

This conclusion is supported by a study of the relative number of tracks having different ranges. If the maximum range of the recoil electrons is S_m, Compton and Hubbard find[7] that the probability that the length of a given track will be S is proportional to

$$(2\sqrt{S/S_m}+\sqrt{S_m/S}-2) . \quad (5)$$

[11] Compton and Hubbard, loc. cit.,[7] p. 449.

[12] That this is true for the β-rays excited by γ-rays has been shown in a similar manner by D. Skobeltzyn, Zeits. f. Phys. **28**, 278 (1924).

This expression assumes that the exciting primary beam has a definite wave-length. To calculate the relative number of tracks for different relative lengths to be expected, we have averaged this expression by a rough graphical method over the range of wave-lengths used in our experiments. These calculated values are given in the last column of Table III, for the relative ranges designated in column 1. A comparison of these

TABLE III

Relative lengths of R tracks.

Range of S/S_M	Per cent of R tracks within this range					
	52kv	74kv	88kv	111kv	Mean	Calc.
0- .2	44	66	60	54	56	53
.2- .4	34	20	26	32	28	22
.4- .6	19	8	4	8	10	14
.6- .8	0	3	5	3	3	8
.8-1.0	3	3	5	3	3	3

calculated values with the observed relative ranges shows a rather satisfactory agreement throughout. It will be noted further that the probabilities of tracks of different relative ranges is found to be about the same for x-rays excited at different potentials. This is in accord with the theoretical expression (5) for the probability, which is independent of the wave-length of the x-rays employed.

Angles of ejection of R tracks. On the view that the initial momentum of an R electron is the vector difference between the momenta of the incident and the scattered quantum, it is clear that these electrons should start at some angle between 0 and 90° with the primary beam. The probability that a given track will start between the angles θ_1 and θ_2 is on this hypothesis,[13]

$$\int_{\theta_1}^{\theta_2} P_\theta d\theta = 3ab \int_{\theta_1}^{\theta_2} \frac{a^2 \tan^4\theta + b^2}{(a \tan^2\theta + b)^4} \frac{\sin\theta}{\cos^3\theta} d\theta \,, \tag{6}$$

where $a = (1 + h\nu/mc^2)^2$, and $b = (1 + 2h\nu/mc^2)$.

In our photographs only those taken at 111 kilovolts have tracks long enough to determine the initial direction with sufficient accuracy to make a reliable test of this expression. In all, the directions of 40 tracks were estimated, with the results tabulated in the second column of Table IV. In view of the fact that the photographs were stereoscopic, it was possible to estimate the angles in a vertical plane roughly, though not closer perhaps than within 10 or 15°. The values in the third column are calculated from Eq. (6). It is especially to be noted that, in accord with the

[13] See Compton and Hubbard, loc. cit.,[7] Eq. (14).

theory, no R tracks are found which start at an angle greater than 90° with the primary x-ray beam. In view of the small number of tracks observed and the approximate character of the angular estimates, the agreement between the two sets of values is as close as could be expected.

A more searching test of the assumption that the R tracks are electrons which have recoiled from scattered quanta is a study of the relative ranges of the tracks starting at different angles. (See columns 4 and 5 of Table IV.) The calculated ranges in column 5 are based on Eq. (2) for

TABLE IV

Number and range of R tracks at different angles, for 111 kv x-rays.

Angle of emission	Per cent of total number (obs.)	(calc.)	Average range (obs.)	(calc.)
0°-30°	34	28	9 mm	11 mm
30°-60°	39	50	4	4
60°-90°	27	22	0.9	0.3

the energy at different angles. In this calculation the effective wave-length, as estimated in connection with Table I, is employed. It will be seen that the observed ranges of the tracks ejected at small angles are much greater than that of those ejected at large angles, in substantial agreement with the theory.

It is worth calling particular attention to the fact that in comparing the theoretical and experimental values in these tables, no arbitrary constants have been employed. The complete accord between the predictions of the theory and the observed number, range, and angles of emission of the R tracks is thus of especial significance.

The evidence is thus very strong that there is about one R track or recoil electron associated with each quantum of scattered radiation, and that this electron possesses, both in direction and magnitude, the vector difference of momentum between the incident and the scattered x-ray quantum. Our results therefore afford a strong confirmation of the assumptions used to explain the change in wave-length of x-rays due to scattering, on the basis of the quantum theory.

RYERSON PHYSICAL LABORATORY,
UNIVERSITY OF CHICAGO.
November 15, 1924.

QUANTUM THEORY OF THE UNMODIFIED SPECTRUM LINE IN THE COMPTON EFFECT

By G. E. M. Jauncey

Abstract

The theory is based on the following assumptions: (a) The energy of the primary quantum plus the kinetic energy of the electron in its Bohr orbit (supposed circular) is equal to the energy of the scattered quantum plus the kinetic energy of the recoil electron after removal from the Bohr orbit and before it has escaped from the electrostatic field of the atom; (b) the vector sum of the momenta of the primary quantum and the electron in its orbit is equal to the sum of the momenta of the scattered quantum and the recoil electron just after removal from its orbit; (c) in order for the scattering to take place according to (a) and (b) the difference between the energies of the primary and scattered quanta must at least equal the binding energy of the electron in its Bohr orbit. From these assumptions it is found that there are certain positions of the electron in its orbit from which the electron cannot be ejected by the primary quantum. In these positions the mass of the whole atom is added to that of the electron, and the change of wave-length is negligible. For MoKα rays scattered by the K electrons of C, the theory indicates that there are no unmodified rays scattered at angles less than 23°, and that the change of wave-length of the modified rays scattered at 90°, lies between .01 and .06 A. These conclusions are in general agreement with experimental results of A. H. Compton and of Clark, Duane and Stifler.

I. Introduction

THE experiments of Compton[1], Ross[2], Compton and Woo[3], and others on the change of wave-length produced when x-rays are scattered, show that part of the rays are scattered with and part without change of wave-length. Compton calls the former the modified, and the latter the unmodified rays. The modified x-rays show a change of wave-length in accord with the formula given in Compton's quantum theory of scattering,[4]

$$\lambda_\phi - \lambda_0 = h(1-\cos\phi)/mc, \tag{1}$$

where ϕ is the angle of scattering. The unmodified scattered rays are however not in agreement with this theory. Compton in a later paper[5] suggests that the existence of the unmodified rays may be explained on one of two hypotheses. The first hypothesis is that the binding energy

[1] A. H. Compton, Phys. Rev. **22,** 408 (1923)
[2] P. A. Ross, Phys. Rev. **22,** 201 and 524 (1923)
[3] Compton and Woo, Proc. Nat. Acad. Sci. **10,** 271 (1924)
[4] A. H. Compton, Phys. Rev. **21,** 483 (1923)
[5] A. H. Compton, Phil. Mag. **46,** 897 (1923)

of the electron is such that the energy imparted to the electron during the process of scattering is insufficient to eject it from the atom; while the second hypothesis is that the primary quantum spreads itself over several electrons and that the quantum is therefore scattered by a group of electrons, the group having a mass of several times that of a single electron. Compton[5] favors the second hypothesis. It seems peculiar however that electrons should sometimes act singly and at other times in groups. Further if there is any truth in the second hypothesis then there should be scattering by groups of two, three, and more electrons. These groups would give one-half, one-third, and so on, respectively, of the change of wave-length predicted by Eq. (1). There is however no experimental evidence that there are modified lines between the unmodified line and the modified line corresponding to Eq. (1). It appears therefore that the second hypothesis is untenable.

Another fact which is unexplained by Compton's simple theory is that the modified spectrum line always has a width greater than that of the unmodified spectrum line and also than that of the primary spectrum line. Some of the excess width of the modified spectrum line is due to the variation of ϕ in Eq. (1). However this explains only a small part of the excess width. In a recent paper[6] the writer has been able to explain qualitatively this width by taking account of the motion of the electrons in their Bohr orbits in the atoms of the scattering substance. The change of wave-length for a given scattering angle then varies with the position of the electron in its Bohr orbit at the time of being hit by the primary x-ray quantum. This suggests that there may be certain positions of the electron in its orbit from which the impinging x-ray corpuscle or quantum may be unable to eject it. In this case the mass of the whole atom would be added to that of the electron. This would cause m in Eq. (1) to be large and therefore the change of wave-length to be negligible. By slightly altering the assumptions given in the paper on the width of the modified spectrum line[6] it is possible to explain the existence of the unmodified rays and also the width of the modified spectrum line. The theory will now be developed.

II. Theory

Assumption I.—The energy of the primary x-ray corpuscle plus the kinetic energy of the electron in its Bohr orbit immediately before impact is equal to the energy of the scattered corpuscle plus the kinetic energy of the recoil electron immediately after impact and before the

[6] G. E. M. Jauncey, Phil. Mag. in print, and Phys. Rev. **24**, 204 (1924)

recoil electron has moved an appreciable distance from the position in the Bohr orbit at which it was struck by the primary x-ray corpuscle.

Let us suppose for simplicity that the Bohr orbit of the electron in the atom is circular. The writer has shown[6] that the momentum p of the electron in a circular orbit is given by

$$p=(mc\cdot\sqrt{2a_s-a_s^2})/(1-a_s) \tag{2}$$

where $a_s=h/mc\lambda_s$ and λ_s is a critical absorption wave-length of the scattering substance. Also it may be shown that the kinetic energy K of the electron in a circular Bohr orbit is given by

$$K=mc^2a_s/(1-a_s)\ . \tag{3}$$

Applying assumption I we therefore have

$$hc/\lambda_0+K=hc/\lambda_\phi+mc^2\{1/\sqrt{1-\beta^2}-1\}\ , \tag{4}$$

where λ_0 is the wave-length of the primary x-rays, λ_ϕ that of the scattered x-rays, and βc is the velocity of the recoil electron immediately after being removed from its Bohr orbit. It should be noted that βc is not the velocity of the electron after it escapes from the electrostatic field of the atom.

Assumption II.—The vector sum of the momentum of the primary x-ray corpuscle and that of the electron in its Bohr orbit before impact is equal to the vector sum of the momentum of the scattered x-ray corpuscle and that of the recoil electron immediately after impact and before it escapes from the electrostatic field of the atom.

Referring to Fig. 1, the direction of the primary x-rays is along OX; OA represents the momentum of the primary x-ray corpuscle; OB represents the momentum of the scattered x-ray corpuscle; AC that of the electron before impact, and BC that of the electron after impact. OB is in the plane XOY, while BC and AC are not necessarily in this plane; AD is the projection of AC on the plane XOZ; ψ and θ are the angles CAD and XAD respectively, and ϕ is the angle of scattering.

We now find BC^2 which represents $m^2\beta^2c^2/(1-\beta^2)$, the square of the momentum of the recoil electron, and we have, after dividing by m^2c^2,

$$\begin{aligned}\beta^2/(1-\beta^2)=a_0^2+a_\phi^2+b^2+2a_0\,b\cos\psi\cos\theta-2a_0a_\phi\cos\phi\\ -2a_\phi\,b\cos\psi\cos\phi\cos\theta-2a_\phi\,b\sin\psi\sin\phi\ ,\end{aligned} \tag{5}$$

where $a_0=h/mc\lambda_0$, $a_\phi=h/mc\lambda_\phi$ and $b=p/mc$.

From Eq. (4) we also have, after dividing throughout by m^2c^4,

$$\beta^2/(1-\beta^2)=a_0^2+a_\phi^2+B^2+2a_0+2B-2a_\phi+2a_0B-2a_0a_\phi-2a_\phi B \tag{6}$$

where $B=K/mc^2$. By equating the right hand sides of Eqs. (5) and (6) we may solve for a_ϕ. However since $a_\phi/a_0=\lambda_0/\lambda_\phi$ we shall write the solution in the form,

$$l=\frac{u-v(\cos\psi\cos\theta\cos\phi+\sin\psi\sin\phi)}{1-v\cos\psi\cos\theta} \tag{7}$$

where $l=\lambda_\phi/\lambda_0$, $u=1+a_0(1-a_s)\operatorname{vers}\phi$, $v=\sqrt{2a_s-a_s^2}$.

For circular orbits the length of AC (Fig. 1) is constant and therefore the locus of C is a sphere. In Eq. (7) u and v are constants for a given value of the scattering angle ϕ. We may take v as representing the length of AC; then the value of l is a function of the angles ψ and θ which give

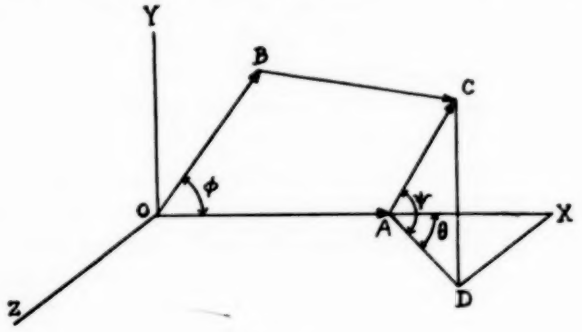

Fig. 1.

the direction of AC. Let us move the origin of coordinates to A; then, if x, y and z are the coordinates of C, we have $v\cos\psi\cos\theta=x$ and $v\sin\psi=y$ and hence, substituting in Eq. (7),

$$l=\frac{u-x\cos\phi-y\sin\phi}{1-x}. \tag{8}$$

For a given value of ϕ, we have from Eq. (8) that the surface $l=$constant is a plane. Further, since there is no term in z in Eq. (8), the plane $l=$constant is parallel to the z axis. Hence the locus of C for $l=$constant on the sphere $x^2+y^2+z^2=v^2$ is the circle where the plane $l=$constant cuts the sphere. The maximum and minimum values of l, and therefore of $\lambda_\phi(\phi=\text{constant})$, are for those values of l which cause two of the planes given by Eq. (8) to touch the sphere. Since these planes are parallel to the z axis the problem reduces to one of two dimensions. The condition that the straight line, Eq. (8), touches the circle $x^2+y^2=v^2$ is that

$$l^2(1-v^2)-2l(u-v^2\cos\phi)+u^2-v^2=0 \tag{9}$$

Solving Eq. (9) for l we have

$$l=\frac{u-v^2\cos\phi\pm v\sqrt{1+u^2-2u\cos\phi-v^2\sin^2\phi}}{1-v^2}. \tag{10}$$

Let l_1 be the maximum value of l as given by Eq. (10) and l_2 the minimum value. Then the maximum change of wave-length on scattering for a given value of ϕ is $\lambda_\phi-\lambda_0=(l_1-1)\lambda_0$, while the minimum change of wave-length is $\lambda_\phi-\lambda_0=(l_2-1)\lambda_0$. On our first and second assumptions the change of wave-length of the scattered x-rays may have any value between these extreme values. So far we have not considered the binding energy of the electron except in so far as we have used it to obtain the momentum of the electron before scattering in its Bohr orbit. Now, however, we take account of the binding energy in the following assumption.

Assumption III.—In order that the scattering process may take place according to Assumptions I and II the kinetic energy of the electron immediately after being hit must be great enough to overcome the binding energy of the electron in its Bohr orbit.

This assumption restricts the possible values of $\lambda_\phi-\lambda_0$. The least possible value of λ_ϕ is such that the energy of the primary x-ray corpuscle equals that of the scattered x-ray corpuscle plus the binding energy of the electron, or

$$hc/\lambda_0=hc/\lambda_\phi+hc/\lambda_s\,. \tag{11}$$

This gives the least possible value of $\lambda_\phi-\lambda_0$ as equal to $\lambda_0^2/(\lambda_s-\lambda_0)$. Let the least possible value of l be designated by l_3; then

$$l_3=\lambda_s/(\lambda_s-\lambda_0)\,. \tag{12}$$

For those directions of AC (Fig. 1) which make $l<l_3$, the electron is not ejected from its Bohr orbit and the mass of the whole atom is added to that of the electron so that scattering takes place without change of wave-length. This type of scattering occurs for all values of the scattering angle ϕ for which $l_2<l_3$.

The number of x-ray corpuscles scattered at a given angle ϕ for which l is between the values l and $l+dl$ is proportional to the area on the sphere $x^2+y^2+z^2=v^2$ between the planes (see Eq. 8) $l=l$ and $l=l+dl$. This area is proportional to the difference between the perpendiculars from A (Fig. 1) on the planes $l=l$ and $l=l+dl$. The perpendicular from A on the plane $l=l$ is

$$P=(l-u)/\sqrt{1-2l\cos\phi+l^2}\,. \tag{13}$$

The area on the sphere between $l=l_1$ and $l=l_3$ is

$$A_{13}=k\int_{l_1}^{l_3}dP=k\left[P\right]_{l=l_1}^{l=l_3}, \tag{14}$$

where k is a constant of proportionality. Similarly the area on the sphere between $l=l_3$ and $l=l_2$ is

$$A_{32}=k\left[P\right]_{l=l_3}^{l=l_2} \tag{15}$$

The ratio of A_{13} to A_{32} gives the ratio of the number of modified to that of the unmodified x-ray corpuscles scattered at a given angle ϕ. However each of the modified x-ray corpuscles has less energy than an unmodified corpuscle. As an approximation we may take the average value of l for the modified corpuscles as being the arithmetic mean of l_1 and l_3 so that on the average a modified corpuscle has an energy of $2/(l_1+l_3)$ times that of an unmodified corpuscle. The ratio of the energy of the modified rays to that of the unmodified rays scattered at a given angle ϕ is then

$$E_{mod}/E_{unmod}=2A_{13}/(l_1+l_3)A_{32}\ , \tag{16}$$

l of course having the value unity for the unmodified rays.

The intensity of a certain wave-length may be defined as being measured by $dE/d\lambda_\phi$ or by dE/dl. The energy dE is proportional to dP/l, since dP is proportional to the area on the sphere between $l=l$ and $l=l+dl$ from which the modified x-ray corpuscles come, and l is inversely proportional to the energy of each corpuscle. Hence the intensity of the wave-length λ_ϕ is given by $I=\text{constant}\times(dP/dl)/l$.
Hence from Eq. (13) we have

$$I=\text{constant}\times\frac{1-(l+u)\cos\phi+lu}{l(1-2l\cos\phi+l^2)^{3/2}}\ . \tag{17}$$

III. Application to Experiment

For molybdenum Kα x-rays scattered by the K electrons of carbon we have $\lambda_0=0.71$ A and $\lambda_s=45$ A, making $a_0=0.034$ and $a_s=0.00054$. In this case we have a_0 fairly small and a_s very small so that Eq. (10) may be written in the approximate form

$$l=1+a_0\ \text{vers}\ \phi\pm 2\sqrt{2a_s}\sin\tfrac{1}{2}\varphi\ . \tag{18}$$

Hence for scattering at 90° by the K electrons of carbon $l=1.034\pm0.046$. Now the least possible value of l other than unity according to assumption III is $\lambda_s/(\lambda_s-\lambda_0)$ or 1.016. Hence $l_1=1.080$, $l_2=0.988$, and $l_3=1.016$. There is in this case therefore both a modified and an unmodified ray. Substituting values in Eq. (16) we have the ratio of the energies equal to 2.2. A curve is given in Fig. 2 showing the variation of the ratio E_{mod}/E_{unmod} with the scattering angle ϕ. It is of interest to note that the ratio becomes zero at $\phi=23°$, hence for $\phi<23°$ there are no modified

rays. Above 23° the ratio has a finite value and becomes larger as ϕ increases to 180°. This is qualitatively in accord with Compton's curves.[1]

Giving l in Eq. (17) values between 1.016 and 1.080 and putting $\phi = 90°$ we may plot the curve between I and λ_ϕ since l is proportional to λ_ϕ. This plot is represented by the full curve of Fig. 3. It is seen that the intensity is greatest for the smallest possible wave-length of the modified x-rays. The full curve of course could only be realized experi-

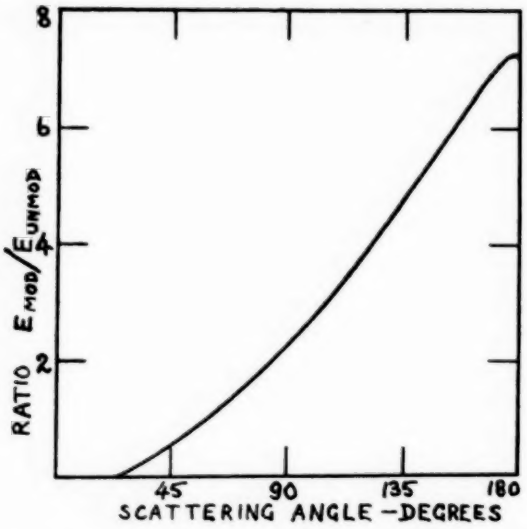

Fig. 2. Ratio of the energies in the modified and unmodified lines for varying angles.

mentally if the x-ray spectrometer had infinite resolving power, and also if the reflecting power of the crystal were the same for all wave-lengths. With an actual spectrometer the experimental curve would be more like the broken curve in Fig. 3. It is interesting to note that the theoretical curve begins at a change of wave-length equal to $\lambda_0^2/(\lambda_s - \lambda_0)$, which has been noted experimentally by Clark, Duane and Stifler[7] and has been explained by Duane on the basis of tertiary radiation.

In a previous paper[6] the formula for the width of the modified spectrum line was given as $\delta\lambda_\phi = 4\lambda_0\sqrt{2a_s}\sin\frac{1}{2}\phi$. This formula is valid for small values of a_s if $l_2 > l_3$. If however $l_3 > l_2$ then the width is smaller and is given by

$$\delta\lambda_\phi = (l_1 - l_3)\lambda_0 \,. \tag{19}$$

[7] Clark, Duane and Stifler, Proc. Nat. Acad. Sci. **10**, 148 (1924)

The theoretical width of the modified line when MoKα x-rays are scattered at 90° by the K electrons of carbon is seen from Fig. 3 to be 0.045 A.

In conclusion it should be noted that the formulas developed in this paper must be taken only as approximations. Experimental curves of I against $\lambda_\phi - \lambda_0$ are made up of curves for the scattering from the L, M etc., electrons as well as the K electrons. Then, as regards the L, M etc., electrons, some of these move in elliptic orbits, whereas we have considered only circular orbits. Then again for assumptions I and II to have any basis in fact, the time of action between the primary x-ray

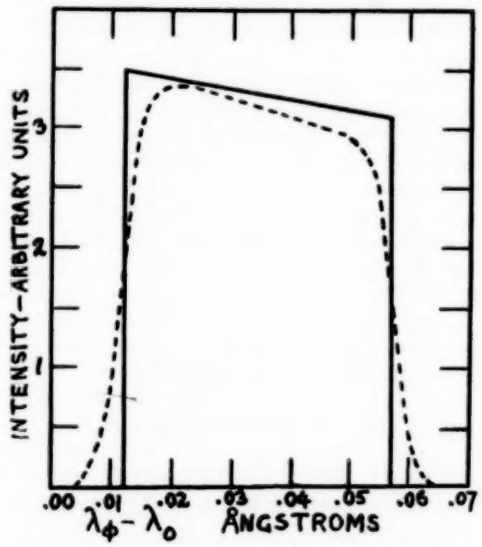

Fig. 3. Scattering of Mo Kα x-rays by K electrons of C at 90°.

corpuscle and the electron must be small compared with the period of revolution of the electron in its Bohr orbit. It would not be surprising therefore if the formulas deviated considerably from the experimental facts when applied to scattering from other than light elements. However in spite of the approximate nature of the paper the writer has been able to show the possibility of explaining the existence of the unmodified x-rays on a corpuscular theory and without having to resort to interference produced by one quantum being scattered by a group of electrons as suggested by Compton.[5]

WASHINGTON UNIVERSITY, ST. LOUIS,
November 29, 1924.

SOFT X-RAYS FROM IRON

By Charles H. Thomas

Abstract

Critical potentials of iron to 900 volts, determined photo-electrically.—Soft x-radiation from a polished iron target bombarded by electrons from a filament heated by a current constant to .01 per cent, produced a photo-electric current from a platinum semi-cylinder which was so placed that all the radiation from the target fell on it and which was protected from stray electricity by a system of radially disposed nickel vanes charged alternately positively and negatively. A vacuum of 10^{-6}mm pressure or better was maintained. When the ratio of the photo-electric current to the thermionic bombarding current was plotted as a function of the exciting voltage a number of breaks appeared. From the similarity of the curves thus obtained to those obtained with gases, breaks at radiation potentials were distinguished from those at ionization potentials. The fact that radiation excited by 2.3 volt electrons produced a photo-electric current, can be explained by taking Einstein's complete equation $h\nu = e(V+\Phi)$ where Φ is the *work function* of iron whose value is calculated to be 5 volts. Correcting for this, about 23 *radiation potentials* were located at 7.3, 14.1, 16.5, 24.3, 28.8, 34.3, 48, etc. volts, and 9 *ionization potentials* at 11.1, 19.4, 41.2, etc., volts. The ionization potentials at 818.5, 704.3 and 54.6 volts are identified with the lines L_I, L_{III}, and M_{III}.

Introduction

A CONSIDERATION of the $eV = h\nu$ relationship, together with the known photo-electric properties of platinum, shows that radiation excited by 5 volt electron impacts is of sufficiently short wave-length to produce photo-electric emission from platinum. However, the observers[1-11] who used the general method of measuring the photo-electric current caused by the radiation from a metal bombarded by electrons, have failed to obtain any photo-electric emission from radiation excited by less than 12.5 volts and no definite results have been reported below

[1] Richardson and Bazzoni, Phil. Mag. **42,** 1015 (1921)
[2] Kurth, Phys. Rev. **18,** 461 (1921)
[3] Horton, Andrewes and Davies, Phil. Mag. **46,** 721 (1923)
[4] Lukirsky, Phil. Mag. **47,** 466 (1924)
[5] Rollefson, Phys. Rev. **23,** 35 (1924)
[6] Boyce, Phys. Rev. **23,** 575 (1924)
[7] Bazzoni and Chu, Jour. Franklin Institute **197,** 183 (1924)
[8] Hughes, Phil. Mag. **43,** 145, (1922)
[9] McLennan and Clark, Proc. Roy. Soc. A **102,** 389 (1923)
[10] Holweck, Ann. der Phys. **17,** 5 (1922)
[11] Holtsmark, Phys. Zeit. **23,** 252 (1923)

16 volts. Milliken[12] by spectroscopical methods has found lines in the spectrum which correspond to voltages even lower than 12.5 volts. Therefore it would seem probable that critical potentials should be observed in the low voltage region if sufficient radiation energy could be made to fall on the photo-electric detecting plate.

The ionization of residual gas in the experimental tubes has frequently led to difficulties and errors in the low voltage regions. Therefore any method for further investigation of this problem at low voltages must provide for the elimination of this error. A modification of the type of apparatus as used by Kurth was adopted because it seemed to offer the best possibilities of success.

Apparatus and Procedure

The essential part of the apparatus is shown in Fig. 1. The cathode source of electrons F, consisting of several turns of helically wound 15 mil

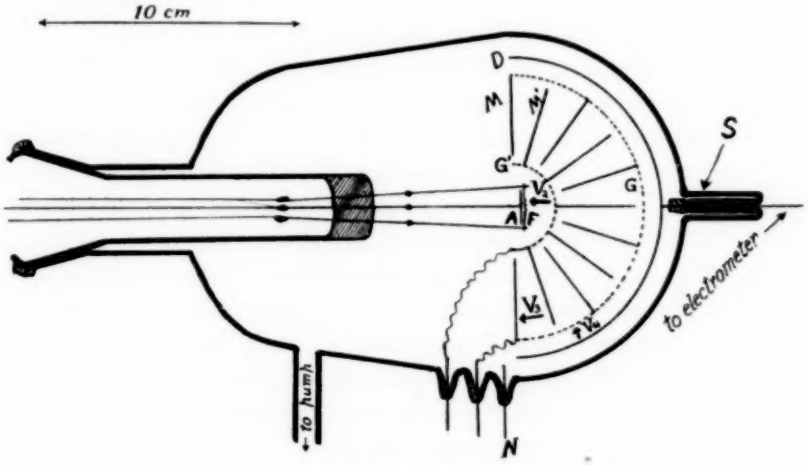

Fig. 1. Apparatus.

(0.375 mm) tungsten wire, was placed 1 mm in front of the anode target A which was a highly polished iron plate 8×12 mm in size. The anode and cathode were supported on tungsten leads through the glass stem, which was fitted to the tube with a ground glass joint and sealed with De Khotinsky cement. This ground glass joint was long and was kept free from cement except at the outside, where it was kept cool by water circulation. Thus, cement vapor pressure was reduced to a minimum and its presence in the experimental tube rendered inappreciable by the diffi-

[12] Milliken, Proc. Nat. Acad. Sci. **7**, 289 (1921)

culty of its diffusion through the ground joint combined with the rapid evacuation by the pump and liquid air traps.

The nickel vanes, M and M', in the form of a hollow semi-cylinder 8 cm in diameter and 8 cm high, were charged alternately positively and negatively, the negative ones being connected to a coarse gauze G', the positive ones M being connected to a coarse gauze G which acted as a receiver for the photo-electrons. The gauzes G and G' were made of fine platinum wire and were of such coarse mesh as not to intercept any appreciable amount of the radiation. These vanes, which were rigidly held together by spotwelding, were supported on two glass rods (not shown in diagram) from the stem S. These rods were carefully wound with a few turns of fine platinum wire which was connected to earth through N, in order to prevent any surface leakage of electricity to the detecting cylinder D.

This semi-cylindrical platinum detector D surrounded the vanes at a distance of 7 or 8 mm, and was supported on a tungsten lead which connected it to the electrometer through S.

A potential V_1 of from 0 to 1500 volts between anode and cathode, was supplied by a small direct current generator and was adjusted by the potentiometer method, using sliding rheostats. This voltage was measured on a 150 volt Weston Laboratory Standard Voltmeter fitted with suitable multiplying resistances to give the proper scale, on which the applied voltage could be measured to 1/30 of one per cent. A retarding potential V_2 of 8 volts was maintained between F and G'. This was found sufficient to keep all electrons from passing through G'. A potential V_3 of 145 volts between the vanes M and M' was furnished by dry cells, and was sufficient to prevent any ions, which might be present, from reaching D. A potential V_4 of 16 volts between D and G pulled off the photo-electrons from the detecting plate.

The filament cathode was heated by a current of 10 to 12 amperes, which was supplied by high capacity lead storage cells. The voltage drop across the cathode was 2 to 2.6 volts. In the early part of this work a carbon rheostat paralleled by a sliding wire rheostat was used to regulate the cathode current but this permitted a slight erratic variation which was sufficient to cause the results to be difficult to interpret, on account of the rapid variation of the thermionic current with small changes of temperature of the cathode. Later a resistance made by immersing in kerosene a nichrome ribbon with clamped contacts gave a current constant to at least one hundredth of one per cent. However, in order to obtain such a degree of constancy the cathode current was turned

on an hour before any readings were taken, to give ample time for the equalization of the batteries.

The thermionic current, varying from 0.5 to 4 milli-amperes, was measured on a Paul Universal Test Set.

The photo-electric current was measured by the constant deflection method on a Dolezalek electrometer with a sensitivity of 2300 mm per volt, shunted by a convenient set of India ink resistances.

An apparently perfect vacuum as indicated by a sensitive McLeod gauge capable of measuring 10^{-6} mm, was maintained by a mercury diffusion pump, backed by an oil pump, and a series of three liquid air traps, two of which contained charcoal. Before each series of runs the tube and charcoal traps were baked at a temperature of 450 to 500°C for a period of three hours by a system of electric heaters. At the conclusion of this baking out process the anode was brought to a bright red heat by bombarding it with electrons. In this manner the target was freed from occluded gases.

The tube and stem were wrapped on the outside by a few turns of fine platinum wire which was connected to earth. The heater coils were earthed during readings. The tube was further protected by a metal shield which covered the heating coil box. With these precautions the possibility of electrostatic disturbances or of surface leakage of electricity from the outside was negligible.

It was possible to get sufficient electrons from the cathode when it was heated to a temperature which should have caused little evaporation of the tungsten from the cathode. However, after ten or twelve hours use, there was a slight deposit on the polished anode. This did not affect the position of the breaks but it did decrease the sharpness of the breaks to a marked degree. When the anode was freshly polished the original intensity of the breaks returned. For this reason the anode was removed frequently and polished carefully, after which it was returned to the tube as quickly as possible and a vacuum obtained so that there would be as little time for oxidation as possible.

When a very hot cathode had to be used in order to obtain sufficiently large readings for accuracy, as at the lower voltages, an electrometer deflection of 15 to 20 mm in the positive direction occurred before the anode voltage was applied. At a lower cathode temperature and with a less sensitive electrometer shunt, with which most of the readings were taken, this effect amounted to only 2 or 3 mm. This deflection was constant for a constant filament temperature and could therefore be easily allowed for by shifting the zero of the electrometer scale. This effect was due to the photo-electric emission caused by the light from the filament.

The heating current through the filament was adjusted so as to give a maximum electrometer scale deflection for each run, which consisted of thirty or less readings over the desired voltage range. By following this plan it was possible not only to keep initial conditions constant for the short period necessary to take the readings but also to obtain greater accuracy by having the readings as large as possible.

When the ratio of the photo-electric current to the thermionic current was plotted as a function of the anode voltage, curves were obtained which show marked changes of slope at critical potentials. These breaks have been interpreted as indicating critical voltages at which new types of radiation set in and the frequency has been computed from the $eV = h\nu$ relation. In the study of iron only upward breaks due to increased radiation were noted.

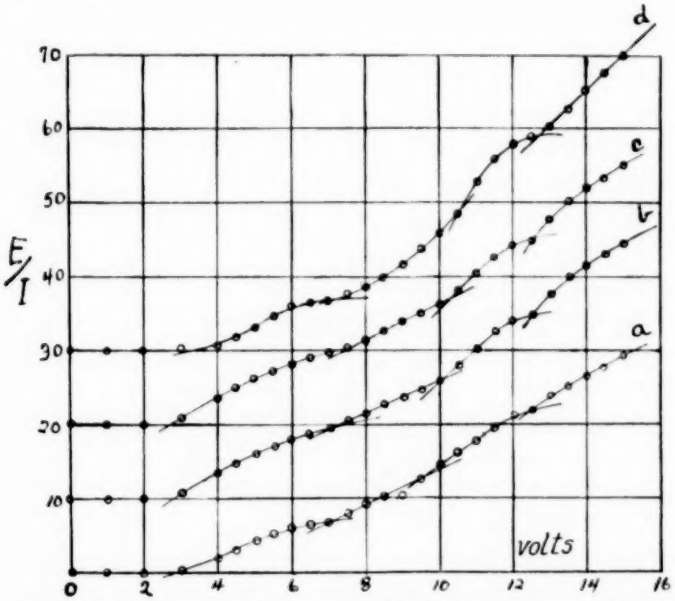

Fig. 2. Ratio of photo-electric current to thermionic current, as a function of anode voltage.

Results

Fig. 2 gives four curves for the low voltage range over which the readings were taken at half volt intervals. Here, as in the following graphs, E/I is plotted on an arbitrary scale. These curves are the results of readings of different days. Each curve shows similar breaks and agrees well with the others except for the point on curve (a) at 9 volts. This discrepancy is assumed to be due to an experimental error. The first break occurs at an average of 3.3 volts. The second, at 7.1

volts, is of a different character because the curve shows no downward curvature or decrease of slope until it reaches the following break. Strong breaks occur at 10.1 and 12.5 volts.

Fig. 3 shows the results of eight runs over the range 38 to 90 volts or less. Curves (a) and (b) were taken from results obtained when the target had been used 12 hours without polishing. Therefore these curves do not show as strong breaks as the remaining curves. Each of these curves was taken under different conditions. These results were taken

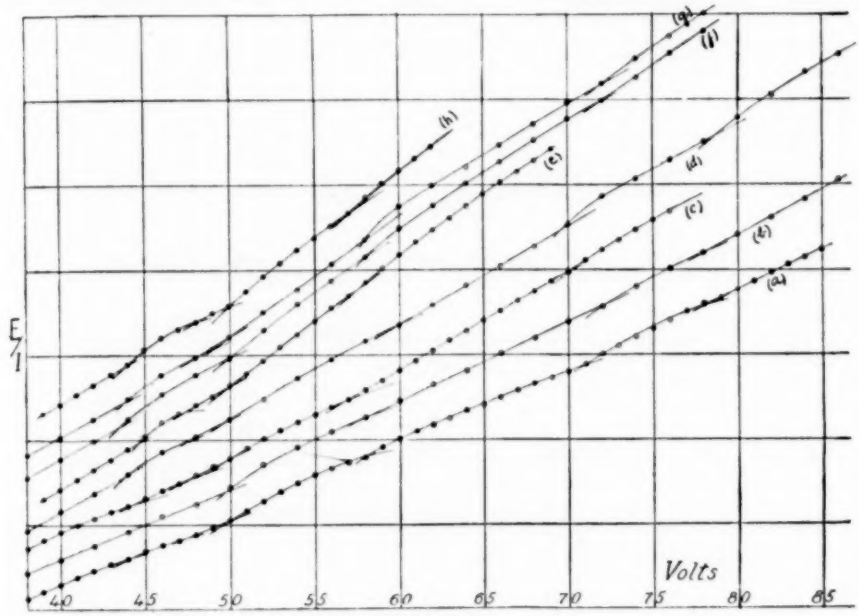

Fig. 3. Results for higher anode voltages, 38 to 87.

on five days, some with and some without fresh polishing of the target, and using three different electrometer shunts. However, their agreement comes within the limits of experimental error. A break occurs on 7 of the curves near 45 volts. Another break, which is shown on the best curves at smaller intervals, appears at 47.3 but this break is questionable because the late spring weather conditions would not permit of a final accurate check of this point.* At 50 volts a strong upward break occurs, also breaks at averaged values of 58.1, 71.3 and 78.7 volts.

Fig. 4 curve (a), the readings of which were taken at 3 volt intervals, shows breaks at 273, 285, 301, and 328 volts. Curve (b), readings at 2 volt intervals, shows breaks at 215 and 226 volts.

* Note added to proof: Since this was written the reality of this break has been verified by additional tests.

Fig. 5 curve (a), the readings of which were taken at 5 volt intervals, shows breaks at 636 and 698 volts. Because the break at 636 volts occurred on only half the curves taken, this break is questionable. Curve

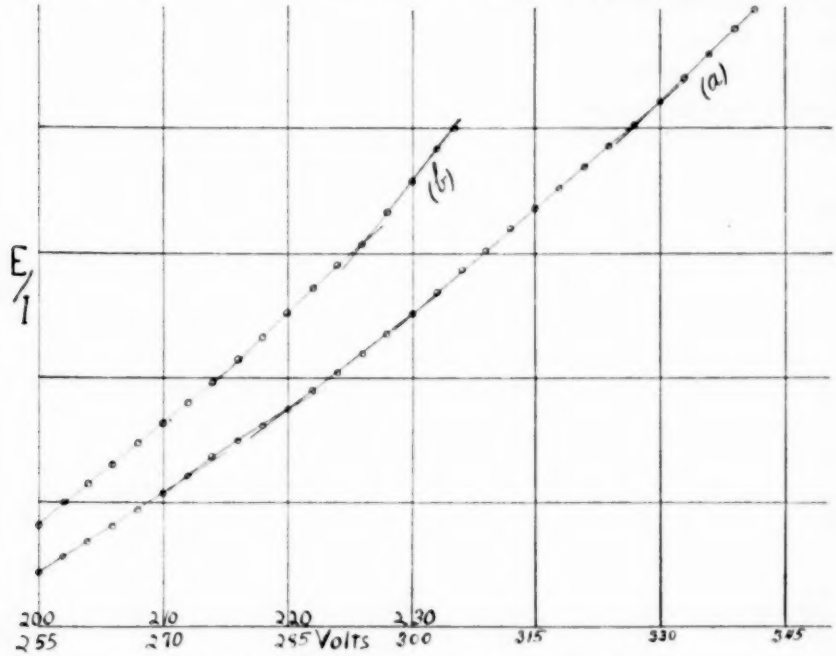

Fig. 4. Results for anode voltages 200 to 345.

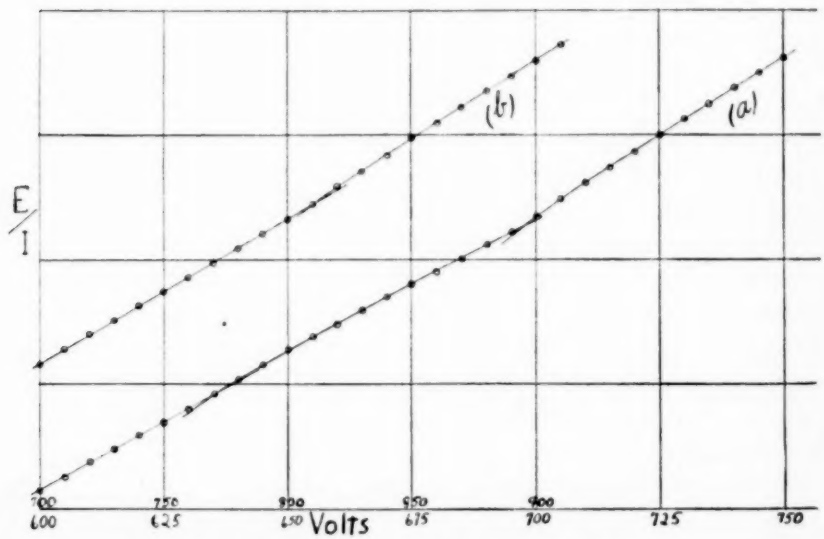

Fig. 5. Results for anode voltages 600 to 910.

(b) taken at 10 volt intervals shows a break at 812 volts. The experimental results from 812 volts to 1500 volts when plotted give an accurately straight line.

In the first column of Table I are given the corrected critical potentials. The second column gives the relative intensities of the breaks estimated

TABLE I

Critical potentials of iron

Critical potentials voltage	intens.	nature	λ	ν/R	Other observations of voltages Rollefson[5]	Kurth[2]	Horton et al.[3]	Stuhlman[17]
								3.3
7.3	2.5	R	1693.8A	.54				8.5
11.1	2.7	I	1112.1	.82				10.4
14.1	2.2	R	875.5	1.04				
16.5	2.9	R	748.1	1.22				
19.4	1.8	I	636.3	1.43	20.			
24.3	1.3	R	508.0	1.80	26.			24.3
28.8	2.5	R	428.6	2.14				
34.3	2.0	R	359.8	2.52				
41.2	2.5	I	299.6	3.04				
48.	2.4	R	257.1	3.53	46.8			45.8
51.3	1.6	R	240.6	3.78				
54.6	3.1	I	226.0	4.03		50		
62.	2.7	R	199.0	4.57				
75.3	2.2	R	163.2	5.56			73	
82.7	2.3	R	149.2	6.10	81.7			
94.8	1.3	R	130.1	7.00	95.4			
103.5	2.0	I	119.1	7.64				
112.2	1.7	R	110.	8.28	111.2			
131.8	1.9	R	93.6	9.72	130.4			
					140.9			
					147.1			
					153.4			
158.5	1.7	R	77.8	11.71	160.1			
169.4	2.3	I	72.8	12.51			166	
181.6	1.2	R	67.9	13.41				
192.	1.8	R	64.3	14.16				200
221.3	1.1	R	55.7	16.32				
228.1	2.8	I	54.1	16.83		227		
277.4	1.4	R	44.5	20.49				
288.6	1.1	R	42.8	21.31				
303.7	1.8	R	40.65	22.43				
331.	1.6	R	37.25	24.44				
					618			
639. (?)	.9	R	19.3	47.29	637			
704.3	1.5	I	17.52	52.01	697			
						757		
818.5	2.0	I	14.96	60.37				

by measuring the average change of slope at each break. Column three gives the nature of the effect producing the break, i.e. whether it is assumed to be a radiation potential R or an ionization potential I; in the

fourth column are the wave-lengths in angstrom units; in the fifth the values of ν/R where ν is the frequency and R is Rydberg's constant, and in the remaining columns are given the results obtained by previous investigators for iron. The potential in column 1 marked (?) is doubtful.

Discussion of Results

The designation R or I was made according to the nature of the break, following the analogy of the interpretation of corresponding curves for excitation of gases by electron impacts.[13,14] In gases the curve beyond a radiating potential is always concave downward, whereas beyond an ionizing potential it is straight or curved upward. It is not certain that the interpretation is the same in the present case, but at any rate, the designation will serve to differentiate between the two types of breaks.

The photo-electric current appeared when the excitation potential reached 2.5 or 3 volts and a definite break occurred at an average of 3.3 volts. Now if $eV = h\nu$ gives the frequency of the corresponding radiation, this radiation would be of too long a wave-length to produce any photo-electric emission from the platinum detector. Therefore it is necessary to seek some explanation for this discrepancy.

As an electron which has energy corresponding to the applied voltage V approaches the iron target, it is pulled in by the surface forces which give rise to the "work function." Thus the electron actually strikes the target with energy

$$\tfrac{1}{2}mv^2 = e(V + \Phi).$$

This equation may now be written

$$h\nu = e(V + \Phi)$$

where the values of the factors except Φ are known. In order to compute a value for Φ it will be necessary to turn to the study of electron emission from some other metals because little is known of the electronic emission from iron.

Dushman[15] gives the ratio X_0/δ for tungsten, tantalum and molybdenum as about .56. In this ratio, X_0 denotes the distance at which an electron leaving the metal begins to be attracted by the charge induced on the surface in accordance with Coulomb's law. Schottky[16] gives

$$\Phi_0 = (7.16 \times 10^{-8}/X_0) \text{ volts}.$$

[13] F. L. Mohler, Phil. Mag. **37**, 33 (1919)
[14] K. T. Compton, Phil. Mag. **40**, 553 (1920)
[15] S. Dushman, Trans. Amer Electrochem. Soc. **44**, 101-116 (1923)
[16] W. Schottky, Phys. Zeit. **15**, 872 (1914) and **20**, 220 (1920); Zeits. f. Phys. **14**, 63 (1923)

δ denotes the atomic diameter calculated from the atomic volume by the relation

$$\delta = (V/N)^{1/3} = 1.33 \times 10^{-8} V^{1/3} \text{cm}$$

where $N = 6.062 \times 10^{23}$ and V is the atomic volume. For iron this value is 7.1, which gives for δ the value 2.556×10^{-8} cm. From the above data Φ_0 for iron comes out 5 volts.

The observed critical potentials must be further corrected for the potential drop across the cathode, for the contact difference of potential between cathode and target, and for the initial energy of emission of the electrons from the cathode. Taking the value of Φ as 5 volts, a final correction factor of 4 volts is obtained which is believed to be correct to $\pm .2$ volts, exclusive of the uncertainty in the value of Φ.

A tabulation of the critical potentials for iron by the different observers has been made in Table I. The uncertainty of the value of the correction factor especially when a cathode of large potential drop is used, together with the failure of the other observers to take into account the work function, leads to discrepancies which make the comparison of results uncertain, especially at lower voltages. However, the results for iron of previous observers agree with the results of the writer within the limit of the correction factor (4 volts), except for the potential at 757 volts by Kurth, those at 140.9, 147.1, 153.9 and 618 volts by Rollefson and those at 3.3 and 200 volts by Stuhlman[17] who used a method of investigation different from that of the others.

Rollefson[5] tested his results for iron by an application of the combination principle to his critical potentials in order to calculate the voltages corresponding to lines of the spectrum which Milliken[12] studied spectroscopically, and he obtained values which agreed within 1 volt with Millikan's values. Because there are 83 lines of intensities 1 to 9 within the range 10 to 42 volts in the Millikan spectrum for iron, any arbitrary value from 10 to 42 would agree within .2 volt with one of these lines if they were equally spaced. This seemed to warrant further investigation. Therefore, the wave-lengths of the lines attributed entirely to iron and having an intensity of 1 or greater, were changed to corresponding volts and from these the probability that an arbitrary value would agree with the voltage of some line, was estimated. If 32 consecutive integers beginning at 10 are assumed to be results of the application of the combination principle, 90 per cent of these values will agree within 1 volt with voltages corresponding to lines found by Millikan, 80 per cent will agree within .5 volt and 50 per cent will agree within .2 volt. Unless

[17] Stuhlman, Science **56**, 344 (1922)

experimental results show much greater precision than those outlined above, the agreements obtained would not seem to have any particular significance.

The ionization potentials at 818.5, 704.3 and 54.6 volts can be identified as corresponding to the lines, L_I, L_{III} and M_{III} with ν/R values of 60.37, 52.01 and 4.03 respectively. Mohler[18] has computed from x-ray data the ν/R value of L_{III} for iron to be 52.2 and of M_{III} to be 4. He has also computed the value of L_I, using $\sqrt{L_{II}} - \sqrt{L_{III}} = .65$, to be 63. The value of L_I cannot be computed with the same accuracy as those for L_{III} and M_{III}. The values just given seem to be the only available data for the prediction of the levels for iron.

Undoubtedly some of the lower voltages correspond to lines of the N series but there is no apparent gap between the M and N series as between the L and M series. Even though the value for ν/R of 16.8 be assigned to M_I, critical potentials apparently belonging to the M series appear above this value. No definite attempt will be made at the present time to assign definite critical potentials to definite series because this work is now being continued with other metals. It is hoped that by a comparison of the results of different metals more definite conclusions may be drawn.

In conclusion the writer wishes to express his thanks to Prof. K. T. Compton, at whose suggestion this work was undertaken, for his encouragement and ever ready assistance during the course of this experiment. He also wishes to thank Dr. S. Dushman for suggesting a method of evaluation of the work function for iron.

PALMER PHYSICAL LABORATORY,
PRINCETON UNIVERSITY,
October 17, 1924

[18] K. T. Compton, and F. L. Mohler, Bull. Nat. Research Council, **9**, part I, No. 48, p. 105 (1924)

THE CRYSTAL STRUCTURE OF METALLIC TELLURIUM AND SELENIUM AND OF STRONTIUM AND BARIUM SELENIDE*

By Mabel K. Slattery

Abstract

X-ray spectrograms were made using the powder method of Hull, with monochromatic MoKα rays. Both tellurium and selenium are found to crystallize in simple triangular lattices with axial ratios 1.33 and 1.14, respectively, and with sides of unit basal triangle equal to 4.44 A and 4.34 A, respectively. In each case three atoms are grouped at each corner. The densities computed from these measurements are 6.25 and 4.84, respectively. Strontium selenide and barium selenide both have a simple cubic structure, with cube edges equal to $3.117 \pm .003$ A and $3.308 \pm .005$ A respectively. In the case of SrSe the ions at the corners are Sr^{++} and Se^{--}, and the calculated density is 4.53.

X-RAY photographs were taken by the well-known powder method described by A. W. Hull.[1] A narrow beam of monochromatic rays is passed through the powdered material and produces a pattern of lines on a film bent on an arc of a circle, at whose center the powdered material is placed. These lines are due to the reflection of the rays from the planes in the small crystals, one line for each kind of plane. From the position and intensity of the lines the crystal structure can be found.

In all of the following work the powdered sample was mixed with about five volumes of wheat flour to decrease absorption and was loaded into a glass capillary tube. The rays used were the molybdenum α doublet, obtained by filtration through zirconium.

Tellurium

Metallic tellurium is listed by Groth[2] as trigonal, isomorphous with metallic selenium.

Two photographs were taken, giving identical patterns. The observations are tabulated in Table I. The intensities were obtained by assigning to the strongest line a value of ten, and estimating the others on this basis. Using the graphs described by Hull and Davey,[3] a match was found on the single triangular lattice, at axial ratio 1.33. The values in column

* The results in this paper have been presented before American Physical Society; see Abstracts in Phys. Rev. **21**, pp. 22 and 378 (1923).

[1] A. W. Hull, Phys. Rev. **10**, 661, (1917); **17**, 571 (1921).

[2] Groth, Chemische Krystallographie, vol. 1, p. 34.

[3] Hull and Davey, Phys. Rev. **17**, 549 (1921).

3 were calculated for the plane spacings of a simple triangular lattice with axial ratio of 1.33 and with the side of unit basal triangle equal to 4.44 A.

TABLE I

Tellurium

Planes	Spacing of planes observed	Spacing of planes calculated	Estimated intensity
10.0	3.83 A	3.832 A	2
10.1, 00.1(2)	3.22	3.224	10
10.2	2.34	2.340	5
11.0	2.22	2.220	4
11.1	2.08	2.078	2
00.1(3), 10.0(2)	1.969	1.967	2
20.1	1.834	1.834	4
11.2	1.777	1.776	2
10.1(2)	1.614	1.614	2.5
12.0, 11.3, 00.1(4)	1.469	1.471	3
12.1	1.412	1.411	2
20.3, 10.4	1.377	1.378	2
12.2	1.307	1.304	1
30.1	1.267	1.256	0.3
00.1(5), 10.2(2) and 12.3, 30.2	1.171	1.171	3
10.5	1.130	1.129	0.8

The density determined from the dimensions of the unit prism comes out 2.083, taking the number of atoms associated with each unit prism as one-half. The specific gravity given by Groth is 6.233 and 6.388. This would mean that at each point of the lattice there are three atoms of tellurium, making the density from crystallographic data equal to 6.225. This has recently been confirmed by A. J. Bradley[4] who gives $a = 4.835$A, the atoms being located on Schoncke's point systems, No. 23 or 24, i.e., a right-handed or left-handed spiral around the trigonal axes. The metals bismuth[5] and antimony[6] have been found to have a similar structure but with two atoms associated with each point.

SELENIUM

Groth gives very little data for metallic selenium, except that it is hexagonal, isomorphous with metallic tellurium.

Two photographs were obtained, each giving the same pattern. Data are tabulated in Table II. A match was found on the simple triangular graph. Values for the third column are calculated for the simple triangular lattice, with an axial ratio $c = 1.14$ and with the side of unit basal triangle equal to 4.34 A.

[4] A. J. Bradley, Phil. Mag. (6) **48**, No. 285 (Sept. 1924)
[5] R. W. James, Phil. Mag. **42**, 193 (1921)
[6] Norman Tunstall and R. W. James, Phil. Mag. **40**, 233 (1920)

The density comes out 1.613 assuming one half atom per unit prism. Since the accepted specific gravity of selenium is 4.47 to 4.6, the calculations would indicate that, as in the case of tellurium, three atoms of selenium are associated with each point of the lattice. Bradley[4] has also confirmed this. The density from crystallographic data, therefore, is 4.84.

TABLE II

Planes	Spacing of planes observed	calculated	Estimated intensity
10.0	3.77 A	3.773 A	8
10.1, 00.1(2)	3.01	3.013	10
11.0	2.17	2.170	2
10.2	2.07	2.069	2.5
11.1	1.997	1.999	2
10.0(2)	1.880	1.879	0.2
20.1	1.770	1.768	1.7
11.2, 00.1(3)	1.638	1.637	1.5
10.3, 10.1(2)	1.505	1.506	1.5
12.0	1.425	1.422	1.5
11.3	1.310	1.310	0.3
10.4	1.175	1.178	0.3
11.4	1.075	1.075	0.2

COMPOUNDS OF SELENIUM

From a study[7] of the compounds of the halides with the alkali metals, using CsI and RbBr as starting points, values for the ionic radii of the monovalent elements have been found. This method might be extended to the determination of the sizes of the divalent ions, provided measurements of BaTe, SrTe, BaSe, and SrSe could be made.

Strontium selenide, a white powder which becomes reddish brown on exposure to air, was made by heating $SrSeO_3$ to a dull red heat in a stream of hydrogen. For calibration purposes, NaCl was photographed on each film with the substance analyzed.

TABLE III

Strontium selenide (No. 494)

NaCl (read)	SrSe (read)	SrSe (corrected)	Log *d*	Planes
2.85 A	3.19 A			
2.020	2.24			
1.640	1.882	1.801	.49407	111
1.419	1.574	1.561	.49443	100(2)
1.269	1.408	1.397	.49468	210
1.158	1.281	1.271	.49312	211
1.002	1.110	1.102	.49372	110
.942	1.046	1.039	.49374	221, 100(3)
.893	.991	.985	.49344	310
	.945	.940	.49382	311
	.836	.835	.49482	321

[7] W. P. Davey, Phys. Rev. **22**, 211-220 (Sept. 1923)

Two photographs were taken, measurements being made directly in angstrom units on a scale described by W. P. Davey.[8] Results for one are given in Table III.

From the planes which appear the structure is seen to be simple cubic. The mean value of logarithm of d, the side of the unit cube, found by use of probability paper is .49400, hence d is 3.119 A. The density, calculated from the dimensions of the unit cube and its weight, comes out 4.512. The other photograph gave $d = 3.116$ A, and density $= 4.544$.

A rough measurement by the displacement method for powders gave the value 4.18. The errors in the displacement method are such as to tend to make the value for the density come out too low. The agreement is, however, sufficiently close to give a check on the interpretation of the diffraction pattern.

The unit crystal of SrSe is then a simple cube of ions, with Sr^{++} and Se^{--} occupying alternate corners of a cube whose side is $3.117 \pm .003$ A.

Barium selenide was made by reducing $BaSeO_3$ with hydrogen at a red heat. Two photographs were taken. Results from one are given in Table IV.

TABLE IV

Barium selenide (No. 457)

NaCl (read)	BaSe (read)	BaSe (corrected)	Log $2d$	Planes
2.81	3.80 A	3.80 A		
1.987	3.30	3.30		
1.621	2.33	2.33		
1.404	1.990	1.994	.82042	311
1.256	1.901	1.905	.81948	111(2)
1.148	1.648	1.652	.82007	100(2)
.994	1.475	1.478	.82108	210(2)
.936	1.348	1.351	.82076	211(2)
.888	1.167	1.169	.82038	110(3)
	1.099	1.101	.81884	100(2) and 221
	1.042	1.044	.81973	310(2)
	.995	.997	.82042	311(2)
	.882	.884	.82054	321

The structure is seen to be simple cubic. The mean logarithm of $2d$ from probability curve is .82025; d then is equal to 3.305 A. The value in the fourth column is $2d$ because the logarithm which is added to the logarithm of the values of corrected measurements of BaSe has been taken for planes of higher order than the first. The second photograph gave $d \pm 3.310$ A.

Density measurements were not made because of the small amount of the sample available. Barium selenide has then a simple cubic structure of ions, with length of side of cube equal to $3.308 \pm .005$ A.

[8] W. P. Davey, J. Opt. Soc. Amer. R.S.I. **5**, (Nov. 1921)

Barium and strontium tellurides. Several attempts have been made to obtain photographs of these compounds. They were made in several different ways, including heating together in hydrogen the oxides of the metals and TeO_2 and heating a mixture of carbon and tellurate in hydrogen, with only moderate success. In every case the x-ray analysis gave photographs of metallic tellurium with additional lines which were too few and too faint to be of any use. The probability is that the telluride was decomposed after it was made, by the moisture of the air to which it was exposed while being packed into the tiny tube. There was certainly telluride present in all of the samples before they were photographed.

VASSAR COLLEGE,
October 10, 1924.

ELECTRON EMISSION FROM TUNGSTEN, MOLYBDENUM AND TANTALUM

By S. Dushman, H. N. Rowe, Jessie Ewald and C. A. Kidner

Abstract

Thremionic emission from tungsten, tantalum and molybdenum as a function of temperature.—The tubes used in these series of careful measurements, each contained a long V-shaped filament and an anode consisting of a calcium surface deposited on the wall, and were thoroughly heat treated so as to get rid of adsorbed gases. The data obtained were corrected for lead losses and for the Schottky effect. *In the case of tungsten*, specially prepared pure metal was used and the temperature scale of Worthing and Forsythe was adopted. The results for a number of filaments agree well with each other and with the equation $I = AT^2e^{-b_0/T}$ where if I is in amp./cm², A has the value 60.2 ($\log_{10}A = 1.779$), the value derived by Dushman[1] from the "chemical" constant, assuming the Sackur-Tetrode theory, and $b_0 = 52{,}600 \pm 250$, which is in good agreement with previous results. *With tantalum*, the accuracy of the results is not as great because of uncertainty as to the temperature scale, but the indication is that the value of A is the same as for tungsten (the most probable value of $\log_{10}A = 1.7 \pm .1$). Assuming the theoretical value, b_0 comes out $47{,}800 \pm 500$. *With molybdenum*, the variation in the results for different runs indicates that the surfaces were not sufficiently cleaned and were contaminated with oxide which would tend to raise the value of A. (The mean value of $\log_{10}A$ obtained is about 2.2.) However assuming $\log_{10}A = 1.779$, b_0 comes out $50{,}000 \pm 500$. *Theoretical constancy of A.* It is pointed out that theoretically A can be expected to be a universal constant only for surfaces for which the surface heat due to positive charge is zero. Experiments with coated filaments show that electronegative atoms like oxygen increase A and electropositive elements like Th and Cs decrease A.

Introduction

AS SHOWN by O. W. Richardson and subsequent investigators, thermodynamical considerations lead to an equation of the form

$$I = AT^2\epsilon^{-b_0/T} \tag{1}$$

where I = electron emission per unit area, and b_0 = work function for the emitting surface.

In a previous paper by S. Dushman,[1] it was shown that if the evaporation of electrons is regarded as analogous to that of a monatomic vapor, the value of the constant A in the above equation may be derived from that of the "chemical" constant. If we adopt the Sackur-Tetrode theory,

$$A = 2\pi k^2 me/h^3 . \tag{2}$$

[1] S. Dushman, Phys. Rev. **21**, 623 (1923)

On the other hand, Lewis, Gibson and Latimer[2] have suggested another derivation for the chemical constant which leads to the relation

$$A = \left(\frac{2^{5/2}\pi^{9/2}\epsilon^{-5/2}}{15}\right) k^2 me/h^3. \tag{3}$$

In these equations,

k = Boltzmann constant = 1.372×10^{-16} erg/degree;

m = mass of electron = 8.995×10^{-28} gm;

e = charge on electron = 4.774×10^{-10} e.s.u.;

h = Planck's constant = 6.55×10^{-27} erg. sec.

Substituting these values in the above equations and expressing I in amperes per square centimeter

$A = 60.2$ according to (2);

$A = 51.2$ according to (3).

As was furthermore shown in the paper mentioned previously,[1] it is impossible at present to decide on the basis of experimental data definitely in favor of either theory. However, if we adhere to the standard temperature scale for tungsten as established by the work of Worthing and Forsythe,[3] the electron emission data for tungsten are in better agreement with the value $A = 60.2$ amps/(cm^2 deg.^{2}).

For the purpose of calculation by ordinary logarithms, Eq. (1) can be written in the form

$$\log_{10}(I/T^2) = 1.779 - (b_0/2.303T). \tag{4}$$

If a series of emission data is taken at different temperatures for the same metal, it is possible to calculate a value of b_0 from each determination by means of Eq. (4), assuming that $\log A = 1.779$. The value of b_0 can also be obtained by plotting $\log (I/T^2)$ against $1/T$. If the equation is valid, the points thus obtained should all lie on a straight line and the value of b_0 from the slope of this line should agree with the average of the values obtained by applying Eq. (4).

The purpose of the following experiments was to determine whether this equation holds for tungsten, molybdenum and tantalum.

Description of Tubes Used for Emission Data

The tubes used for measuring electron emission were constructed as shown in Fig. 1. These were made of lime-glass and were approximately 3 cm in diameter and 20 cm in over-all length. The filament F whose

[1] Lewis, Gibson and Latimer, J. Amer. Chem. Soc. **44**, 1008 (1922)

[3] A. G. Worthing and W. E. Forsythe, Phys. Rev. **18**, 144 (1921). This scale is based on the following values: melting point of Au = 1336°K (m.p. of Pd = 1828°K) and C_1 (in Wien-Planck equation) = 14350 microns × deg. K.

emission was to be determined, was usually V-shaped and had a total length of 10 or 15 cm. The leads through the glass were of fairly heavy "dumet" wire (such as used in lamp practice), and a short length of molybdenum wire was inserted between the dumet and the filament itself. The anode was prepared in each tube by evaporating calcium from the tungsten wire spiral *S*. In order to obtain electrical connection with the calcium volatilized on the walls, two platinum wires *P* were sealed so that the wire inside the wall was just flush with the surface. The resistance of the deposit as measured between these two seals was always below 1 ohm.

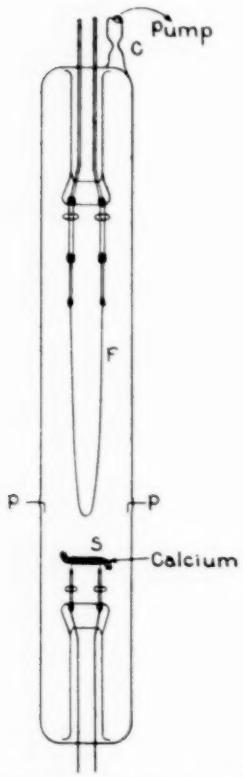

Fig. 1. Design of tube used for determining emission data.

The procedure in preparing such a tube for a series of measurements was as follows. The tube was exhausted by means of a condensation pump with simultaneous bake-out of the glass walls at 360°C for 1 hour. After allowing the tube to cool down, the filament *F* was flashed for a few minutes at a high temperature (2700° to 2800°K in case of tungsten) and then run at a somewhat lower temperature for an hour until all gas evolution had practically ceased. The spiral *S* was then raised gradually to a red heat and the calcium volatilized on the walls. The exhaust was then continued for a few minutes longer and the tube finally sealed off at *c*.

Before taking emission data, the filament *F* was aged by running it at a suitable temperature for 15 to 24 hours. The tube was then immersed in liquid air and the filament flashed again at a very high temperature for about a minute. The temperature of the filament was then lowered to the desired value and emission data taken at different anode voltages. Before taking data at any other temperature the flashing at high temperature was usually repeated.

It is evident that under these conditions the surface of the cathode was quite free from adsorbed gas. The calcium surface at liquid air temperatures maintained an excellent vacuum and it was found that emission

data taken under these conditions were satisfactorily reproducible not only on the same tube but on samples of the same wire made up in different tubes.

Temperature Scales

The temperature scale for tungsten at temperatures above 1200°K has been derived by Langmuir[4] and also, more recently, by Worthing and Forsythe.[3] In view of the extremely accurate determinations made by the latter of the values of the different factors involved, the temperature scale established by them has been adopted in the present connection.

According to this scale, the energy radiated by tungsten as a function of the absolute temperature is given in watts per cm² by the relation.

$$\log_{10}E=3.680(\log_{10}T-3.3)-(1040/T)+1.900\,. \qquad (5)$$

In the determination of temperatures for any given sample of wire a vacuum lamp was made up with a V-shaped filament, and after suitable ageing this lamp was pyrometered against a standard lamp furnished by Worthing and Forsythe, using light of wave-length 0.665μ. In this manner a relation was obtained between the filament current F_i and the absolute temperature. A number of the lamps containing filaments from the same sample of wire as that used for electron emission measurements were also sent to Dr. Forsythe for check determinations on the relation between temperature and filament current. The relation between log F_i and log T was then plotted on a large scale so that interpolation could be made quite accurately. It may be observed in this connection that the pyrometry data obtained in this laboratory and by Dr. Forsythe on pure tungsten filaments were found to be in splendid agreement with the temperatures calculated by means of Eq. (5) from the energy radiated, after a correction had been made for the lead losses (see subsequent section).

In the case of molybdenum, a vacuum lamp containing a sample of the wire used for electron emission work was also pyrometered by Dr. Forsythe. The temperature scale used depends upon some recent determinations of the emissivity of molybdenum for λ0.665μ, according to which this metal is less like a black body than tungsten.

Regarding the temperature scale for tantalum, there are much less accurate data available than in the case of tungsten. The current-temperature relation for the wire used was obtained by pyrometering a vacuum lamp against the standard tungsten lamp mentioned already.

[4] Langmuir, Phys. Rev., 7, 302 (1916)

The true temperature of the tantalum was then derived from that of the tungsten at the same brightness by the relation,

$$\frac{1}{T}-\frac{1}{S}=\frac{\lambda \log_e E_\lambda}{C_2} \tag{6a}$$

where S = brightness temperature;

T = true temperature;

E_λ = emissivity for wave-length λ;

C_2 = 14,350 microns × deg. K.

For any two substances at the same brightness temperature it follows that

$$\frac{1}{T'}-\frac{1}{T''}=\frac{\lambda \log_e (E'_\lambda / E''_\lambda)}{C_2}. \tag{6b}$$

Data on the emissivity of tantalum have been published by Foote and Fairchild.[5] The emissivity for λ 0.65μ is given as 0.60 at $T=1373$, and 0.48 at $T=2873°$K. On the other hand, Dr. Worthing finds as a result of some recent determinations that at approximately all temperatures, E_λ for tantalum is $1.088 \times E_\lambda$ for tungsten.[6] Using these data and those for tungsten published by Worthing[7] we obtain the following equivalent brightness temperatures for the two metals. The second column gives the temperatures calculated on the basis of Foote and Fairchild's values of E_λ, while the third column gives the temperatures calculated by means of Worthing's values, which are those used in the present investigation.

Corresponding true temperatures for equivalent brightness

Tungsten	Tantalum	
	(F. & F.)	(W)
1200	1180	1194
1400	1375	1392
1600	1570	1590
1800	1765	1788
2000	1960	1984
2200	2155	2181
2400	2350	2378

Corrections for Lead-Loss

It is obvious that in order to calculate electron emission per unit area from the emission observed for any given filament, a correction must be applied for the fact that the temperature along a filament decreases to practically room temperature as the lead is approached.

[5] P. D. Foote and C. O. Fairchild, Trans. Am. Inst. Mining Eng. 1919, p. 1389.

[6] Personally communicated to the writers.

[7] A. G. Worthing, Phys. Rev. **10**, 377 (1917); Trans. Am. Inst. Min. Eng. 1919, p. 1895.

Corrections for the cooling effect of the leads have been derived by Langmuir,[8] and are expressed by the following relations.

When the ends of a V-shaped filament are cooled by large leads, the voltage correction for the two ends, that is the decrease in voltage due to the cooling effect of the leads, is

$$\Delta V = .00026\,(T-400) \text{ volts} . \tag{7}$$

But the cooling also affects the electron emission, and the correction for this is

$$\Delta V_H = 2(0.00017 T\phi - 0.05) \text{ volts} . \tag{8}$$*

Here ΔV_H represents the voltage of a length of uncooled filament which would give the same effect as the *decrease* caused by the cooling of the leads. In this equation ϕ is a number which depends upon the temperature coefficient of the quantity H which may represent any property of the metal, such as electron emissivity, candlepower, etc. If we let n represent the exponent of the power of the temperature with which H increases, then the values of ϕ depend upon n as follows;

$n=$	0.5	1.0	2	2.5	5	10	20	30	50
$\phi=$	0.48	0.85	1.23	1.44	1.72	2.10	2.47	2.69	2.95

For the case of electron emission,

$$n = d \log I / d \log T = 2 + b_0/T . \tag{9}$$

Thus, corresponding to any values of b_0 and T, a value of ϕ is obtained and from this ΔV_H can be calculated.

Formulas for the end-loss corrections have also been derived by Worthing.[9] That for ΔV (correction for energy input) agrees substantially with that derived by Langmuir and is

$$\Delta V = 1.00\sqrt{2\rho\eta}/Q . \tag{10}$$

In this equation ρ is the resistivity, η the radiation intensity and Q a function of the maximum temperature. The correction for electron emission varies with the value of b_0. For tungsten (and the same correction may be applied to tantalum and molybdenum) the correction as given by Worthing is

$$\Delta V_H = 3.85\sqrt{2\rho\eta}/Q . \tag{11}$$

[8] I. Langmuir, Phys. Rev. **7**, 151 (1916);
Gen. Elec. Rev. **19**, 210 (1916);
Trans. Far. Soc. **17**, part 3, 2 (1921)

* In a paper published by S. Dushman and Jessie Ewald (General Electric Review, 26, 154, 1923) the factor 2 in this equation was omitted.

[9] A. G. Worthing, J. Franklin Inst. 597 (1922)

This equation gives practically the same results as Eq. (8) for values of T below about 2400°K, but gives much greater corrections for higher temperatures.

If now i_{obs} represents the actually observed electron emission, the corrected emission i_{cor} for the total area of the filament is given by the relation

$$i_{cor} = i_{obs} \times (V+\Delta V)/(V+\Delta V-\Delta V_H) \,. \tag{12}$$

In the following tables this correction factor is denoted by f.

Inadvertently the factor 2 in Eq. (8) was omitted by Dr. Langmuir in his paper. Since his was the relation used by the writers for calculating f and the corrected emission per unit area, it is evident that the values of b_0 thus obtained are slightly higher than those obtained by means of Worthing's relation. However, as the difference amounts, in the case of the filaments discussed in the present paper, to an increase in the calculated value of b_0 of not more than 125 (about 1/4 per cent of the value of b_0) it may be neglected in comparison with the effect of other experimental errors.

Correction for Schottky Effect

In measuring the electron emission from any filament it is observed that the actual value of the emission increases gradually with the anode voltage, even when the current is considerably below the limit due to space charge.

W. Schottky pointed out[10] in 1914 that, owing to the influence of the "electric image," the electron emission must increase with the field strength at the cathode in accordance with the following relation

$$i_v = i_0 \epsilon^{(4.39/T)(dV/dx)} \tag{13}$$

where i_v = electron current at anode voltage V:

i_0 = electron current at zero field strength:

dV/dx = voltage gradient at the cathode.

Since the fundamental Eq. (1) for electron emission was derived on the assumption that there is no field gradient at the cathode it is obviously necessary to correct the actually observed emission data for this affect.

In the case of a filament of radius r along the axis of a cylindrical anode of radius R,

$$\frac{dV}{dx} = \frac{V}{r \log (R/r)} \,. \tag{14}$$

[10] W. Schottky, Phys. Zeits. **15**, 872 (1914)

For most of the tubes used in connection with the present investigation it is difficult to calculate the value of dV/dx accurately. However, the magnitude of the exponential factor in Eq. (13) can be obtained by actually measuring the emission for a range of anode voltages. Writing this equation in the form

$$\log_{10} i_v = \log_{10} i_0 + (4.39/2.303T)\sqrt{dV/dx}$$

it is evident that if log i_v is plotted against $\sqrt{V}$ a straight line should be obtained, and the following relation should exist

$$2.303\ T\ \frac{\Delta \log_{10} i}{\Delta \sqrt{V}} = 4.39\sqrt{s} \tag{15}$$

where s is a *constant* for any tube and depends upon the geometrical arrangement of the electrodes. Thus, if Schottky's equation is valid, it ought to be observed that $T\ \Delta \log i/\Delta\ \sqrt{V}$ is a *constant* for any tube. Furthermore, by means of the value of $\Delta \log i/\Delta\sqrt{V}$ thus obtained it is evidently possible to calculate i_0, the emission that would be obtained if there were no field gradient at the cathode.

Eqs. (1) and (15) can be combined in the form

$$I_v = A\,T^2 \epsilon^{-(b_0 - \Delta b_0)/T} \tag{16}$$

where

$$\Delta b_0 = 4.39\sqrt{dV/dx} = 4.39\sqrt{Vs} = 2.303\ T(\Delta \log_{10} i/\Delta\sqrt{V})\sqrt{V}. \tag{17}$$

That is, for any tube, the value of Δb_0 varies as $\sqrt{V}$.

Emission Data for Tungsten

In the following tables, the data are given from which values of I and b_0 were calculated. F_i denotes the filament amperes, and F_v the filament volts. From measurements of the electron current at different anode voltages, a value of $T\Delta \log_{10} i/\Delta\sqrt{V}$ was obtained, and from the average of these values for all the temperatures a corrected value of $\Delta \log_{10} i/\Delta\sqrt{V}$ was obtained, which was then used to calculate i_0.

The value of the lead-loss correction factor was calculated as described in a previous section, from the filament potential drop and the pyrometered value of T. The value of I, the emission in amp./cm², was then obtained by the relation

$$I = i_0 \times f/\text{area}.$$

Data obtained with several tubes are given in detail in the following tables. Specially prepared pure tungsten was used in order to avoid any effects due to slight traces of impurities.

TABLE I

Results for pure tungsten filament, in tube 107-1

Weight of wire = 1.517 mg/cm; diameter = 0.01003 cm; total length of filament = 15.0 cm; area = 0.474 cm²

F_i	F_r	T	Anode volts	i	$T\frac{\Delta\log_{10} i}{\Delta\sqrt{V}}$	$\left(\frac{\Delta\log_{10} i}{\Delta\sqrt{V}}\right)_{cor}$	$\log_{10} i_0 + 8$	i_0
0.550	3.98	1470	475	1.95×10^{-8}				
			400	1.89				
			225	1.75				
			100	1.61	10.29	0.00728	0.1310	1.35×10^{-8}
0.608	4.68	1543	475	1.240×10^{-7}				
			400	1.195				
			225	1.110				
			100	1.020	10.51	0.00693	0.940	8.71×10^{-8}
0.688	5.74	1640	475	1.080×10^{-6}				
			400	1.050				
			225	0.970				
			100	0.905	10.66	0.00653	1.889	7.745×10^{-7}
0.792	7.22	1761	475	1.160×10^{-5}				
			400	1.120				
			225	1.040				
			100	.975	11.09	0.00608	2.929	8.492×10^{-6}
0.912	9.12	1897	475	1.065×10^{-4}				
			400	1.040				
			225	0.975				
			100	0.910	10.21	0.00563	3.903	7.998×10^{-5}
1.065	11.77	2065	475	1.150×10^{-3}				
			400	1.124				
			225	1.060				
			100	0.996	10.95	0.00518	4.9465	8.841×10^{-4}
1.235	15.30	2239	475	1.154×10^{-2}				
			400	1.124				
			225	1.050				
			100	0.984	11.20	0.00478	5.9155	8.231×10^{-3}

TABLE II

Values computed from data in Table I.

T	$10^3/T$	$V+\Delta V^*$	$V+\Delta V-\Delta V_B^*$	f^*	$\log I + 8$	$\log(I/T^2)+14$	b_0	T (calc.)
1470	0.6803	4.22	3.30	1.275	0.5606	0.2260	52,600	1472
1543	.6482	4.94	3.95	1.25	1.3614	0.9848	52,580	1546
1640	.6098	6.02	4.94	1.215	2.2978	1.8682	52,530	1644
1761	.5679	7.54	6.34	1.19	3.3280	2.8366	52,480	1765
1897	.5271	9.47	8.12	1.167	4.2949	3.7387	52,590	1897
2065	.4842	12.17	10.64	1.143	5.3296	4.6996	52,710	2062
2239	.4467	15.75	14.03	1.122	6.2900	5.5900	52,520	2244
						Average:	52,580	
			Value from slope in log (I/T^2) vs $(1/T)$:				52,560	

* Calculated by means of Eqs. (10) and (11). As mentioned previously the values of b_0 calculated by use of Langmuir's uncorrected relation for ΔV_H lead to values of b_0 which are about 1/4 percent higher.

The average value of $T\Delta\log_{10}i/\Delta\sqrt{V}$ was 10.70. From this the corrected value of the slope $\Delta\log_{10}i/\Delta\sqrt{V}$ was derived as given in Table I. In Fig. 2, values of $\log_{10}i_v$ for each temperature are plotted against those of $\sqrt{V}$. The ordinates give the increase in $\log_{10}i_v$ as compared with $\log_{10}i_0$. The latter was obtained by drawing a straight line with the corrected slope through as many of the points as possible. The actual values of $\log_{10}i_0$ are given in Table I. It will be observed that within the limits of experimental accuracy $T\Delta\log_{10}i/\Delta\sqrt{V}$ is constant.

As shown in Table II, the values of b_0 are remarkably constant although the actual electron emission values vary over a range of 500,000: 1 and the extreme temperatures are as 1.52:1.

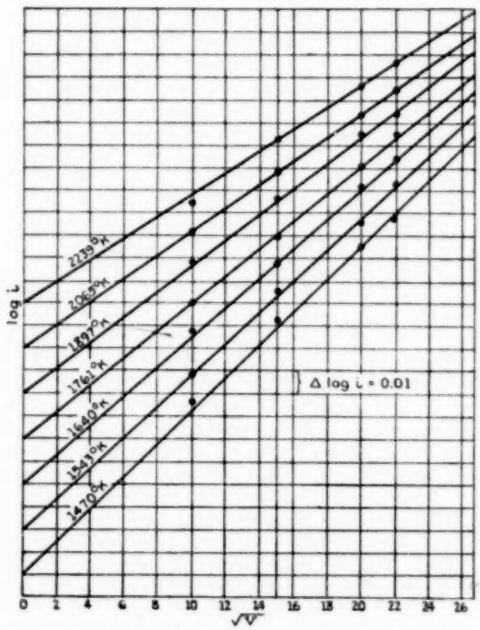

Fig. 2. Variation in emission with anode voltage.

An additional test of the validity of Eq. (1) is furnished by plotting $\log (I/T^2)$ against $1/T$ as shown in Fig. 3. The slope of the best straight line through all the points as obtained by the method of least squares (see subsequent section) corresponds to a value $b_0 = 52{,}560$, which is practically identical with that obtained as the average value in Table II.

The last column in this table gives the value of T calculated for the given value of $\log I$ on the basis $b_0 = 52{,}600$, which, as is pointed out more fully in a subsequent section, we believe to be the best value for tungsten.

The agreement between these two sets of values must be regarded as very satisfactory.

TABLE III

*Results for pure tungsten filament, in tube 107-2**

T	$10^3/T$	log $I+8$	log $(I/T^2)+14$	b_0	T(calc.)
1477	0.6770	0.6065	0.2677	52,760	1475
1543	.6482	1.3432	0.9666	52,620	1543
1640	.6098	2.2850	1.8554	52,570	1641
1761	.5679	3.3158	2.8248	52,520	1764
1897	.5271	4.2696	3.7134	52,690	1895
2065	.4842	5.3043	4.6743	52,790	2057
2239	.4467	6.2659	5.5659	52,640	2239
			Average	52,660	
			Value from slope	52,570	

* This filament was from the same wire as in tube 107-1

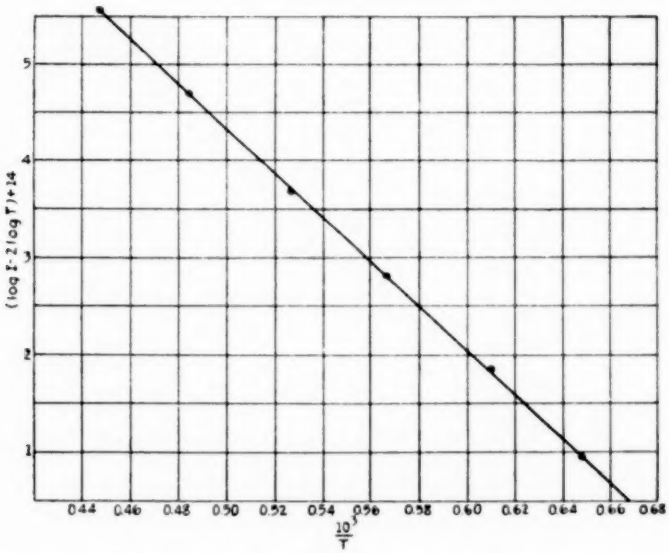

Fig. 3. Variation in emission from tungsten with temperature; b_0 from slope = 52,560.

In the case of tube 54, the sample of pure tungsten wire used was from a different metal lot from that used in the other tubes. The average value of b_0 is 52, 710, with a maximum of 52,880 and minimum of 52,410. From the slope of log (I/T^2) against $1/T$, $b_0 = 52{,}000$. This series of data was, however, not quite as reliable as the other series given above.

In the case of tube 162-2, the tungsten wire used was a sample of unthoriated wire such as is used in regular lamp production. In order to obtain a comparison with the specially pure tungsten wire used in ob-

taining the previous data, two similar V-shaped filaments were inserted in the tube, one of the specially pure wire and the other of the regular wire. Thus emission data were obtained under identical conditions of vacuum. In taking emission data from either filament the other filament

TABLE IV

*Results for pure tungsten filament, in tube 162**

T	$10^3/T$	log $I+7$	$\log(I/T^2)+14$	b_0	T calc.
1533	0.6524	0.1750	0.8040	52,890	1525
1653	.6049	1.3492	1.9126	52,810	1650
1770	.5649	2.3238	2.8278	52,790	1765
1884	.5308	3.1521	3.6019	52,840	1877
1993	.5017	4.8592	4.2600	52,890	1985
2101	.4760	5.4992	4.8544	52,830	2095
2204	.4537	6.0593	5.3792	52,830	2200
			Average	52,830	
			Value from slope (Fig. 4)	52,860	

* The filament in this tube was from the same wire as that in tube 107-1.

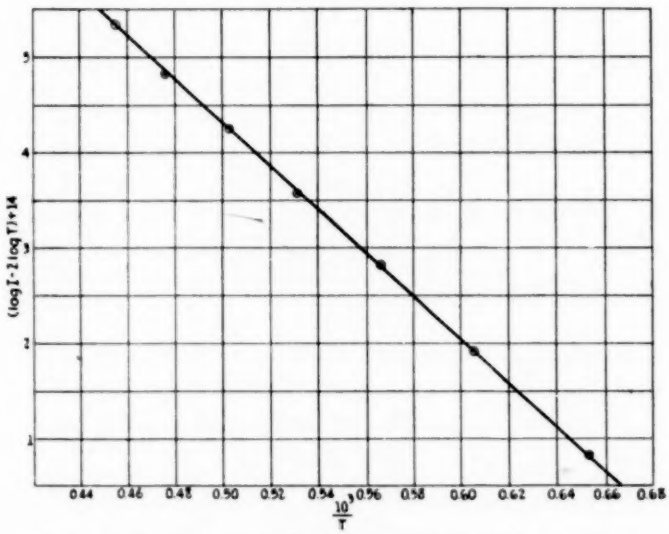

Fig. 4. Variation in emission from tungsten with temperature. $b_0 = 52{,}860$.

was connected to the negative end of the heated filament. The data for the specially pure tungsten filament used in this tube have been given already in Table IV. Table V gives the results obtained with the regular wire. The value of b_0 obtained from the slope by the method of least squares is 51,390 (see Fig. 5). The difference between this and the average value 52,470 is probably due to some slight trace of impurity in the wire.

Emission data were also taken on a sample of regular unthoriated wire obtained from another metal lot. In this case the average value of b_0 was 52,950.

TABLE V

Results for commercial unthoriated tungsten filament, in tube 162-2.

T	$10^3/T$	log $I+7$	log $(I/T^2)+13$	b_0	T(calc.)
1535	0.6515	0.4036	0.0314	52,140	1550
1621	.6169	1.1892	0.7696	52,300	1632
1702	.5876	1.9094	1.4476	52,250	1715
1786	.5599	2.4982	1.9944	52,580	1787
1868	.5353	3.0875	2.5447	52,610	1867
1946	.5146	3.6011	3.0229	52,710	1946
2020	.4950	4.0701	3.4593	52,670	2017
2090	.4785	4.4962	3.8560	52,550	2091
2159	.4633	4.8736	4.2052	52,550	2162
2225	.4493	5.2579	4.5631	52,370	2235
			Average	52,470	
			Value from slope (Fig. 5)	51,390	

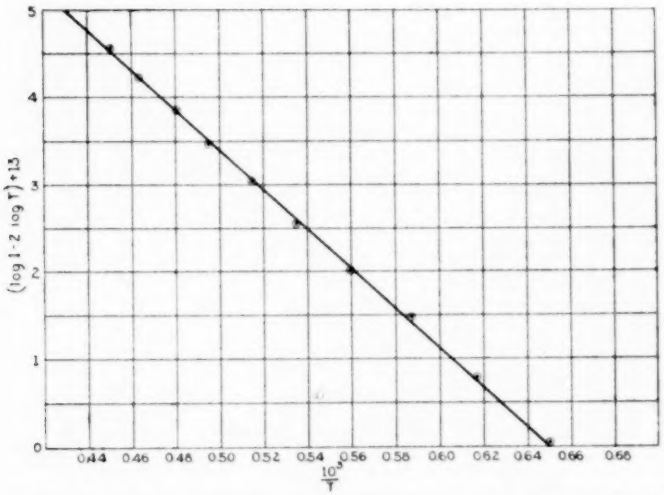

Fig. 5. Emission data for commercially pure tungsten; $b_0 = 51,390$.

In order to obtain data which would be free from lead loss correction, a tube (No. 79) was made up similar in size to that described already, but with a filament along the axis and with guard rings of quartz put in so that on evaporating the calcium the anode would consist of three portions not connected electrically. The central part was made 10 cm long, while each of the guard ring anode portions was about 5 cm in length. Pure tungsten wire was used, from the same lot as for tube 107-1. The data obtained in this case are given in Table VI.

Some further measurements were carried out with a sample of unthoriated tungsten in which the crystals were very long. This was prepared by special treatment and it appeared of interest to determine in this case the effect of crystalline structure on the emission. The average value of b_0 obtained for four different temperatures was 52,400, which may be considered as in very good agreement with the values obtained for the regular wire.

TABLE VI

Results for pure tungsten wire in special tube 79.

T	$10^3/T$	$\log I+5$	$\log (I/T^2)+11$	b_0	T(calc.)
1810	0.5524	0.6118	0.0964	52,860	1803
1930	.5180	1.4971	0.9259	52,690	1928
2000	.5000	1.9733	1.3714	52,550	2002
2090	.4785	2.4720	1.8318	52,710	2087
2170	.4608	2.9325	2.2595	52,580	2172
			Average	52,680	
			Value from slope	53,850	

Value of b_0 for tungsten. Summarizing the values of b_0 obtained in all the above series of measurements it will be observed that the maximum value obtained was 52,950, and the minimum, 52,400. The most reliable measurements gave values ranging around 52,600.

It is evident that in a determination of b_0 as carried out in this investigation, there are many possible sources of error. First, pyrometric data were never determined for the actual filament in the tube, but for a sample of the same wire in a vacuum lamp. Now while the actual temperature for a given filament current can be measured on the same filament with a high degree of accuracy (2 to 3 degrees at 2000°K) such accuracy is difficult to obtain where two samples are made up in different lamps. Slight variations in the ageing schedule will alter the emissivity at a given wave-length, and there is no doubt that in many cases the differences between the pyrometered values of T and those calculated from the electron emission on the basis $b_0=52{,}600$ are to be ascribed to this cause.

It is to be observed in this connection that a 1 per cent error in T causes approximately the same error in the calculated value b_0. Hence an error in pyrometry of 10 degrees at $T=2000$ would lead to an error of 0.50 per cent in that of b_0.

There is, furthermore, some uncertainity as to the exact magnitude of the lead loss correction. From Eq. (9) it follows that an error of 5 per cent in the determination of I leads to an error of approximately 0.2 per cent in the value of b_0. Such an error was quite possible with the lengths of filaments used when it is considered that both Langmuir's and Worth-

ing's formulas for lead loss correction assume that the leads are maintained at room temperatures.

In addition, account must be taken of the fact that in order to obtain accurate emission data from a filament, the latter must be flashed for a considerable time to get rid of residual traces of adsorbed oxygen. As has been shown by Langmuir even a very low pressure of this gas increases the value of b_0 enormously. This effect is much more pronounced at lower temperatures where the rate of evaporation of oxygen is low.

In view of these considerations it would be reasonable to conclude that the lower values of b_0 are the more reliable, and that the best value for tungsten is 52,600, with an error of ± 250 (corresponding to an estimated error of 0.5 per cent in the determination of temperature). The agreement between the pyrometered values of T and the values calculated from I on this basis tends to confirm this conclusion.

Emission Data for Molybdenum

Regular molybdenum wire (0.0129 cm in diameter) was used in the form of V-shaped filaments. As mentioned previously, pyrometer data were determined for us by Dr. Forsythe, on a vacuum lamp containing a filament of the same wire. In the following table only the essential data are given and details regarding corrections for lead loss and the Schottky effect have been omitted.

Tube No. 54. Length of filament = 10 cm. Data obtained with this tube are given in Table VII. The value of b_0 from the slope of log (I/T^2) against $1/T$ is 52,770, while the average value of b_0 is 50,230. However the emission data, especially at lower temperatures, were not very constant. Probably there was a residual gas effect in this tube.

Table VII

Results for molybdenum filament in tube 54.

T	$10^8/T$	log $I+8$	log$(I/T^2)+14$	b_0	T (calc.)
1438	.6954	0.8260	0.5106	50,560	1425
1502	.6658	1.4538	1.1004	50,790	1480
1553	.6440	2.4786	1.6610	50,490	1536
1599	.6254	2.4786	2.0708	50,490	1585
1643	.6087	2.8891	2.4579	50,400	1632
1685	.5934	3.2618	2.8086	50,330	1675
1728	.5788	3.5916	3.1166	50,390	1717
1890	.5291	4.8195	4.2665	50,100	1885
1930	.5181	5.1173	4.5461	49,910	1930
1968	.5081	5.3704	4.7822	49,860	1965
2006	.4985	5.5922	4.9876	49,850	2012
2045	.4890	5.7995	5.1815	49,730	2050
			Average	50,230	
			Value from slope	52,770	

Tube No. 167. Length of filament = 14.85 cm. Data obtained with this tube are given in Table VIII. The agreement between the average value of b_0 and that derived from the slope (51,180) is only fair . There was no evidence of residual gas effects in this tube and the data were very constant.

TABLE VIII

Results for molybdenum filament in tube 167

T	$10^3/T$	$\log I+7$	$\log (I/T^2)+14$	b_0	T(calc.)
1466	0.6821	0.3020	0.9696	50,010	1466
1599	.6253	1.6577	2.2499	49,830	1600
1685	.5934	2.3923	2.9391	49,800	1690
1849	.5409	3.6418	4.1080	49,690	1860
2006	.4985	4.6500	5.0456	49,630	2023
2116	.4726	5.2880	5.6370	49,410	2140
			Average	49,730	
			Value from slope	51,180	

Value of b_0 for molybdenum. It will be observed that the values of b_0 consistently decrease with increase in T, and that the average value obtained by means of Eq. (4) is less than that obtained from the slope. On the other hand, the difference between the latter values (1,590) is greater than that between the maximum (50,560) and minimum (49,410) values calculated by means of Eq. (4).

These results can be accounted for as due to the presence on the surface of the filaments of adsorbed layers of oxygen. The amount of this adsorbed gas decreases with increase in temperatures and, therefore, causes a decrease in the values of b_0. Furthermore, the amount of adsorbed gas must depend on the exact ageing schedule and other factors in the previous history of the tube. This would account for the difference observed between the values of b_0 in the two tubes. Thus the surface of the filament in tube 167 must have been more free from contamination than that used in 54.

Observations with other tubes containing molybdenum filaments were in agreement with the conclusion that in the case of this metal, it is difficult to obtain emission data on absolutely clean surfaces; average values of b_0 were obtained ranging from 50,900 to 49,700 for different samples, with individual variations in any set of observations which were considerably greater than those shown in either Table VII or Table VIII.

It would, therefore, seem logical to conclude that the lowest values of b_0 are probably the most accurate. On the other hand, the temperature scale for molybdenum is not known with anywhere near the same degree of accuracy as that for tungsten, and this may account to some extent

for the differences between the values of b_0 obtained by applying Eq. (4) and those obtained from the slope.

In view of these considerations, it is evident that the results obtained for this metal cannot be regarded as evidence either for or against the validity of Eq. (4). Tentatively the writers believe that there is justification for assuming that the emission from molybdenum may be represented (as accurately as the data permit) by the parameters $\log A = 1.779$ and $b_0 = 50{,}000$. From the maximum and minimum values given in Tables VII and VIII, it would also appear that the maximum deviations are approximately ± 500.

Emission data for tantalum

The temperature scale for tantalum has been discussed in a previous section. Two different samples of wire were used. The first came from Germany (Osram Co.) about ten years ago, and was, therefore, the same kind of material as was used in the tantalum lamp of about 1910-11; the second sample was obtained from the Fansteel Co., Chicago.[11]

As in the case of molybdenum, the oxide of tantalum is quite non-volatile and the filaments must, therefore, be heated to as high a temperature as possible (2400°K) in vacuum in order to obtain thoroughly clean surfaces. Furthermore, it has been found desirable in the preparation of the filaments, not to arc weld them to the leads in hydrogen (as is customary with tungsten) but to spot-weld the joints. As is well known, tantalum at higher temperatures absorbs hydrogen, and on subsequent flashing in vacuum, there is not only considerable evolution of gas, but also apparently a disintegration of the filament so that the glass walls became blackened with the deposited metal.

Before taking emission data on the evacuated tubes, the filaments were aged for a number of hours at 2200° to 2400°K until the cold resistance remained constant. It should be observed that occluded gases increase the resistance of tantalum, so that the measurement of this property forms a guide to the degree of evacuation of the wire.

Osram wire (Tubes No. 269, 270 and 271). The data on the three tubes made up with this wire were so similar that only those obtained with one of these (No. 271) are given in Table IX. The wire used was 0.222 mm (8.75 mil) in diameter, and the total length of the filament was 15.1 cm, corresponding to an area of 1.055 cm². The measurements on the Schottky effect gave for the slope $T\Delta \log i\Delta/\sqrt{V}$ the average value

[11] See C. W. Balke, Ind. Eng. Chem. **15**, 560 (1923) for full description of the properties of this material.

7.36, corresponding to $\Delta b_0 = 170$ for 100 volts on the anode. As shown in Fig. 6, the agreement between the value of b_0 from the data in Table IX and that from the slope of log (I/T^2) against $(1/T)$ is fair.

TABLE IX

Results for Osram tantalum filament, in tube 271

T	$10^3/T$	log $I+6$	$\log(I/T^2)+13$	b_0
1482	0.6747	0.2565	0.9147	47,320
1586	.6304	1.1091	1.7083	47,740
1718	.5821	2.1448	2.6748	47,870
1798	.5560	2.7315	3.2217	47,940
1872	.5342	3.2498	3.7052	47,710
1978	.5055	3.8989	4.3063	47,690
2048	.4883	4.2943	4.6717	47,670
			Average	47,700
			Value from slope	46,840

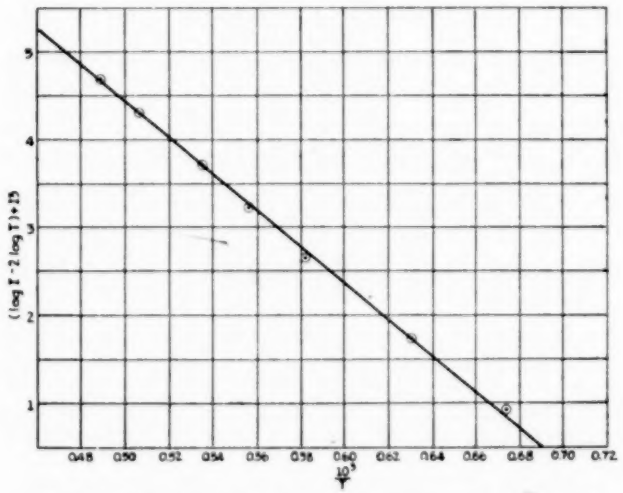

Fig. 6. Plot of emission data for tantalum; $b_0 = 46{,}840$.

Fansteel wire (Tubes No. 267, 268). The data on these two tubes also showed very good agreement. The wire used was 0.254 mm (9.9 mil) in diameter and had a total length of 15.0 cm (area = 1.19 cm²). The correction for the Schottky effect was found to be the same as for the other tantalum filaments. Table X gives the results obtained with this wire.

Value of b_0 for tantalum. The agreement between the values of b_0 obtained for the two different samples of tantalum may be regarded as very satisfactory, and we have, therefore, taken as an average, the value

$b_0 = 47{,}800 \pm 500$. The accuracy is probably not much better than within one per cent, since the temperature scale has not been determined as accurately as in the case of tungsten.

TABLE X

Results for Fansteel tantalum filaments.

T	$10^3/T$	$\log I + 7$	$\log(I/T^2) + 13$	b_0
1450	0.6896	0.8094	0.4866	47,720
1562	.6401	1.7880	1.4006	48,140
1676	.5967	2.7517	2.3031	48,170
1746	.5728	3.2988	2.8148	48,090
1848	.5412	4.0006	3.4672	48,140
1904	.5252	4.3980	3.8386	48,000
1964	.5091	4.7601	4.1737	48,000
2022	.4945	5.0904	4.4788	47,600
			Average	48,000
			Value from slope	47,550

VALUE OF CONSTANT A

The results discussed in the previous sections show that for tungsten and tantalum, the value of A is the same, within the limits of experimental errors, and corresponds to that given by the Sackur Tetrode theory, that is, 60.2 amp. cm^{-2} deg^{-2}. This conclusion was reached by finding that in the large majority of cases, the individual values of b_0 calculated from observations at different temperatures by means of Eq. (4) were in agreement with the values obtained by plotting $\log (I/T^2)$ against $1/T$.

In the case of molybdenum, as stated previously, the evidence for the validity of the value $\log A = 1.779$ is not so good. On the other hand, since there is a possible explanation of this discrepancy, it cannot be stated that the observations obtained in this case are in definite disagreement with equation (4).

As a check on the validity of Eq. (4), the values of $\log A$ and b_0 were calculated for each set of data by the method of least squares. Table XI gives a summary of the values thus obtained. In a recent paper N. Campbell[12] has advocated the use of the so-called method of "zero sum." The values of $\log A$ and b_0 calculated in this manner are given in the last two columns.

Undoubtedly the most accurate data are those given in Tables II, III and IV. The values of $\log A$ obtained from these data are so nearly the same as the theoretical value 1.779 that the difference must be ascribed to experimental errors in temperature determination.

[12] N. Campbell, Phil. Mag. **47**, 816 (1924)

While the data for tantalum and (much more so) those for molybdenum are not in as good agreement with Eq. (4) as those for tungsten, the writers believe that there are two possible causes for these differences: (1) Insufficient knowledge of the radiant emissivity of these metals as a function of the temperature, and (2) the practical difficulty in obtaining absolutely clean surfaces free from adsorbed oxygen.

TABLE XI

Average Values of b_0 and of log A

Metal	Table	By Eq. (4) b_0	Least square method b_0	Least square method $\log_{10}A$	Zero sum method b_0	Zero sum method $\log_{10}A$
Tungsten	II	52,580	52,560	1.773	52,500	1.759
	III	52,660	52,570	1.753	52,450	1.725
	IV	52,830	52,860	1.787	52,740	1.757
	V	52,470	51,390	1.532	51,540	1.566
	VI	52,680	53,850	2.034	53,910	2.047
	Averages:	52,640	52,650	1.776	52,630	1.771
Molybdenum	VII	50,230	52,770	2.404	52,700	2.385
	VIII	49,730	51,180	2.133	51,130	2.120
	Averages:	49,980	51,980	2.268	51,920	2.252
Tantalum	IX	47,700	46,840	1.567	47,350	1.693
	X	48,000	47,550	1.663	48,040	1.785
	Averages:	47,850	47,200	1.615	47,700	1.744

In view of these considerations, it has seemed best to adopt, for the present, the mean values of b_0 derived by means of Eq. (4), although it is quite possible that the emission from molybdenum actually is not in accord with this equation.

Initially it was concluded that the same constant A ought to be valid for electron emission data from all substances. Preliminary investigations with thoriated filaments seemed to be in agreement with this conclusion, but more careful observations by Dr. K. H. Kingdon and also by the writers, have shown that for these filaments, the value of A is smaller and varies with the amount of the surface covered by thorium.

Furthermore the observations of K. H. Kingdon on caesiated tungsten filaments and published data on the emission from oxide coated filaments, lead to the conclusion that for *coated filaments* the value of the constant A may be either greater or lower than both the values derived from Eq. (2) and (3). By coated filaments we mean all filaments in which the emission is due to, or is affected by, a surface layer. Thus an adsorbed layer of oxygen atoms on the surface of tungsten lowers the emission enormously, and as Kingdon has shown, while the value of A is much greater than for pure tungsten, the value of b_0 is also increased considerably.

An explanation for this apparent discrepancy between the theoretical and observed values of the constant A has been suggested by I. Langmuir and L. Tonks.*

As pointed out by P. W. Bridgman,[13] the latent heat of evaporation of electrons consists of two portions, that corresponding to the energy which would be absorbed at constant surface charge, and a heating effect due to the appearance of a positive charge on the surface (surface heat). It is only when this surface heat is zero that A has the value derived from the Third Law of Thermodynamics and given by Eq. (2) or (3). Thus the fact that the value of A actually observed for tungsten is in accord with Eq. (4) may be taken as indicating that for that metal at least the surface heat is negligibly small.[14]

It is of interest in this connection to point out that apparently the effect of monatomic layers of various substances on the value A varies according to whether the atoms composing this layer are electropositive or electronegative. Thus oxygen increases the value of the constant. In fact for a layer of oxygen on tungsten, Kingdon[15] obtains the value $A=5\times10^{11}$. On the other hand, in the case of electropositive atoms, such as thorium and caesium on tungsten, the values of A are considerably lower. According to Kingdon, the values of A for thorium is about 7 (and independent experiments by the writers give results in agreement with this value). For caesium the value is less than 0.003.†

Similarly, in the case of platinum filaments coated with oxides of the alkaline earths, A is very high, approaching that of oxygen on tungsten. The writers are obtaining more data on this subject in the hope that some general relations will be obtained between the nature of the monomolecular layer and the effect on the value of A.

Discussion of Previous Data on Emission from Tungsten, Molybdenum, and Tantalum

Tungsten. According to Langmuir's[16] earlier investigation, the constant A (Richardson's equation) is given as 2.36×10^{7} amp. cm^{-2} deg$^{-\frac{1}{2}}$, while b is given as 52,500. The temperature scale for tungsten as used by Langmuir at that time is somewhat different from that used in the present paper. Thus 2000°K on Langmuir's scale of 1913 corresponds

* A discussion of this theory will appear in the near future.

[13] P. W. Bridgman, Phys. Rev. **14**, 325 (1919)

[14] See also a recent paper by H. A. Wilson, Phys. Rev. **23**, 38 (1924)

[15] K. H. Kingdon, Phys. Rev. **24**, 510 (1924)

† The high value of log A obtained for molybdenum (see Table XI) may probably be explained in the same manner as due to adsorbed oxygen.

[16] I. Langmuir, Phys. Rev. **2**, 402, 450 (1913)

to 2016°K on the present scale. At this temperature, the emission according to Langmuir is .0042 amp. cm^{-2}, while on the basis of the value $b_0 = 52{,}600$, the emission is .0042 amp. cm^{-2} at $T = 2115°K$. To account for Langmuir's observed emission at $T = 2016°K$, we would have to assume $b_0 = 50{,}000$ approximately. This is much lower than any of the values obtained in the present investigation. The difference is probably due to the presence in Langmuir's samples of slight traces of some more active emittor, such as thoria, alkali, or alkaline earth. In fact, the writers have obtained samples of tungsten which were substantially free from all active additions, and which, nevertheless, showed abnormally high electron emission for quite a long period.

The same reasons undoubtedly account for the rather high emission observed by K. K. Smith[17] for one sample of tungsten. Assuming the correctness of his temperature scale, the emission data recorded on p. 811 of his paper give a value for b_0 of 51,700. On the other hand, the data given on p. 820 of the same paper correspond to a value for b_0 of 56,000 (from the slope of $\log (I/T^2)$ against $1/T$). This high value of b_0 was most probably due to the presence of adsorbed gas on the surface of the filament.

The most recent measurements of the emission from tungsten are those obtained by C. Davisson and L. H. Germer.[18] As shown in the paper by S. Dushman,[1] these data are in excellent agreement with Eq. (4). The average value of b_0 is 51,860. As the anode voltage was 196, it is necessary to correct this value for the Schottky effect. From the description of the tube used in the investigation, it is reasonable to conclude that for $V = 0$, the value of b_0 would have been $51{,}860 + 500 = 52{,}360$ approximately.

Molybdenum. Langmuir[16] gives for molybdenum the values $A_1 = 2.1 \times 10^7$ amp. cm^{-2} $deg.^{-\frac{1}{2}}$ and $b = 50{,}000$. Hence, at $T = 2000$, $I = 0.013$ amp. cm^{-2}, while on the basis of Eq. (4), using the value $b_0 = 50{,}000$, we obtain the result $I = 0.0033$ amp. cm^{-2} at that temperature. Probably the difference in the temperature scales used in the two investigations and differences in the state of the surface account for this difference in emission data.

Stoekle[19] has obtained the values $A_1 = 11 \times 10^7$ and $b = 53{,}600$, but there is some doubt as to whether his results were not affected by the presence of gas.

Tantalum. Langmuir[16] gives for this metal the values $A_1 = 1.12 \times 10^7$ amp. cm^{-2} $deg.^{-1/2}$ and $b = 50{,}000$. Converting to Eq. (4) we obtain for

[17] K. K. Smith, Phil. Mag. **29**, 802 (1915)
[18] Davisson and Germer, Phys. Rev. **20**, 300 (1922)
[19] Stoekle. Phys. Rev. **8**, 534 (1916)

temperatures around $T=2000$, $b_0=48{,}200$, which is very close to the mean value obtained in the present investigation.

F. Deninger's[20] observations were not made under as good vacuum conditions as are available at present, and, therefore, correspond to values of b_0 which are much too high.

Quite recently Suhrmann[21] investigated the effect on the emission from tantalum of repeated treatments at high temperatures in vacuo. Owing to the form of cathode used by him, it is impossible to apply any cooling correction, but assuming even the whole cathode area to have been effective, the emission per unit area at any temperature is much higher than that obtained in the present investigation. The value of b_0 calculated from his data is about 42,000, and would certainly be less if a correction could be applied for the cooled area. In view of the observations made by the writers, it would seem necessary to conclude that the tantalum used by Suhrmann was not free from traces of active emittors.

RESEARCH LABORATORY,
GENERAL ELECTRIC COMPANY,
October 25, 1924.

[20] F. Deninger, Ann. d. Physik **25,** 298 (1908)
[21] Suhrmann, Zeits. f. Physik **29,** (1923)

AN EXPERIMENTAL STUDY OF THE ELECTRICAL CONDUCTIVITY OF DISPERSE SYSTEMS. I. CREAM

HUGO FRICKE AND STERNE MORSE

ABSTRACT

Conductivity of suspensions of cream in its skimmed milk.—The well known formula for the conductivity of a suspension of non-conducting spheres is $(k_1-k)/(2k_1+k)=\frac{1}{2}\rho$, where k and k_1 are the specific conductivities of the suspension and of the suspending medium and ρ is the volume concentration of the disperse phase. This formula was experimentally verified within about 0.5 per cent for values of ρ up to 62 per cent, by comparing the values of ρ given by the formula with the values obtained directly from the known dilutions. Since the conductivity was found to change with the age, due to incipient souring, measurements were made quickly. Stirring was used instead of shaking to avoid introducing finely divided air, and was effected by using a special cell in which a bead rolled back and forth as the cell was rocked. After stirring was stopped there was a rapid increase of resistance due, perhaps, to the particles taking up an ordered arrangement. The *temperature coefficient* was found to be the same for the cream as for the skimmed milk, decreasing from 2.65 per cent at 6° to 2.12 per cent at 25°C. The *variation with frequency* was a 2 per cent decrease of conductivity as frequency was increased from 1600 to 200,000. These results indicate that the measurement of conductivity furnishes a practical method of determining the butter fat in milk and cream, which is as accurate as those now used.

A. INTRODUCTION

THIS paper is the first in a series in which it is proposed to show the application to different problems of a theory which has been recently developed[1] for the electrical conductivity of a suspension of homogeneous fortuitously distributed polarizable spheroids. For the case of non-polarizable spheres the formula has the familiar form (Maxwell, Clausius-Mossotti, Lorenz-Lorentz):

$$\frac{(k-k_1)}{(k+2k_1)}=\rho\frac{(k_2-k_1)}{(k_2+2k_1)} \tag{1}$$

in which k is the conductivity of the suspension, k_1 that of the suspending liquid, k_2 that of the suspended particles, and ρ the volume concentration of the latter. For nonconducting spheres, using specific resistances in place of conductivities, it becomes $(r-r_1)/(2r+r_1)=\frac{1}{2}\rho$.

[1] Hugo Fricke, Phys. Rev. **24**, 575 (1924); Jour. Gen. Physiol. **6**, 741 (1924).

Although no strict derivation of this important formula seems to exist, direct experimental tests of it have been made only for fairly low volume concentrations; the most extensive experiments were made by Millikan,[2] who investigated the dielectric constant of suspensions of mixtures of benzol and chloroform in water for volume concentrations up to 15 per cent; his measurements verify the formula within about 1 per cent. Lord Rayleigh[3] has carried through an exact calculation of the conductivity of suspensions of spheres arranged in cubic order and has found that for this case formula (1) holds only approximately. The deviations of Rayleigh's formula from (1) with regard to ρ for the special case of the non-conducting disperse phase are as follows: 1.06 per cent for $\rho = 0.30$, 2.93 per cent for $\rho = 0.40$ and 6.5 per cent for $\rho = 0.50$, his values for ρ being the smaller for the same value of k/k_1. Since the two formulas agree closely for ρ less than .30 experimental test is of interest chiefly for values of ρ over 0.30. We may add that a test of (1) for high volume concentrations of the disperse phase seems of special value at the present time because of the recent applications of this formula to the calculation of the deformation of the atom when it passes from the gaseous or solute state to that of the liquid or solid.[4] In addition to its theoretical interest, this investigation is also of practical importance, since the measurement of the conductivity of milk and cream affords a very practical method of determining their content of butter fat, comparing advantageously with standard methods such as the Babcock test.

B. Method of Verification

A series of creams of differing concentrations were prepared by exact dilutions of a heavy cream with the skimmed milk originally separated from it; then the value of ρ found for each sample as computed from the conductivity data was compared with that obtained by multiplying the value found for the lowest cream by the dilution factor for that sample. Furthermore, on account of its importance for the practical application, a determination of ρ by the Babcock test has been made in each case. Agreement between the values of ρ thus determined with those computed above were nearly within experimental error, slightly lower values for ρ being found by the Babcock test, as would be expected. However, as the

[2] R. A. Millikan, Wied. Ann. **61**, 377 (1897); see also, F. Beaulard, Compt. Rend. **129**, 149 (1899) and F. Hwlawti, Wien Akad. Ber. **110**, 454 (1901)

[3] Lord Rayleigh, Phil. Mag. **34**, 481 (1892)

[4] K. Fajans, and G. Joos, Zeits. f. Physik **23**, 1 (1924)

precision obtainable with the Babcock test is far less than that obtainable by the two other methods, results secured thereby will not be given much weight.

C. Experimental Technique

The conductivities were determined with a Wheatstone bridge, employing a substitution method, the frequency for the most accurate set of data being 83,000 cycles per second. Throughout the work we have utilized a conductivity cell of a special type, designed to permit stirring while a measurement was being made. As will be shown later, some such device is essential in working with suspensions and is of convenience in any conductivity measurement.

This cell, which is shown in Fig. 1, consists of a short horizontal cylindrical vessel, mounted on pivots which permit it to be rocked back and forth on a central axis which is perpendicular to its own axis. By this motion a bead within the cell which nearly fills its lumen, is caused to travel back and forth, the platinized electrodes placed in the axis of motion being slightly recessed so as not to be touched by the bead.

A small hand-regulated mercury bath contained in a quart thermos jar was used as a constant temperature bath. Because of its high heat conductivity, its density and the fact that it does not wet glass, mercury has advantages over any other liquid as a constant temperature bath for conductivity measurements. The temperature used in these experiments was about 25°C, being kept constant within $\pm 0.01°$ in each series of measurements. Measurements were also made at other temperatures from 6 to 25°C in order to determine the temperature coefficient of conductivity for both skimmed milk and cream. This coefficient was found to be the same for any cream and the milk from which it was skimmed, varying from about 2.65 per cent per degree at 6°C to 2.12 per cent at 25°C. This result indicates that for the state of dispersion existing in ordinary cream there occurs no significant variation in absorptive phenomena dependent on temperature, a fact which made it unnecessary to measure the conductivities of the cream and skimmed milk at the same temperature as that at which the separation of the cream was made.

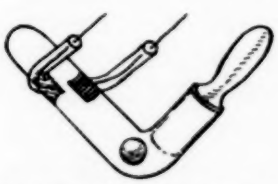

Fig. 1. Conductivity cell used in determining the conductivity of suspensions for the case of cream.

The primary cream was obtained by separating raw, fresh milk in a De Laval cream separator. After a short centrifugation at low speed, in order to remove air, this was diluted with its skimmed milk by a very exact volumetric method depending on a displacement principle which had an accuracy of 0.01 per cent or better. Two dilutions of each cream were made, each in duplicate. The fact that the skimmed milk always contains a slight amount of butter fat (about 0.15 per cent) does not have to be taken into consideration as long as we compare only conductivity and volumetric data; but we have taken it into consideration in comparing conductivity data with the Babcock test data, even though it amounts to only about 0.3 to 0.4 per cent of the value of ρ for the heavy creams and thus is well within the error of the Babcock test.

It may perhaps be doubted whether the skimmed milk obtained from the separator is identical with that which remains in the cream. For the purpose of deciding on this point we sometimes recentrifuged the cream in a bottle for a long time in order to separate most of the skimmed milk remaining therein. This gave the same conductivity figures as those secured from the skimmed milk obtained from the separator. This procedure, while not entirely conclusive, is the only way which has occurred to us whereby this point could be tested.

One source of experimental error which was present in the earlier experiments was the fact that cream as it comes from the separator, especially if it is mixed by being shaken in a bottle rather than stirred with a rod, contains in suspension a small percentage of very finely divided air, the amount of which depends on the plasticity of the cream and consequently on its fat content. This source of error produced a curiously constant deviation of the experimental findings from the theoretical. The presence of this air was first indicated by applying pressures to the cream contained in a dilatometer, and later by applying pressures within the cell during conductivity measurements, thereby inducing changes of volume and conductivity of approximately the right magnitudes. These air bubbles were subsequently eliminated by subjecting the primary heavy cream to a short centrifugation at low speed, and making all mixtures by stirring and not by shaking. This removed the difference between the experimental and theoretical findings to within the accidental errors (errors of sampling, mixing, etc.), these being of the magnitude of 0.2 per cent for the mean figures.

Three phenomena which we observed in the measurements of the conductivity of cream should be especially noted. In the first place the conductivity of milk and cream, unless they are very fresh, changes con-

tinually with time, owing presumably to the processes which initiate souring. The rate at which this change in conductivity takes place is always higher for cream than for milk, in one instance, for example, being approximately five times higher in a 40 per cent cream than in its skimmed milk, 24 hours after milking, samples of each having been kept for the same periods at room and icebox temperatures. More rapid but also irreversible changes, probably partly due to a somewhat different mechanism, occur within the conductivity cell. For these reasons the measurements must be made rather rapidly.

A continuous and rather rapid increase in resistance which occurs when stirring is discontinued but which is reversed when stirring is resumed also takes place. This change can hardly be due to the rising of the fat particles as it is much too rapid to depend on this phenomenon and appears to be independent of the form of cell. It may perhaps be due to a tendency of the particles to take up an ordered arrangement.* In this connection it is of interest to note that according to Lord Rayleigh's formula, an arrangement of the particles in cubic order would increase the resistance to about the magnitude which we have observed. In his studies of suspensions of red blood corpuscles Fraenkel[5] observed phenomena of a similar kind, which he decided were not due to settling. For these reasons we made it a rule to make the reading immediately after stirring.

The third phenomenon is the fact that both skimmed milk and cream exhibit a decrease in resistance with increase of frequency, this undoubtedly being due to a polarization resistance at the electrodes of the cell and amounting to some two percent of the total value of the resistance in the case of skimmed milk, when the frequency is varied from 1600 to about 200,000 cycles per second. The presence of this polarization resistance does not introduce any systematic error in the verification of the formula, since as would be expected theoretically, in creams of varying concentration it is proportional to the resistance of the cream.

* It may be noted that J. Perrin (Compt. Rend. **158,** 1168, 1914) and R. Costantin (Compt. Rend. **158,** 1171, 1914) found it necessary to introduce the same hypothesis to explain their observations of the dependence of the concentration of suspensions of gamboge in water on the osmotic pressure of the suspension. They attributed the ordered arrangement to the existence of a dipole layer of appreciable thickness around each gamboge particle. The thickness of the dipole layer would theoretically be expected to vary in opposite sense to variations in the conductivity of the suspending phase. This would agree with our observation that the effect is decreased when the conductivity of a cream is increased by the addition of electrolytes.

[5] P. Fraenkel, Zeits. Klin. Med. **52,** 470 (1904)

In Table I are given all the original data in one out of some thirty experiments, this experiment having been chosen because the primary cream was the heaviest used. In other experiments the primary creams

TABLE I

Resistance of a primary cream, its dilutions and its skimmed milk.

Cell No. III Frequency 83 kilocycles/sec. Temperature 25.01°C

			Primary cream		
Samples:	1	2	3	4	5
	[560.2	573.9	569.4	572.8	574.3
	559.5	573.0	567.0	571.7	572.3
	555.9	[570.2			[569.6
	555.4	571.0]			568.9
	555.0]				568.5
					568.3
					566.9]
Averages		573.4	568.2	572.2	573.3
Averages for all samples			571.8 ± 0.9		

		Dilution No. 1 (54.51/84.82)			
Samples:	1A	2A	3A	1B	2B
	[325.2	327.0	327.1	326.4	327.3
	325.0]	327.4	327.1	326.1	327.4
Averages		327.2	327.1	326.2	327.3
Averages for all samples (weighted)			327.12 ± .06		

		Dilution No. 2 (30.31/84.82)			
Samples:	1A	2A	3A	1B	2B
	233.7	232.3	233.2	232.9	232.7
	232.3	232.1	233.3	233.1	232.6
	233.2		233.3		232.5
	233.0				
Averages	233.0	232.2	233.2	233.0	232.6
Averages for all samples			232.81 ± .14		

			Skimmed milk	
Samples:	1	2	3	4
	162.6	161.8	162.0	162.4
	162.5	161.8	162.1	162.4
	162.6			
Averages	162.6	161.8	162.0	162.4
Averages for all samples			162.21 ± .14	

varied from about 25 per cent to about 50 per cent. Among other points this experiment illustrates the criteria which we have employed in order to judge the reliability of individual measurements, the most important of which are the following. Inasmuch as the heavier creams are very thick liquids and the cell is small it is extremely difficult either

to get homogeneous samples or to be assured that the cell has been adequately cleaned of the preceding sample. Consequently after the cell has been filled several times with samples of a new liquid, measurements have been made on successive samples without accepting any until the readings on different samples became concordant. Sample 1 of the primary cream and sample 1A of dilution No. 1 represent such rejected samples. The different columns under each heading represent successive samples of that material, and in each column from above downward are given successive measurements on a given sample, each measurement having been taken immediately after the stirring. Rejected measurements are bracketed.

Because of the irreversible change of conductivity which heavier creams undergo within the cell, with such creams, as a rule, only the first two readings are accepted, though in the table some bracketed figures are included in order to illustrate this change.

TABLE II

Test of formula for conductivity of suspensions

	Volume concentration per cent	
	Calc. from resistances	Calc. from dilution factors
Primary cream:	62.73 ± .12	62.93 ± .19
Dilution No. 1:	40.40 ± .08	40.44 ± .12*
Dilution No. 2:	22.49 ± .06	Standard

* Babcock test gave 37.6 volume per cent. The deviation of this figure, −6 per cent, from the calculated value is unusually high. In our other series the deviations averaged about −2 per cent, with a probable accidental variation of from 1 to 2 per cent.

Table II gives a comparison of the values for ρ calculated from the conductivity data for each dilution with those obtained by dividing the value of ρ for the lowest cream as standard by the respective dilution factors, thus obtaining a value of ρ for each of the two heavier creams which is based on the value of ρ for the lowest cream as calculated from the electrical conductivity data and on the known amount of dilution. Agreements substantially as good as those shown in Table II were obtained in all of the last series of experiments in which the technique outlined above was employed. The data from these experiments are accordingly omitted. They cover completely the range of values of ρ from 8 to 62 per cent.

DEPARTMENT OF BIOPHYSICS,
CLEVELAND CLINIC FOUNDATION,
October 8, 1924.

THE THEORY OF A SIMPLE ELECTROSTATIC ALTERNATOR

By Alfred W. Simon

Abstract

The quantitative theory of a simple electrostatic alternator, that is a static machine which reverses its potential periodically, is given. The machine studied is one with four fixed inductors and four revolving carriers, and reverses its potential once every revolution. Assuming there is no leakage, the formulas for the potentials of the inductors are deduced; and, provided the potentials of two opposite inductors were initially zero and those of the other pair equal and opposite, take a very simple form. If the inductors nearly completely surround the carriers and if the inductors are relatively far apart, during every revolution the potential of any inductor is theoretically quadrupled and at the same time reverses its sign. The machine is therefore self-exciting. Experiments made with an actual machine are described and are in good qualitative agreement with the theory.

ELECTROSTATIC alternators, that is static machines which show the phenomenon of periodic reversal, have been described by various authors.[1] Among them is a noteworthy machine invented by Wimshurst,[2] which is self exciting and yet reverses its polarity regularly every three quarters of a revolution.

The present work gives, for the first time, the quantitative theory of these machines, and it will be shown that most of the important phenomena observed with this class of machines can be deduced directly from ordinary electrostatics.

As the subject of our analysis we shall take a simple electrostatic alternator of four inductors and four carriers, one which when at work reverses its polarity regularly every revolution.

Theory of a Simple Alternator

Consider a machine (Fig. 1) which has four fixed inductors 1, 3, 5, 7, and four revolving carriers 2, 4, 6, 8, and which is so constructed that when the carriers are in the position shown, each carrier is connected by means of a brush and an insulated arm to the inductor next in the direction of rotation. It is assumed that the machine possesses four-fold geometrical symmetry so that each quarter revolution brings the elements again into the same geometrical configuration. Let the inductors 1, 3, 5, 7, be initially raised to potentials $V_{1,0}$, $V_{3,0}$, $V_{5,0}$, $V_{7,0}$, respectively.

[1] V. E., Johnson, "Modern High Speed Influence Machines" Chap. IX, London, 1922

[2] J. Wimshurst, Phil. Mag. **31**, 567 (1891)

It is then required to find the potentials $V_{1,n}$, $V_{3,n}$, $V_{5,n}$, $V_{7,n}$, of the inductors after n quarter turns or cycles. With regard to the notation, it will be observed that the first subscript refers to the inductor and the second to the cycle (quarter turn).

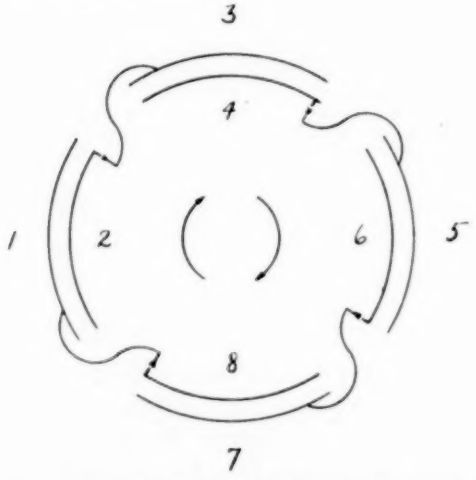

Fig. 1. A simple alternating electrostatic generator.

Let $q_{i,n}$ represent the charge on the element which occupies the position i of the figure after n cycles. For example, let $q_{1,n}$ represent the charge on the inductor 1 after n cycles, $q_{2,n}$ the charge on the carrier which occupies position 2 after n cycles, and so on. Attention is called to the fact that the separate carriers are not indexed but referred to by the position they occupy. Keeping this in mind, we have at once, if we assume no leakage,

$$q_{1,n+1}+q_{8,n+1}=q_{1,n}+q_{6,n} \tag{1}$$

$$q_{3,n+1}+q_{2,n+1}=q_{3,n}+q_{8,n} \tag{2}$$

$$q_{5,n+1}+q_{4,n+1}=q_{5,n}+q_{2,n} \tag{3}$$

$$q_{7,n+1}+q_{6,n+1}=q_{7,n}+q_{4,n} \tag{4}$$

If we substitute for each of the q's its value in terms of the coefficients of capacity, of the coefficients of induction of the elements in the configuration of the figure, and of the corresponding potentials, the above equations become, respectively,

$$aV_{1,n+1}+dV_{3,n+1}+cV_{5,n+1}+bV_{7,n+1}=a'V_{1,n}+d'V_{3,n}+c'V_{5,n}+b'V_{7,n} \tag{5}$$

$$bV_{1,n+1}+aV_{3,n+1}+dV_{5,n+1}+cV_{7,n+1}=b'V_{1,n}+a'V_{3,n}+d'V_{5,}+c'V_{7,n} \tag{6}$$

$$cV_{1,n+1}+bV_{3,n+1}+aV_{5,n+1}+dV_{7,n+1}=c'V_{1,n}+b'V_{3,n}+a'V_{5,n}+d'V_{7,n} \tag{7}$$

$$dV_{1,n+1}+cV_{3,n+1}+bV_{5,n+1}+aV_{7,n+1}=d'V_{1,n}+c'V_{3,n}+b'V_{5,}+a'V_{7,n} \tag{8}$$

in which the coefficients a,b,c,d,a',b',c',d' have been substituted for the expressions

$$\begin{aligned} a &= a_{18,18} = a_{32,32} = a_{54,54} = a_{76,76} \\ b &= a_{18,32} = a_{32,54} = a_{54,76} = a_{76,18} \\ c &= a_{18,54} = a_{32,76} = a_{54,18} = a_{76,32} \\ d &= a_{18,76} = a_{32,54} = a_{54,76} = a_{32,18} \end{aligned} \tag{9}$$

$$\begin{aligned} a' &= a_{18,16} = a_{32,38} = a_{54,52} = a_{76,74} \\ b' &= a_{18,38} = a_{32,52} = a_{54,74} = a_{76,16} \\ c' &= a_{18,52} = a_{32,74} = a_{54,16} = a_{76,38} \\ d' &= a_{18,74} = a_{32,16} = a_{54,38} = a_{76,52} \end{aligned} \tag{10}$$

where $a_{pq,rs}$ is defined by

$$a_{pq,rs} = a_{pr} + a_{ps} + a_{qr} + a_{qs} , \tag{11}$$

any a_{ij} denoting as usual the coefficient of induction of the bodies i, j. In problems where a large number of coefficients must be dealt with, as in this case, the above notation greatly simplifies the work. Moreover, any $a_{pq,rs}$ has a physical significance; for example, $a_{18,18}$ represents the coefficient of capacity of the two bodies 1,8 connected together: $a_{18,32}$ represents the coefficient of induction of the pair 1,8 connected together, and the pair 3,2 connected together.

The reason for the fact that these coefficients are equal in groups of four [Eqs. (9) and (10)] is that our assumption of four-fold geometrical symmetry has as a consequence fourfold electrical symmetry. Further, it is important to note that in addition we have $b=d$, since the mutual coefficients of two pairs of bodies connected together are equal, that is to say

$$a_{pq,rs} = a_{rs,pq} . \tag{12}$$

In electrostatics we usually meet this law in the form

$$a_{ij} = a_{ji} .$$

Eq. (12) is simply a more general form of the same law.

The four equations (5), (6), (7), (8), are the fundamental equations of the machine under consideration, and our problem now becomes a purely mathematical one of deducing the formulas for the sequences $V_{1,n}$, $V_{3,n}$, $V_{5,n}$, $V_{7,n}$, from these equations.

If we subtract (7) from (5), and (8) from (6), and put

$$D_{1,n} = V_{1,n} - V_{5,n} \tag{13}$$

$$D_{3,n} = V_{3,n} - V_{7,n} \tag{14}$$

we obtain

$$(a-c)D_{1,n+1}+(d-b)D_{3,n+1}=(a'-c')D_{1,n}+(d'-b')D_{3,n} \quad (15)$$

$$(b-d)D_{1,n+1}+(a-c)D_{3,n+1}=(b'-d')D_{1,n}+(a'-c')D_{3,n} \quad (16)$$

and, raising the subscripts by unity:

$$(a-c)D_{1,n+2}+(d-b)D_{3,n+2}=(a'-c')D_{1,n+1}+(d'-b')D_{3,n+1} \quad (17)$$

$$(b-d)D_{1,n+2}+(a-c)D_{3,n+2}=(b'-d')D_{1,n+1}+(a'-c')D_{3,n+1} \quad (18)$$

By eliminating the terms of the $D_{3,n}$ sequence from these four equations, we obtain an equation of the form

$$D_{1,n+2}+k_1D_{1,n+1}+k_0D_{1,n}=0$$

where

$$k_1=2(a'-c')/(a-c)$$

$$k_0=[(b'-d')^2+(a'-c')^2]/(a-c)^2 .$$

Now the roots of the algebraic equation $r^2+k_1r+k_0=0$, are $r_1=\alpha+i\beta$ $r_2=\alpha-i\beta$, where $\alpha=(a'-c')/(a-c)$ and $\beta=(b'-d')/(a-c)$. Hence according to the theory of finite differences,[3]

$$D_{1,n}=\rho^n(C_1\cos n\theta+C_2\sin n\theta) \quad (19)$$

where $\rho=\sqrt{\alpha^2+\beta^2}$, $\theta=\arctan \beta/\alpha$ and C_1, C_2, are constants to be determined from the initial values of $D_{1,n}$, that is from $D_{1,0}$ and $D_{1,1}$.

Now from Eqs. (15) and (16) we find that

$$D_{1,1}=[(a'-c')D_{1,0}/(a-c)]+[(d'-b')D_{3,0}/(a-c)]$$

or in terms of θ and ρ

$$D_{1,1}=\rho\cos\theta\, D_{1,0}-\rho\sin\theta\, D_{3,0} .$$

Putting successively $n=0$ and $n=1$ in Eq. (19) and substituting for $D_{1,1}$ the value just found, we have as the determining equations for C_1 and C_2

$$C_1\cos(0)+C_2\sin(0)=D_{1,0}$$

$$\rho C_1\cos(\theta)+\rho C_2\sin(\theta)=\rho D_{1,0}\cos\theta-\rho D_{3,0}\sin\theta ,$$

from which it follows at once that

$$C_1=D_{1,0} \text{ and } C_2=-D_{3,0} .$$

Our formula for $D_{1,n}$ is therefore

$$D_{1,n}=\rho^n(D_{1,0}\cos n\theta-D_{3,0}\sin n\theta) . \quad (20)$$

[3] G. Boole, "A Treatise on the Calculus of Finite Differences," p. 212, London 1880.

By exactly the same method, if we solve Eqs. (15), (16), (17), (18), for $D_{3,n}$, we find

$$D_{3,n}=\rho^n(D_{3,0}\cos n\theta+D_{1,0}\sin n\theta)\ . \tag{21}$$

If next we add Eqs. (5) and (7), and Eqs. (6) and (8), and put

$$S_{1,n}=V_{1,n}+V_{5,n}$$
$$S_{3,n}=V_{3,n}+V_{7,n}\ ;$$

we obtain

$$(a+c)S_{1,n+1}+(d+b)S_{3,n+1}=(a'+c')S_{1,n}+(d'+b')S_{3,n}$$
$$(b+d)S_{1,n+1}+(a+c)S_{3,n+1}=(d'+b')S_{1,n}+(a'+c')S_{3,n}$$

and, raising the subscripts by unity

$$(a+c)S_{1,n+2}+(d+b)S_{3,n+2}=(a'+c')S_{1,n+1}+(d'+b')S_{3,n+1}$$
$$(b+d)S_{1,n+2}+(a+c)S_{3,n+2}=(d'+b')S_{1,n+1}+(a'+c')S_{3,n+1}$$

Eliminating the terms of the $S_{3,n}$ sequence, we obtain an equation of the form

$$S_{1,n+2}+k_1'S_{1,n+1}+k_0'S_{1,n}=0$$

where

$$-k_1'=2\{(d+b)\ (d'+b')-(a+c)\ (a'+c')\}/\{(d+b)^2-(a+c)^2\}$$
$$k_0'=\{(d'+b')^2-(a'+c')^2\}/\{(d+b)^2-(a+c)^2\}\ .$$

Now the roots r_1 and r_2 of the algebraic equation $r^2+k_1'r+k_0=0$ are

$$r_1=\{d'+b')+(a'+c')\}/\{(d+b)+(a+c)\}\ ,$$
$$r_2=\{(d'+b')-(a'+c')\}/\{(d+b)-(a+c)\}$$

and are both real, so that the theory of finite differences gives for $S_{1,n}$ an equation of the form

$$S_{1,n}=C_1r_1^n+C_2r_2^n\ .$$

By a method exactly similar to that employed in the case of the D's we can evaluate the constants C_1 and C_2, and we then find, that

$$2S_{1,n}=(S_{1,0}+S_{3,0})r_1^n+(S_{1,0}-S_{3,0})r_2^n \tag{20'}$$
$$2S_{3,n}=(S_{3,0}+S_{1,0})r_1^n+(S_{3,0}-S_{1,0})r_2^n\ . \tag{21'}$$

The four Eqs. (20), (21), (20′), (21′) enable us to calculate any of the potentials $V_{1,n}$, for from the definition of the D's and S's we have

$$\begin{aligned} 2V_{1,n}&=D_{1,n}+S_{1,n}\ ; \quad -2V_{5,n}=D_{1,n}-S_{1,n}\ ; \\ 2V_{3,n}&=D_{3,n}+S_{3,n}\ ; \quad -2V_{7,n}=D_{3,n}-S_{3,n}\ . \end{aligned} \tag{22}$$

If we substitute for the D's and S's their values, we have

$$2V_{1,n}=\rho^n\{(V_{1,0}-V_{5,0})\cos n\theta-(V_{3,0}-V_{7,0})\sin n\theta\}$$
$$+\tfrac{1}{2}\{V_{1,0}+V_{5,0}+V_{3,0}+V_{7,0}\}r_1^n+\tfrac{1}{2}\{V_{1,0}+V_{5,0}-V_{3,0}-V_{7,0}\}r_2^n \tag{23}$$

$$2V_{3,n}=\rho^n\{(V_{3,0}-V_{7,0})\cos n\theta+(V_{1,0}-V_{5,0})\sin n\theta\}$$
$$+\tfrac{1}{2}\{V_{1,0}+V_{5,0}+V_{3,0}+V_{7,0}\}r_1^n-\tfrac{1}{2}\{V_{1,0}+V_{5,0}-V_{3,0}-V_{7,0}\}r_2^n \quad (24)$$
$$-2V_{5,n}=\rho^n\{(V_{1,0}-V_{5,0})\cos n\theta-(V_{3,0}-V_{7,0})\sin n\theta\}$$
$$-\tfrac{1}{2}\{V_{1,0}+V_{5,0}+V_{3,0}+V_{7,0}\}r_1^n-\tfrac{1}{2}\{V_{1,0}+V_{5,0}-V_{3,0}-V_{7,0}\}r_2^n \quad (25)$$
$$-2V_{7,n}=\rho^n\{(V_{3,0}-V_{7,0})\cos n\theta+(V_{1,0}-V_{5,0})\sin n\theta\}$$
$$-\tfrac{1}{2}\{V_{1,0}+V_{5,0}+V_{3,0}+V_{7,0}\}r_1^n+\tfrac{1}{2}\{V_{1,0}+V_{5,0}-V_{3,0}-V_{7,0}\}r_2^n \quad (26)$$
$$n=0\,,\ 1\,,\ 2\,,\ 3\,,\ \ldots\ldots$$

These are the general formulas for the potentials of the inductors after n cycles, and from them we can draw a number of interesting conclusions. In order to do this we need, however, to examine the quantities r_1, r_2, ρ, and θ, in detail.

If we substitute in the expression for r_1 the values given by Eqs. (9) and (10), we find that $r_1=1$, hence it disappears from our equations. The term involving r_1^n is therefore a constant, and we note that it is, in fact, the sum of the original potentials of the inductors.

If we substitute in the expression for r_2 and make use of the known properties of the electric coefficients as explained in a previous paper,[4] we readily find that $-1<r_2<1$. This shows that the terms involving r_2^n are transient terms, which vanish for large values of n.

If we examine similarly the expression for ρ, we find that ρ ordinarily will be greater than unity. Hence for large values of n, irrespective of what the initial conditions were, there remain only the trigonometric terms.

Examining these we find $V_{1,n}=-V_{5,n}$, and $V_{3,n}=-V_{7,n}$, and we have therefore established the important result that for large values of n the potentials of oppositely situated inductors become equal and opposite, and approach infinity as n approaches infinity. It will be noted that we have assumed no leakage; in practice, of course, the potentials will increase only until the increase is balanced by the leakage. This explains also why such machines are "self-exciting," for any difference of potential, no matter how small it may originally be, is rapidly multiplied.

The second important result which we see directly from the formulas is that the potentials will alternate, with a period dependent on θ. Let us next determine the magnitude of θ. If we substitute in the expression for $\tan\theta$ and simplify, we find

$$\tan\theta=\frac{1+\dfrac{a_{22}-a_{26}}{a_{25}-a_{12}}}{1+\dfrac{a_{11}-a_{15}}{a_{25}-a_{12}}}\,. \quad (27)$$

[4] A. W. Simon, Phys. Rev. **24**, 690 (1924)

The period is therefore a function of a certain number of the electric coefficients of the elements of the machine, and by varying these we can vary the period.

If the carriers nearly completely surround the inductors and if the inductors are relatively far apart, then we may put, to a close degree of approximation,

$$a_{22}=a_{11}=-a_{12}$$

$$a_{26}=a_{25}=a_{15}=0\ .$$

Substituting these values in (27) we find $\tan\theta=1$, whence $\theta=\pi/4$. This shows that under these conditions the complete period is 2 revolutions, and that the potential of each inductor reverses every revolution.

If we simplify the expression for ρ we have

$$\rho^2=\left\{(a_{11}+a_{16}-a_{12}-a_{15})^2+(a_{22}+a_{16}-a_{12}-a_{26})^2\right\}/\left\{a_{11}+a_{22}-a_{15}-a_{26}\right\}^2\ .$$

Under the same assumptions as made above, this reduces to

$$\rho^2=\left\{(2a_{11})^2+(2a_{11})^2\right\}/\left\{(2a_{11})^2\right.$$

whence $\rho=\sqrt{2}$. If we assume further that $V_{1,0}=-V_{5,0}$ and $V_{3,0}=V_{7,0}=0$, there result the following simple formulas

$$V_{1,n}=-V_{5,n}=(\sqrt{2})^nV_{1,0}\cos(n\pi/4)$$

$$V_{3,n}=-V_{7,n}=(\sqrt{2})^nV_{1,0}\sin(n\pi/4).$$

In order to picture the action of the machine under these conditions a series of values of $V_{1,n}$ and $V_{3,n}$ corresponding to a complete period have been computed and are given in Table I.

TABLE I

n	$V_{1,n}$	$V_{3,n}$	Revolutions
0	$+V_{1,0}$	0	0
1	$+V_{1,0}$	$+V_{1,0}$	$\frac{1}{4}$
2	0	$+2V_{1,0}$	$\frac{2}{4}$
3	$-2V_{1,0}$	$+2V_{1,0}$	$\frac{3}{4}$
4	$-4V_{1,0}$	0	1
5	$-4V_{1,0}$	$-4V_{1,0}$	$1\frac{1}{4}$
6	0	$-8V_{1,0}$	$1\frac{2}{4}$
7	$+8V_{1,0}$	$-8V_{1,0}$	$1\frac{3}{4}$
8	$+16V_{1,0}$	0	2

EXPERIMENTAL VERIFICATION OF THE THEORY

The above theory represents only an approximation to actual practice since we have excluded leakage phenomena; in particular, the potential of the inductors does not rise indefinitely but approaches a final value which is determined by the amount of leakage.

However, in spite of leakage phenomena, a great many of the results deduced theoretically can be verified experimentally.

A machine, such as that represented in Fig. 1, was actually constructed and found to be self-exciting and alternating. The potential of each inductor reversed regularly every revolution. When electroscopes were connected to the inductors, the action of the machine could be exhibited in a very striking way. When two electroscopes were connected to a pair of *opposite* inductors the leaves diverged and collapsed *in synchronism*, and, if the sign of the charge on each was tested by means of an electrified stick of sealing wax, it was found that the leaves were *oppositely* charged; if the electroscopes were connected to two *adjacent* inductors, one leaf *lagged* a quarter period behind the other, and for successive quarter turns the signs of the potentials were exactly those given in Table I.

By adding four variable condensers, one to each inductor, the period of reversal could be increased exactly as demanded by Eq. (27).

For a complete quantitative verification it would be necessary to actually measure the various electric coefficients involved and compare the observed values of ρ with those calculated from the measured coefficients. It is hoped to carry this out in the near future.

In conclusion I wish to express my thanks to Professor L. E. Dickson of the Department of Mathematics for some valuable suggestions regarding the mathematical treatment of the problem.

RYERSON LABORATORY,
UNIVERSITY OF CHICAGO,
December 1, 1924.

VISIBLE RADIATION FROM COLUMBIUM OXIDE

By E. L. Nichols

Abstract

Radiation from columbium oxide, heated in the hydrogen flame to various temperatures below 1000°C, was studied with the spectrophotometer. Two distinct and strikingly different types of visible radiation were found. *Phase O* (in the oxidizing region of the flame) is selective with luminescence bands superimposed upon the radiation due to temperature. *Phase R* (in the reducing region) resembles that of a black body both as to spectral distribution and intensity. This phase was traced to the formation of a lower oxide Cb_2O_4 which is jet black at temperatures of incandescence and radiates as a black body. The change from one phase to the other was instantaneous when the oxide was shifted in the flame.

Formation of black suboxides in the hydrogen flame.—Similar black suboxides were observed in the *case of titanium oxide and tantalum oxide*, and to the formation of these in the reducing flame, phase R is doubtless to be ascribed whenever radiation of that type occurs.

THIS white and highly refractory oxide (Cb_2O_5) exhibits certain remarkable peculiarities as to the character of its visible radiation at the lower temperatures of incandescence. When a fragment a few millimeters in diameter is gradually inserted from the side into the outer layers of a hydrogen flame, instead of becoming "red hot" it glows with a pale greenish blue color. Pushed further into the flame the color of the incandescent fragment changes abruptly to a deep red.

The contrast is a most striking one and the transition may readily be shown to depend on the position of the oxide within the flame rather than upon any change of temperature. These two types of radiation, which in conformity with the previous study of somewhat similar conditions in the incandescence of titanium oxide[1] we shall call respectively *phase O* and *phase R*, are mutually and instantly interchangeable. So sharp is the boundary between the portions of the flame where they occur that it is easy to move the bit of oxide into a position where the inner part, lying nearer to the axis of the flame, is red, and the outer, in the oxidizing layer, is green-blue. If now the piece of oxide be made to oscillate at right angles to the axis of the flame this boundary will be seen to be fixed with reference to the flame. There is no perceptible lag, such as would be easily observable if the change depended upon alternate heating or cooling of the oxide.

[1] Nichols, Phys. Rev. (2) **22**, 420 (1923).

Approximate Analysis of the Visible Radiation

Through a spectroscope of low dispersion the spectra of both phases are seen to be continuous but the appearance of that of phase O suggests a group of very broad nearly submerged bands covering the entire range of the visible region. For the comparison of these spectra the following scheme was adopted.

Across the outer surface of the base of an alundum crucible a shallow depression was cut about .05 cm deep and 1.0 cm in width. This served as a holder for a thin layer of the oxide which could be pressed into the channel in powdered form, completely filling it, with the smooth face of the layer flush with the alundum surface on either side. Thus mounted it could be raised into a vertical plane and heated by means of the hydrogen flame without breaking down. With a camel's hair brush half of the surface of the oxide was moistened with a solution of uranyl chloride leaving a sharp dividing line *LL* (Fig. 1). After heating, the moistened region remained impregnated with uranium oxide, which imparted to it the radiating properties of a very nearly perfect black body.

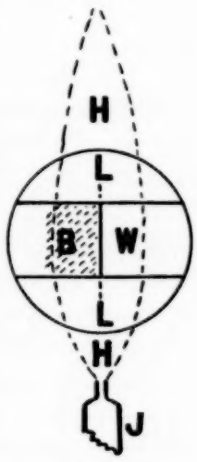

Fig. 1.

When a flame of hydrogen *HH* from a small vertical jet *J* was brought up until its outer layers were in contact with the layer of oxide, the region *B* to the left of the median line, became red hot, while the corresponding region *W* to the right assumed the radiating condition known as *phase O*. An image of the contiguous fields of glowing material was then sharply focussed in the vertical transverse plane, passing through one collimator slit of a large Hilger spectrophotometer with the line *LL* parallel to the slit. By turning a sheet of plate glass *G* (Fig. 2) in the path of the beam of light, the image of *BW* could be shifted to the right or left so that the portion corresponding to *B* alone or to *W* alone would fall upon the slit *S*. Thus any desired wave-length of the spectrum of the light from *B* or *W* could be compared with the corresponding wave-length of the comparison lamp which was mounted, in the manner described in various earlier papers, on a photometer bar before the other slit of the spectrophotometer. The comparison source was a tungsten filament of low voltage maintained by a storage battery at approximately 2000°K. By turning *G* through a predetermined angle the spectrum under observation could be shifted back

and forth between B and W at will and thus, by the method of substitution, the relation of these spectra to one another was readily determined.

By moving the hydrogen flame a trifle nearer to the base of the crucible and thus converting phase O of the radiation of the Cb_2O_5 into phase R, a similar set of observations gave the relations between the spectrum of this phase and the spectrum of the comparison lamp or of the uranium oxide. These measurements give directly the composition of the visible radiation from the glowing oxides in terms of the composition of the light from the comparison lamp.

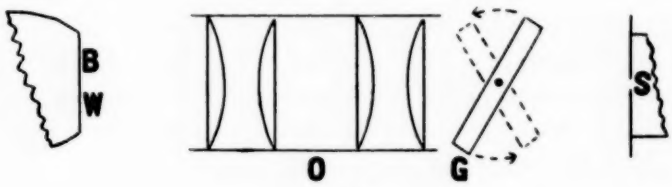

Fig 2.

In Table I, as already stated, I_0 is the brightness of the glowing columbium oxide (phase O) in terms of that of the corresponding region in the spectrum of the comparison lamp. The conditions of the measurements were such that the two spectra were very nearly of equal brightness in the yellow (at .5890μ). Similarly I_B is the brightness, under the same conditions of comparison, of the glowing uranium oxide. To make the values of I_0 and I_B as nearly as possible strictly comparable, measurements of the two were made alternately throughout the spectrum.

TABLE I

Distribution of intensities in the spectrum Cb_2O_5.

λ	I_0	I_B	I_0/I_B	λ	I_0	I_B	I_0/I_B
.4590μ	.0930	.0240	3.88	.5771μ	1.320	2834	4.76
.4675	.1551	.0266	5.83	.6018	.9766	4852	2.01
.4793	.2488	.0310	8.02	.6298	1.008	.5333	1.89
.4918	.2825	.0363	7.79	.6620	.8503	.8547	0.996
.5052	.2644	.0472	5.99	.6765	1.468	1.294	1.134
.5175	.2644	.0643	4.13	.6924	1.276	1.693	0.754
.5372	.6645	.1480	4.49	.7007	1.562	1.762	0.886
5557	.1457	.2635	5.53				

In Fig. 3, I_0 is plotted as function of the wave-length and the corresponding intensity of the spectrum of the comparison lamp is represented by the horizontal line TT having the ordinate unity. Clearly the spectrum of Cb_2O_5 under conditions which give radiation of phase O, consists of several rather broad overlapping bands. Uranium oxide, on the contrary, at the same temperature (820°C as determined by the optical

pyrometer), shows no indications of a banded spectrum. The curve I_B (also given in Fig. 3) is of the character which one would expect to obtain for a non-selective radiator at the temperature in question.

Knowing the distribution of intensities in the spectrum of the comparison lamp, the values of I_0 might readily be expressed in terms of relative energy, but it is more interesting for our present purpose to compare the radiation of the glowing columbian oxide with that of a black body at the same temperature. This comparison is afforded by the ratio I_0/I_B for the various regions of the spectrum and is given graphically in Fig. 4 where

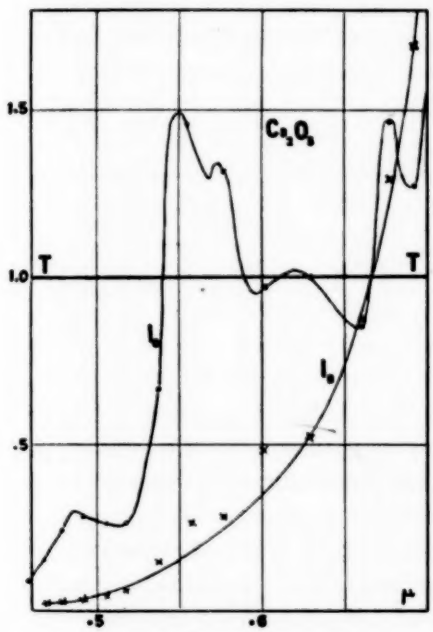

Fig. 3. Intensity distribution I_0 of spectrum of Cb_2O_5, taking the comparison spectrum as unity, *TT*.

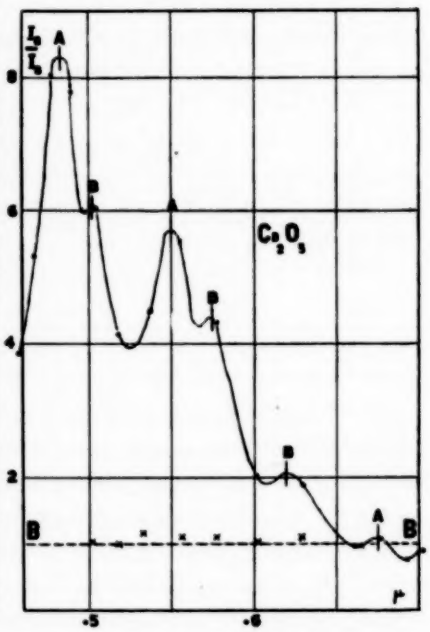

Fig. 4. Intensity distribution of spectrum of Cb_2O_5 referred to that of a black body taken as unity, *BB*.

I_B is represented by the horizontal line *BB* of ordinate unity. The curve for I_0/I^B in this diagram brings out the crests of the overlapping bands more definitely than does the corresponding curve in Fig. 3. The resolution is not sufficient to bring out the finer structure of the spectrum but six crests may be quite closely located.

H. L. Howes[2] in a study of calcium oxide and of certain sulphides when excited to luminescence by the hydrogen flame, has found their spectra to be made up of overlapping bands equidistant as to frequency and coinci-

[2] H. L. Howes, Phys. Rev. (2) **17**, 469 (1921).

dent with the bands of the same substances when excited by cathode rays.[3] More recently, Tanaka[4] in an exhaustive investigation of the cathodo-luminescent substances, made under the present writer's direction, has established a definite relation between the frequency interval between bands and the atomic weight of the activating element. A consideration of the frequency relations of the crests in Fig. 4 is therefore not without interest. Tanaka's interval for columbium would be very close to 21 and an inspection of the location of the bands in the spectrum now under consideration shows that they may in fact be arranged in two sets such that the distance, measured in frequency units, between neighboring members of a set is an even multiple of Tanaka's interval. Calling these sets *A* and *B* we find the following relations.

TABLE II

Frequency relations of the bands of phase O.

Set A			Set B		
λ	$1/\lambda\times10^3$	Differences	λ	$1/\lambda\times10^3$	Differences
.4831μ	2070		.5020μ	1992	
		$252=21\times12$			$252=21\times12$
.5500	1818		.5747	1740	
		$336=21\times16$			$126=21\times6$
.6748	1482		.6196	1614	

It is believed that the crests recorded in Table II represent groups of bands rather than single bands, and experiments are in progress to determine by a photographic method the finer structure of this spectrum and of the spectra of other glowing oxides.

In the present investigation, as in some earlier studies of incandescent oxides, the visible radiation from uranium oxide has been taken as representing with sufficient closeness that of a black body of the same temperature. In support of this assumption the following observation may be cited. Into one end of a cylindrical copper block about 5 cm long and 2.5 cm in diameter, a hole about .5 cm in diameter and 4 cm in depth, was bored parallel to the axis. When the block was suspended over a large Bunsen burner and heated to uniform incandescence, the appearance of the end with the hole was as follows.

(1) With the flame adjusted so as to maintain the surface of the copper in a reduced metallic state, the aperture, because of the radiation under black body conditions from within, appeared as a cherry red disk on a very dark background.

[3] Nichols, Howes and Wilber, Phys. Rev. (2) **12**, 351 (1918).
[4] Tanaka, Jour. Opt. Soc. Amer. **7**, 287 (1924).

(2) With the flame shifted so as to oxidize the surface of the copper, the radiation from the end of the rod was so nearly equal to that from the hole that the latter was *just barely perceptible.*

(3) The flame having been extinguished and a small portion of the oxidized surface contiguous to the hole having been moistened with a solution of uranium chloride, the block was again heated to incandescence. It was now observed that in the oxidizing flame the patch to which the uranium chloride had been applied and which was now covered with a very thin layer of uranium oxide was scarcely to be distinguished from the surrounding surface *or from the hole.* In the reducing flame, however, this patch, which was not reduced by the flame, stood out against the much weaker radiation from the metallic copper and, so far as could be judged by the eye, was almost of the same brightness and color as the hole from which it could be distinguished only by its shape. Settings with the optical pyrometer when the block was at 870°C confirmed the judgment of the eye, the relative brightness being as follows; hole, 1.00; CuO, .954; uranium oxide, .954; metallic copper, .14. The value for copper is what one would expect, being intermediate between that given for the green .17 and for the extreme red .09.[5]

Quite aside from the above measurement, there can be no doubt in the mind of one who has seen them side by side upon the incandescent surface, of the essential equality of the two oxides, nor of their approximately complete blackness to one who has viewed them by reflected light at a temperature of 500° or more. This last observation was checked by measuring the melting point of minute crystals of KCl placed upon the incandescent oxide. The pyrometer, using the calibration given by the Bureau of Standards, yielded the accepted melting point within 3° when the settings were made upon the uranium oxide. It will be understood that these very high values of relative emissivity apply only to oxides formed by the hydrogen flame in the manner described and used practically in the nascent state, and not necessarily to these two substances in general.

Phase O: A Luminescent Effect

That the visible radiation indicated graphically in Fig. 4, is partly at least to be ascribed to luminescence is obvious when we consider that all intensities above the horizontal line *BB* or a line very near to that, are in excess of the black body intensities for the various wave-lengths and at the given temperature. That the portion of the area under the curve

[5] LeChatelier, Measurement of High Temperatures, Trans. by Burgess, p. 497.

which is due to temperature radiation must be much smaller than that which would correspond to a black body becomes obvious when we flood the radiating surface with white light strong enough to quench the incandescence. It is then seen that we have to do with an oxide which is *nearly white*, and therefore capable of relatively feeble radiation in accordance with the Kirchhoff relation.

In addition to the above criterion there are the following characteristics which suggest luminescence.

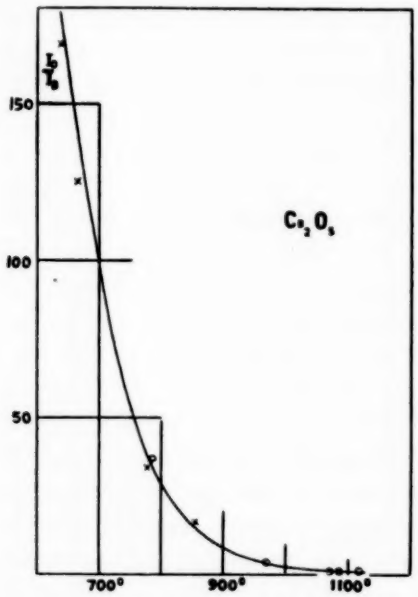

Fig. 5. Ratio of brightness to that of a black body, as a function of temperature.

(a) *The spectral structure.* The band structure, which has already been described, is characteristic of all known luminescence spectra.

(b) *The ratio of brightness to that of a black body* of the same temperature diminishes rapidly with rising temperature and approaches unity at temperatures above 1000°. The change of the ratio of I_0/I_B with the temperature is shown in Fig. 5 in which the observations grouped along the logarithmic curve indicate the ratios obtained in two overlapping runs, one for the lower, designated by crosses, and one for the higher ranges, designated by circles.

The curve in Fig. 5 is similar to those found for the *blue glow*[6] of such oxides as CaO, MgO, BeO, Al_2O_3, and ZrO_2; but the luminescent bands

[6] Nichols and Howes, Jour. Opt. Soc. Am. **6**, 42 (1922); also Phys. Rev. (2) **19**, 300 (1922).

in the case of Cb_2O_5 extend through the entire spectrum and the color of the glow is a very pale blue-green.

The point of lowest temperature in Fig. 5 represents very nearly the threshold for this type of luminescence for Cb_2O_5; that is, at lower temperatures nothing is visible while when 640° is reached the effect appears quite suddenly.

(c) *Fatigue.* When a coating of the oxide not previously heated to incandescence is suddenly brought to a given temperature its initial brightness exceeds any subsequent value and it falls at first rapidly and then more and more slowly to a nearly constant state. This effect of fatigue, which is another of the characteristics of luminescence as distinguished from temperature radiation, is shown in the curve in Fig. 6, in which the abscissas are the times in minutes from the application of the flame, and the ordinates are intensities as expressed by the ratio I_0/I_B. It will be noted by comparison with Fig. 5 that the brightness falls to the value for the temperature in question, 860°C, after about 25 minutes.

Among the substances tested by the present writer in collaboration with Professor H. L. Howes in the preliminary study of incandescent oxides[7] was a mixture supposed to consist chiefly of the oxides of columbium and tantalum. This was designated tentatively as niobium oxide (and wrongly as Nb_2O_4). The behavior of this substance corresponded in some respects to that of Cb_2O_5. It was, for example, luminescent throughout the visible spectrum with the greatest excess of radiation in the blue violet. It also ceased to luminesce at about 1100°C. It differed from our present oxide in showing signs of fusion just above 1100° instead of melting at 1300°, and it was strongly luminescent below the threshold value of 640°. Phase R, if it existed, was not observed.

Observations on Radiation of Phase R

As has been stated in the opening paragraph of this paper, a sudden transition in the type of radiation occurs when the columbium oxide is moved from the outer oxidizing zone of the hydrogen flame into the inner reducing regions. Upon comparing the appearance of the glowing oxide with that of uranium oxide at the same temperature, it is seen at once that the two glowing surfaces are scarcely to be distinguished either as to color or brightness.

Spectrophotometric measurements by the method used in the study of Phase O, readings being made alternately of the brightness of the radiation from the columbium oxide (Phase R) and from the contiguous surface

[7] Nichols and Howes, Phys. Rev. (2) **19**, p. 309

of uranium oxide, confirm the impression as to the approximate identity of the two, both as to the composition of the light and as to the equality of temperature.

In Fig. 7 are plotted the results of such a run. The curve portrays the radiation from the uranium oxide at various wave-lengths, the points marked by crosses showing the departure of the brightness of the radiation of the columbium oxide from that of the uranium oxide. These departures, while all in the same direction, are insignificant as compared with the departure of the luminescent Phase O as is more strikingly

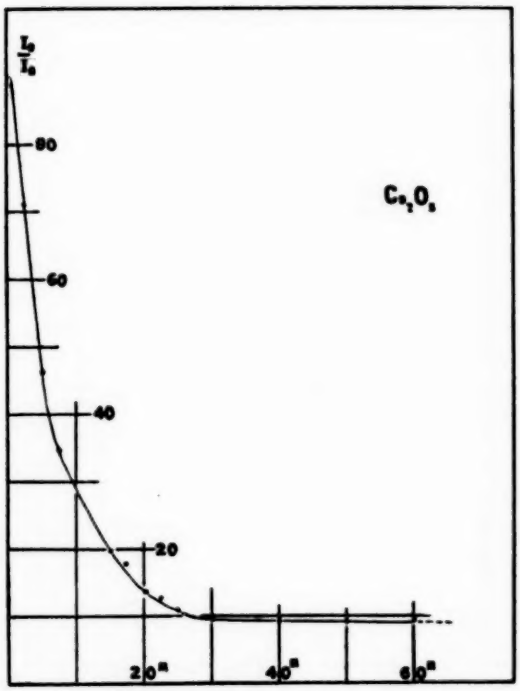

Fig. 6.
Brightness of oxide coating heated to 860°, as a function of time in minutes.

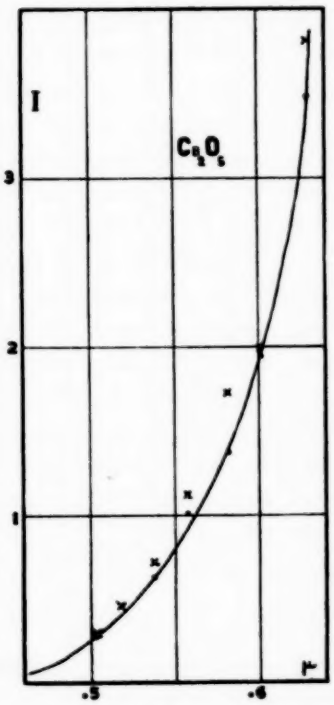

Fig. 7.
Comparison of Phase R radiation with that of uranium oxide (full line).

shown by means of the points marked by crosses along the horizontal line in Fig. 4, where the radiation from the uranium oxide is taken as unity throughout the spectrum. The variation is perhaps most reasonably to be accounted for by supposing that the luminescence was almost but not entirely suppressed.

If now the effect of moving the coating across the boundary between the oxidizing and the reducing zones of the flame were merely to deprive

it of the exciting action which produces luminescence, we should have a white oxide of relatively very feeble radiating power instead of a surface which, as appears to the eye and also as determined by the optical measurements just given, radiates *like a black body*.

The very simple explanation of this apparent anomaly is at once afforded by illuminating the glowing oxide strongly with white light, for then the regions from which radiation of Phase R come *are seen to be jet black* while the surrounding and luminescent regions in the oxidizing portions are a yellowish white. The boundary between black and white shifts instantly with every movement of the flame, like a shadow. Evidently the surface of the oxide within the reducing regions of the flame is converted into a black and consequently into a non-luminescent substance, probably into the black tetra-oxide Cb_2O_4 known to the chemists.

Analogous Changes in TiO_2 and Ta_2O_5

After the completion of the above observation, titanium oxide, the substance first known to have two phases of radiation,[1] and tantalum pentoxide were similarly tested. The titanium oxide darkened within the regions giving radiation of Phase R but the color as viewed by reflected light was a blue-gray rather than black, possibly due to the formation of Ti_2O_3. Tantalum oxide under similar conditions blackens, reducing probably to the well known black tetraoxide Ta_2O_4.

It is probable, in view of these observations, that whenever an incandescent oxide shows two distinct types of radiation in the hydrogen flame, the effect is due to the formation of a superficial layer of a black oxide within the reducing regions of the flame whereby the luminescence of the substance is partly or entirely destroyed, while its temperature radiation proper is raised from the lower intensity characteristic of a white substance to that pertaining to a black body.

Physical Laboratory of Cornell University,
September, 1924.

THE TRANSPARENCY AND COLOR OF THE SEA

By K. R. Ramanathan

Abstract

The theory of the Secchi disk given by Shoulejkin[1] is discussed and a correct expression derived for the depth to which the disk, painted white, should be sunk in an ocean of pure dust-free water so as to be just visible. With ordinary paint the maximum depth is computed to be about 120 meters, whereas the greatest observed depth in the ocean is about 60 meters. The difference is due (1) to the presence of suspended matter and (2) to a possible extra absorption in the blue and violet. Contrary to the opinion expressed by Shoulejkin, it is shown that in the blue region the *brightness* due to molecular scattering alone would be appreciable, in fact about one-sixth that of blue sky. This is confirmed by rough observations made in the Bay of Bengal.

IN two recent papers,[1] Prof. Shoulejkin has discussed the question of the color of the sea and has published interesting experimental observations in connection with them. He is of the opinion that the return of light from the sea is mainly due to the scattering of light by small particles suspended in it, the color and intensity of the returned light being modified by the selective absorption of the water. While agreeing with Prof. Shoulejkin that in many cases the scattering of light by suspended particles is of primary importance, the writer wishes to point out that it is not always so. Shoulejkin has also derived an expression for the relation between the scattering and absorption coefficients of sea-water and the maximum depth to which a disk (painted white) should be sunk in order to be just visible. Making use of this relation, he concludes that in seas where water occurs in its purest form, and hence where molecular scattering[2] is mainly responsible for a return of light, there would be very little light returned from within the ocean and that the color and the brightness of such seas would depend mainly on the state of the sky at the time. Since this is contrary alike to theory and observation, it is felt desirable to examine Shoulejkin's paper in some detail.

Shoulejkin's arguments rest on his theory of the Secchi disk[1a] and on the expression for the brightness of the sea which he derived[1b]. It seems to the writer that serious errors have been made, especially in connection with the theory of the Secchi disk. Both on that account and on account of its intrinsic interest, it is proposed to discuss the problem afresh.

[1] Shoulejkin, (a) Phys. Rev. **22**, 85 (1923) and (b) **23**, 744 (1924).
[2] C. V. Raman, Proc. Roy. Soc. A **101**, 64 (1922) and
K. R. Ramanathan, Phil. Mag. **46**, 543 (1923)

When a plate is gradually lowered in water to such a depth that it ceases to be visible, what we look for is the difference in *brightness* between the plate and the surrounding column of water. In a transparent medium, the brightness of an object which subtends a finite angle at the eye is independent of its distance, while in an absorbing medium, the brightness varies as $e^{-\gamma r}$ where γ is the coefficient of extinction in the medium and r is the distance.[3] When a matt surface of albedo A is sunk in water to a depth z, it will have a brightness $AI_0e^{-2\gamma z}/\pi$ where I_0 represents the intensity of the normally incident light at the surface of the sea. To get the apparent brightness of the disk, we have also to add to this the brightness of the superincumbent column of water due to scattering. If $2B/\lambda^4$ represents the scattering per unit solid angle by unit volume of water against the direction of the incident light, this amounts to

$$\frac{2BI_0}{\lambda^4}\int_0^z e^{-2\gamma x}dx=\frac{BI_0}{\gamma\lambda^4}(1-e^{-2\gamma z})$$

and the total apparent brightness of the disk is therefore

$$(A/\pi-B/\gamma\lambda^4)I_0\,e^{-2\gamma z}+BI_0/\gamma\lambda^4\,. \qquad (1)$$

The brightness of the surrounding unobstructed column of water is $I_0B/\gamma\lambda^4$ and the relative contrast is therefore

$$(A/\pi-B/\gamma\lambda^4)e^{-2\gamma z}/(B/\gamma\lambda^4)\,. \qquad (2)$$

In estimating what minimum relative difference in brightness we may reasonably expect to detect, we have to remember that at the depths at which the disks usually disappear in tropical waters, practically all the red, yellow and green have been cut off and the light is mostly indigo and violet where the sensitiveness of the eye in detecting differences of brightness is small and the fatigue is rapid; the disk is but a small patch in an otherwise continuous and uniformly bright area; and moreover, the observations are made from an unsteady support so that the eye cannot be properly focussed. Ten per cent will not, under these circumstances, be an overestimate for the minimum contrast necessary for proper seeing. Indeed, according to Buchanan,[4] the contrast should be very much larger. The value for the least perceptible difference in brightness adopted by Shoulejkin, 1/133, is decidedly too low. Even in calm days and with

[3] Shoulejkin's assumption that the coefficient of extinction as measured in transmission experiments is $\frac{1}{2}a/\lambda^4+f(\lambda)$ where a/λ^4 is the coefficient of scattering and $f(\lambda)$ the coefficient of absorption is erroneous. What is measured is $a/\lambda^4+f(\lambda)$.

[4] Buchanan, Nature, July 1910, p. 87.

large disks, it is doubtful if one could detect a difference of less than 5 per cent.

Another point of importance is the value of the albedo for the disk. With white light incident, the albedo for ordinary white paint is about 0.6, but the usual paints exercise an absorption in the blue and violet parts of the spectrum, so that in this region, the albedo is much less. When we go down to depths of 50 meters and more, the transmitted light is mostly of wave-lengths below .5μ and we cannot therefore use the usual value of the albedo. Buchanan's statement that at a depth of 25 fathoms, the brightness of the uninterrupted sea was of much *greater* intensity than that of the disk supports this.

Considering as an ideal case an ocean of dust-free distilled water and taking primary scattering alone into account, the following table gives the values of the brightness of a sufficiently large white disk sunk under different depths of water. The data for scattering and absorption coefficients are the same as those used in my paper on the color of the sea. The value of the albedo has been assumed to be 0.6 for all wave-lengths except the last two for which it has been taken to be 0.4 and 0.3 respectively.

TABLE I.

Proportion of incident light scattered per unit solid angle by a Secchi disk

Depth	.578μ	.546μ	.475μ	.436μ
50m	1.55×10^{-3}	9.1×10^{-3}	2.9×10^{-2}	4.3×10^{-2}
100	1.2	3.0	1.3	2.8
150	1.2	2.8	1.05	2.3
∞	1.2	2.8	1.0	2.1

To get the visual effect of all the wave-lengths taken together, we have to take the radiations in different spectral regions in proportion to the energies of the incident radiations and also to the corresponding luminous efficiencies. Remembering that the luminous efficiencies at .475μ and .436μ are only about 1/8 and 1/35 of that at .550μ (Ives), we can easily see from the table above that the maximum depth at which we can expect to distinguish a sufficiently large disk is about 120 meters.[5]

The greatest observed depth of disappearance of the disk, about 60 meters, is in the tropical parts of the Pacific ocean and in the Sargasso sea. In the transparent parts of the Indian ocean, the depth is about 50 meters. These are decidedly less than the depth calculated for pure

[5] We have in the above neglected the illumination of the disk and of the water by scattered light. A rough calculation shows that this will not greatly affect the depth of disappearance in pure water. A detailed calculation would however be of interest.

dust-free water; the difference may be due either (1) to scattering by suspended particles, such as were found by the writer to be present in small quantities in the Bay of Bengal, or (2) to an increase in the coefficient of absorption in the violet end of the spectrum, or to both causes combined.

The presence of suspended particles affects the depth of sinking in two ways; it increases the coefficient of scattering which causes the return of a greater percentage of incident light from the water, the contribution of the surface layers being comparatively greater; it also reduces the transparency of the medium. A reference to Eq. (2) shows that both these would reduce the critical depth of sinking. When the quantity of suspended matter is, however, small, the increase in the scattering is mostly on the forward side of the incident light and the scattering against the incident direction is hardly affected. For example, with one of the samples from Bay of Bengal, the scattering was about 1.2 times that of dust-free distilled water between the angles 0° and 60° (measured from a direction opposite to the incident light), 1.5 times between 60° and 90°, 3.0 times between 90° and 120°, and 6 times between 120° and 180°. Since the solid angle contained between each of these limits is the same, namely π, the total scattering is increased to about 3 times that of pure dust-free water. But the total light returned from within the ocean is not increased in the same ratio, because the scattering against the direction of the incicent light is only slightly more than that of the dust-free water, and thus the return of light from within the sea is primarily due to molecular scattering. Although, therefore, the presence of these particles would to some extent diminish the depth at which an immersed white disk can be seen, it cannot account for the entire difference between the observed and calculated depths.

There is evidence to show that the actual absorption of sea-water in the violet end of the spectrum is really greater than that of dust-free distilled water. Even water from the deep-blue portions of the Bay of Bengal shows a very feeble but distinct green fluorescence when excited by blue and violet light. This implied an extra absorption in this region and this is, I think, another important reason why we are not able to see a white disk at depths greater than about 60 meters in even the most transparent parts of the ocean. Actual measurements of extinction coefficients in water collected from the transparent parts of the ocean would be of interest.

In connection with Shoulejkin's statement that molecular scattering by itself cannot give rise to any appreciable brightness of the sea, it may

be pointed out that according to the figures given in Table I, the brightness of a dust-free sea when viewed normally is in the blue region of the spectrum about one per cent of the incident intensity of illumination. When secondary scattering is taken into account, this will be raised to about 1.2 per cent. Now it is known that the average blue sky has about 1/7 the brightness of white paper illuminated by the zenith sun.[6] Taking the albedo of white paper to be 0.80, the brightness of the latter is AI_0/π i.e. about 25 per cent of the incident intensity of illumination, and that of the average blue sky is therefore 3.5 per cent. If we confine ourselves to the blue region of the spectrum, the value would be higher, say about 7 per cent. An ocean of dust-free distilled water would thus have a brightness about 1/6 that of the average blue sky, while sky-light normally reflected at the surface of the sea would give rise to a brightness of only 2 per cent of the sky-brightness. Some rough photometric measurements (with a blue filter) carried out by the author from the upper deck of a steamer in the blue waters of the Bay of Bengal between the hours 9 a.m. and 3 p.m. on a day when the sky was *very clear*, showed that the zenith sky was 4 to 5 times as bright as the sea when viewed nearly normally.

UNIVERSITY COLLEGE,
RANGOON, INDIA,
September 29, 1924.

[6] Recueil des Constantes Physiques, p. 209.

OPTIMUM REVERBERATION FOR AN AUDITORIUM

By Samuel Lifshitz

Abstract

The time of reverberation of a room depends upon the number of people present. The optimum time has been determined experimentally for a number of halls by having the audience gradually increase while musicians play as constantly as possible, the judgment of trained musicians being obtained as to when the best acoustics were secured. The optimum reverberation (for a sound $10^6 \times$threshold intensity) was found to be the same for speech and for singing as for instrumental music within .05 sec., the mean being 1.03 sec. for a room of less than 350m³. For larger rooms the optimum T is given by the equation $(10.23-\log_{10}V)T+0.97(0.4-\log_{10}V)T^{\frac{1}{2}}=6$. The acoustics of various concert halls and of the Big Theater in Moscow are in agreement with the formula, which has previously been published.

WALLACE SABINE[1] has determined how the reverberation depends upon the architectural features of a room, but it is not yet known definitely what value the reverberation in a given closed room should have in order that its acoustics may be perfect. Paul E. Sabine[2] in a recent paper gives the following rule; "The time of reverberation for an audiorium with its maximum audience . . . . should lie between 1 and 2 seconds. For speech and light music it should fall in the lower half of this range, while for music of the larger sort it may lie nearer the upper limit." Our investigations, as we shall see, are in agreement with the first part of the rule, but not with the second part. According to our results the difference between speech and orchestral music of the larger sort exists only for imperfect rooms. In the case of too great reverberation we should prefer to listen to an orchestra than to speech, which in these conditions may be quite unintelligible; and on the other hand, in case of not enough reverberation the music will appear dry and lifeless, while the speech will be quite acceptable and comprehensible. However, this difference disappears when the acoustics of the closed room become perfect, that is, when there is an optimum of reverberation.

In the beginning our investigations only dealt with the conditions of musical reception in a small room. The room which was studied was the auditorium of the Government Institute of Musical Science in Moscow. The volume of this room was equal to 126 m³. The experiment consisted

[1] Wallace Sabine, Collected Papers on Acoustics, 1922; Harvard Univ. Press
[2] Paul E. Sabine, The American Architect, June 1924

in a singer or a musician repeating the same piece with different audiences in the room. A board of highly qualified musicians gave judgment as to the beauty of the music heard. In the beginning, when the room was empty, the voice sounded very sonorously, then as the audience of the auditorium increased the effect became more and more agreeable, the optimum was reached, and then the music began to sound dry and lifeless. Experienced performers tried to play or sing without changing any more than possible either the intensity or the manner of the performance. Under these conditions, the determination of the optimum could be made within narrow limits. A change in the reverberation of a few hundredths of a second gave a perceptible change in the character of the sound. In this way the following results were obtained.

For the baritone, the violin and the violoncello, the best times of reverberation were found to be 1.00 sec., 1.03 sec. and 1.05 sec. respectively. In the mean $T_{op}=1.03$ sec. As the mean of our determinations and of the results obtained by Sabine for the piano (1.08 sec.), we will take $T_{op}=1.06$ sec. Here, as also further on, T_{op} is the time of reverberation of a sound initially a million times as intense as the threshold of audibility.

An orator's speech in the room investigated sounded best, considering the beauty of quality of the voice, under the same conditions, that is when $T_{op}=1.06$ sec.

Later, as a result of a series of theoretical considerations and experiments,[3] we came to the conclusion that this optimum holds for rooms of dimensions up to 350 m³. For larger rooms, the optimum time increases in accordance with the equation:

$$(10.23-\log_{10}V)T_{op}+0.97(0.4-\log_{10}V)T_{op}^{\frac{1}{3}}=6 \qquad (1)$$

Here V indicates the volume of the room in cubic meters.

Fig. 1 shows the relation between the optimum time of reverberation in seconds and the volume in cubic meters. To test the formula we ininvestigated many music-halls and the Big Theater in Moscow. The following results were obtained.

1. *The Column Hall of the House of Unions.* This hall has a volume of 12,500m³ and seats 1600 persons. The reverberation of the empty room is 3.55 sec. and that of the filled hall 1.75 sec. The optimum of reverberation from Eq. (1) is also 1.75 sec. This hall, when full, appears perfect from the point of view of acoustics. In it the voice of an orator, that of a singer, the music of a piano and that of an orchestra sound

[3] Samuel Lifshitz, Lectures on Architectural Acoustics, Moscow, 1923; Journal of (Russian) Physical and Chemical Society, **40**, 1924.

equally well. The renowned orchestra director Nikish considered this hall the best in Europe. The sound spreads equally throughout the whole volume of the room.

2. *The Small Hall of the Conservatory.* The volume of the room is 2550m³ and it seats 550 persons. The reverberation of the empty room is 3.46 sec. and that of the filled room is 1.30 sec., while the optimum from Eq. (1) is 1.32 sec. This hall is considered one of the best among the smaller halls of Moscow. In it, singing and playing on the piano and on the violin, all sound equally well. The sound fills the room equally and only in the last rows of the amphitheater may be noticed a considerable

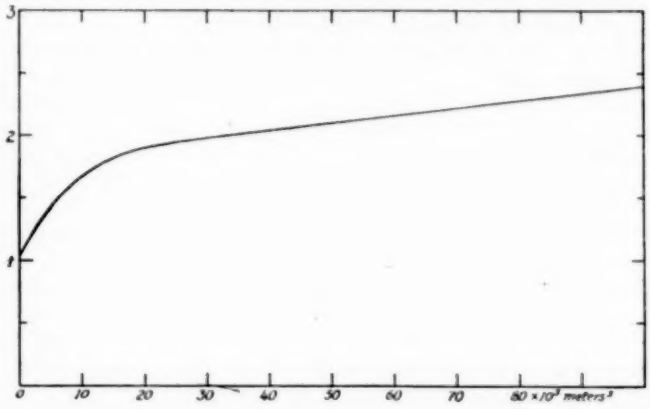

Fig. 1. Optimum time of reverberation in seconds as function of volume of auditorium.

decrease on the intensity of the sound. This comes from the amphitheater being divided from the rest of the hall by an arch of considerable breadth, which throws a part of the sound waves back into the hall. In shadowed places the reverberation appears considerably smaller than elsewhere in the room.

3. *The Big Hall of the Conservatory.* This hall has a volume of 17,000m³, and holds, with the orchestra, 2150 persons. The reverberation of the empty hall is 4.60 sec., that of the filled hall 2.00 sec., while the optimum from Eq. (1) is 1.85 sec. The reverberation of this room is comparatively large and the sound is somewhat too loud. This is true as well for the singing as for the sounds from musical instruments.

4. *The Big Theater.* The volume of the theater (to the second curtain) is 13,800m³; the number of auditors is 2300 persons; the reverberation of the empty theater is 2.06 sec. and the reverberation of the filled theater is 1.55 sec. The optimum from Eq. (1) is 1.79 sec. The theater, when

empty, sounds rather loud and when full sounds rather dry. The theater has ideal acoustics at rehearsals, being only falf filled. The features which partly affect the acoustics of the Big Theater are the great amount of ornamentation, and the soft curtains in the boxes, which give a great absorption even in the empty room. Therefore, the increased absorption of sound, due to the audience, is not as marked as usual. The audience in the boxes along the walls from the top down to the orchestra do not diminish the reverberation. That is why the deviations from the optimum one side or the other are comparatively small, and the theater, with respect to acoustics, appears tolerably good when full as well as when empty.

PHYSICAL INSTITUTE OF THE UNIVERSITY OF MOSCOW,
ACOUSTIC LABORATORY OF THE GOVERNMENT INSTITUTE OF MUSICAL SCIENCE.
November, 1924.